The localisation and activity of xanthine oxidoreductase in human endothelial and epithelial cells

Hoare, Catherine Anne

Award date:
2002

Awarding institution:
University of Bath

THE LOCALISATION AND ACTIVITY OF XANTHINE OXIDOREDUCTASE IN HUMAN ENDOTHELIAL AND EPITHELIAL CELLS

Submitted by Catherine Anne Hoare
for the degree of PhD of the University of Bath
2002

ProQuest LLC
789 East Eisenhower Parkway
P.O. Box 1346
Ann Arbor, MI 48106-1346

ABSTRACT

The following report attempted to show the true sub cellular location of human xanthine oxidoreducatse (XOR) and, together with cellular activity studies, assign a physiological function for the enzyme.

Localisation of XOR was facilitated by a high specificity anti-human XOR monoclonal antibody. Localisation was studied in human endothelial and mammary and gut epithelial permenant cell lines. Both confocal microscopy and electron microscopy was used. In all the cell lines XOR appeared in discrete punctate pockets and this, along with an association with the golgi apparatus, gave strong indication that the enzyme was being trafficked through the cell in vesicles. The destination of the enzyme varied in all three cell types although in all cases it seemed to be destined for secretion and then attachment to the outside of the plasma membrane.

The localisation and activity in endothelial cells supported a role for XOR in NO mediated vasodilation. This occurred under hypoxic conditions, indicating that the enzyme could be complimenting the oxygen dependent nitric oxide synthase (NOS). The localisation and activity of XOR in mammary epithelial cells, along with other work studying the enzyme in human milk, strongly suggested that XOR produced superoxide, NO and peroxynitrite served an anti-microbial role in the neonatal gut. A similar role was suggested for XOR in gut epithelial cells, with the localisation giving a strong indication that the enzyme may serve to produce an anti-microbial response upon breach of the gap junction between enterocytes.

Overall the most striking evidence was that the enzyme appeared to be trafficked through the secretion pathway of all the cells studied.

ACKNOWLEDGEMENTS

Firstly I would like to thanks my supervisors, Roger Harrison and Robert Eisenthal for giving me the opportunity to undertake this work and the support needed to complete it. I would also like to thank The University of Bath for funding.

My gratitude also goes to David Tosh, Chris Davey and Barbara Reaves for help with the confocal microscopy, as well as Ursula Potter for her help, guidance and extreme patience with the electron microscopy. My thanks also go to John Hancock and Roger Hurst for their significant scientific input, emotional support and friendship.

My thanks also to past and present members of Lab 1.28: Arwen Pearson, Sharmy Chouhdury, Hannah Martin, Tracey Goult, JJ Doel, Zoe Symons and Stephanie Hazelhurst, for both their ongoing help and friendship.

Special thanks to Christine Chester (the truest friend) and to my ever-understanding mum for always being my inspiration, and to my excellent friends Rachel Strong, Cedric Meyer, Charlie Chester, Matthew Hoare and Karen Franklin. And not forgetting my Father, Alan Hoare, who may not have been here to witness me undertake this project but was undoubtedly the person who believed in me so utterly that I could not help but believe in myself.

And finally my infinite thanks to Neil, soul mate, companion and fellow dreamer.

ABBREVIATIONS

ATP – adenosine triphosphate

BBB – blood brain barrier

BRLE – buffalo rat epithelial cell line

BSA – bovine serum albumin

DMSO – dimethylsulphoxide

ECACC – European collection of cell cultures

EDTA – ethylenediaminetetraacetic acid disodium salt dihydrate

ELISA – enzyme linked immunosorbent assay

ER – endoplasmic reticulum

FAD – flavine adenine dinucleotide

FBS – foetal bovine serum

FeS – iron sulphur

FITC – fluorescein isothiocyanate

GTN – glyceryl trinitrate

HBSS – hanks buffered saline solution

HUVEC – human umbilical vein endothelial cell

IgG – immunoglobulin G

IgM – immunoglobulin M

IR – ischemia reperfusion

KDa – kiloDaltons

Mo – molybdenum

NAD^+ – nicotinamide adenine dinucleotide

NADH – reduced nicotinamide adenine dinucleotide

NADPH –nicotinamide adenine phosphate dinucleotide

NO – nitric oxide

NOS – nitric oxide synthase

PBS – phosphate buffered saline

rER – rough endoplasmic reticulum

ROS – reactive oxygen species

SDS – sodium dodecyl sulphate

SDS PAGE – sodium dodecyl sulphate polyacrylamide gel electrophoresis

TBS – tris buffered saline

TRITC – tetramethylrhodamine isothiocyanate

TUNEL – transferase dUTP nick end labeling

UV – ultra violet

XDH – xanthine dehydrogenase

XO – xanthine oxidase

XOR – xanthine oxidoreductase

Table of Contents

	Page No.
Title Page	i
Acknowledgements	ii
Abstract	iii
Abbreviations	iv
Table of Contents	vi
1 Introduction	1
1.1 A brief introduction to xanthine oxidoreductase	1
1.2 Enzymology	4
1.2.1 Substrates	4
1.2.2 Dehydrogenase and oxidase forms	7
1.2.3 Reactive oxygen species	7
1.2.4 Nitric oxide metabolism	8
1.2.5 Inactive forms.	10
1.3 Properties of human XOR	11
1.4 Tissue and cellular distribution	11
1.5 Proposed pathogenic roles	13
1.6 Normal physiological roles	15
2 Aims	18
3 Materials	19
3.1 Chemicals	19
3.2 Instruments	19
3.3 Cell culture	20
3.4 Cells	20
3.5 Antibodies, apoptotic markers and ELISA	21
3.6 Electron microscopy reagents	21
4 Methods	22
4.1 Routine maintenance of cells	22
4.1.1 Medium for HB4a cells	22
4.1.2 Medium for BRLE and Caco-2 cells	22
4.1.3 Medium for EA-hy-926 and ECV-304 cells	23
4.1.4 Medium for CPA cells	23
4.1.5 Establishing cultures from cryopreserved cells	23
4.1.6 Subculturing cells	24
4.1.7 Cryopreservation of cells	25
4.1.8 Cell Harvesting for fluorimetric Assay	25
4.1.9 Induction of apoptosis	26
4.2 White blood cell preparation	26
4.3 Pterin assay for enzyme activity	26

4.4 Protein estimations 27
4.5 Nitric oxide assay 28
4.6 Confocal microscopy 29
4.6.1 Preparation of cells 29
4.6.2 Staining of cells 29
4.6.3 Image collection 31
4.7 Electron microscopy 31
4.7.1 Pre-embedding labeling 32
4.7.2 Embedding cell samples 33
4.7.3 Sectioning 35
4.7.4 Post-embedding labelling 36
4.7.5 Staining grids for viewing under transmission electron microscope 37
4.7.6 Data collection 38
4.8 Western blot analysis 38
4.8.1 Nuclear preparation 38
4.8.2 SDS Page 39
4.8.3 Western blot 40

5 Activity and localisation of XOR in endothelial cells 42
5.1 Growth curve and pterin-dependent XOR activity 43
5.2 Nitric oxide generation 44
5.3 Localisation of XOR in endothelial cells by electron microscopy 46
5.3.1 Cell morphology 46
5.3.2 Localisation of XOR in cells embedded in LR White resin 48
5.3.3 Localisation of XOR in cells embedded in epoxy resin 51
5.3.4 Controls 53
5.4 Localisation by confocal microscopy 54
5.4.1Loclaisation of XOR in primary and permanent endothelial cells 54
5.4.2 Localisation of XOR in barrier-positive and barrier-negative endothelial cells 56
5.4.3 Localisation of XOR in apoptotic endothelial cells 58
5.4.4 Localisation of XOR in CPA co-culture 61
5.4.5 Localisation of XOR and actin 61
5.5 Discussion 63

6 Activity and localisation of XOR in mammary epithelial cells 71
6.1 Growth curve and pterin-dependent XOR activity 71
6.2 Nitric oxide activity 73
6.3 Localisation of XOR by electron microscopy 73
6.3.1 Cell morphology 74
6.3.2 Localisation of XOR in cells embedded in LR White resin 74
6.3.3 Localisation of XOR in cells embedded in epoxy resin 77
6.3.4 Controls 81

6.4 Localisation by confocal microscopy 81
6.4.1 Localisation of XOR in HB4a mammary epihelial cells 82
6.4.2 Localisation of XOR in apoptotic cells 82
6.4.3 Localisation of XOR and actin
6.5 Discussion 87

7 Activity and localisation of XOR in gut epithelial cells 91
7.1 Growth curve and pterin activity 92
7.2 Nitric oxide activity 92
7.3 Localisation by electron microscopy 94
7.3.1 Cell morphology 94
7.3.2 Localisation of XOR in cells embedded in LR White resin 96
7.3.3 Localisation of XOR in cells embedded in epoxy resin 100
7.3.4 Controls 100
7.4 Localisation by confocal microscopy 101
7.4.1 Localisation of XOR in mature and immature Caco-2 cells 101
7.4.2 Localisation of XOR in barrier-positive and barrier-negative Caco-2 cells 105
7.4.3 Localisation of XOR in apoptotic Caco-2 cells 109
7.4.4 Loalisation of XOR, zonular ocludens and catenin beta 109
7.5 Discussion 114

8 Overall discussion 122
9 Appendix 131
10 References 138

1 INTRODUCTION

1.1 A brief introduction to xanthine oxidoreductase

Xanthine oxidoreductase (XOR) is a widely distributed molybdenum-containing flavoenzyme that plays a key role in purine catabolism, catalysing the hydroxylation of hypoxanthine and xanthine to xanthine and uric acid, respectively (Bray, 1975) with concomitant reduction of NAD^+ or molecular oxygen.

XOR has been found in all species studied, from bacteria through to man. The level of amino acid identity among XOR species homologs is very high, indicating a remarkable level of conservation along phylogeny (Terao *et al,* 1997), see Fig 1.1. XOR is readily available from milk, where it forms a major component of the milk fat globule membrane (Bray, 1975). Because of this availability, the enzyme has been known for over 100 years and has been studied in purified form for the last 60 years (Massey and Harris, 1997).

XOR is a homodimer of 150kDa subunits and exists in two interconvertible forms, xanthine dehydrogenase (XDH) and xanthine oxidase (XO). Each monomeric subunit contains two Fe-S redox centers, an NAD^+ and a molybdenum-cofactor-binding site (see Fig 1.2). The dehydrogenase form preferentially reduces NAD^+, in contrast to the oxidase form, which does not reduce NAD^+, preferring molecular oxygen (Bray, 1975, Hille, 1996).

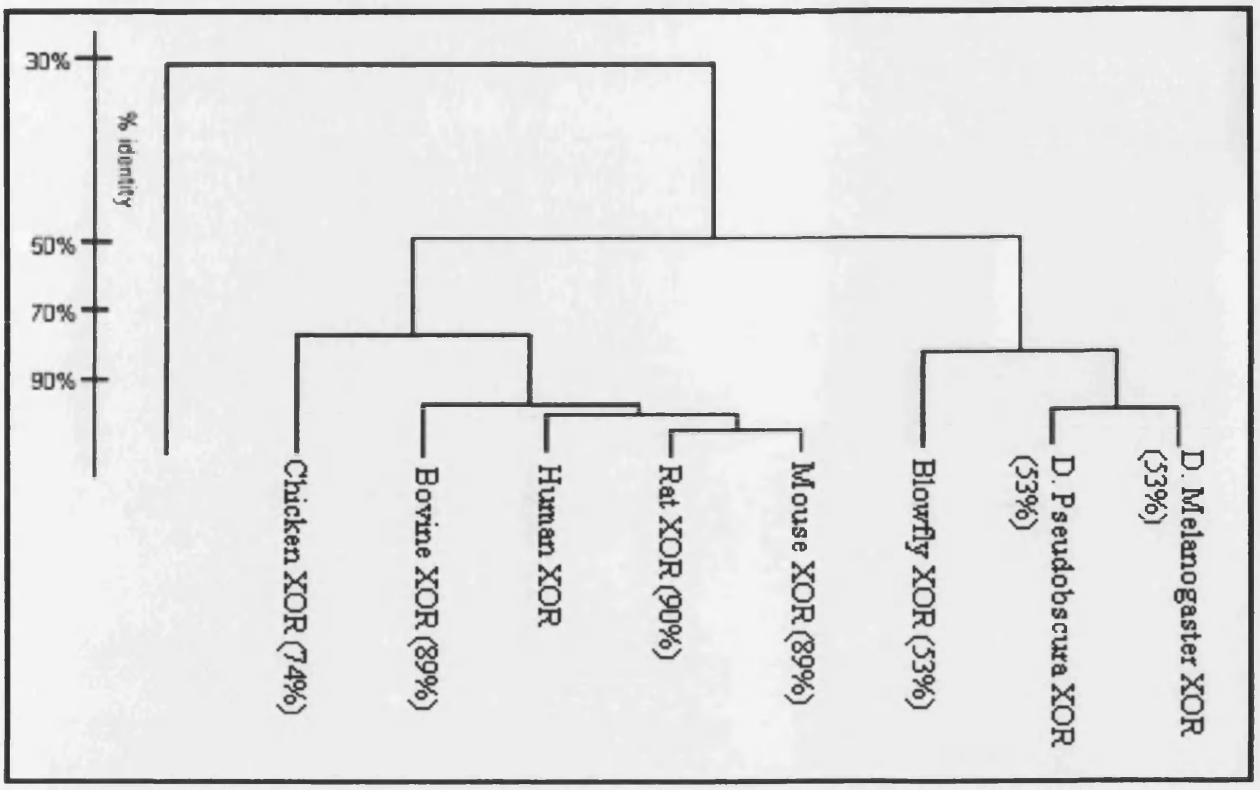

Fig 1.1: *Phylogenic tree showing the % identity to human liver XOR between species of XOR. (Courtesy of Arwen Pearson)*

Interest in XOR has increased over the past few decades as our knowledge about its molecular activity has increased. Its ability to produce reactive oxygen (Granger *et al* 1981) and nitrogen (Millar *et al,* 1998) species has inspired a great deal of research and debate into the enzyme's true physiological purpose and function.

Fig 1.2: *A ribbon diagram depicting bovine XO. FAD and molybdopterin are shown as capped cylinders and the iron sulphur centres as atoms. The Mo domain is blue, the FAD domain green and the FeS domain red. (Courtesey of Arwen Pearson)*

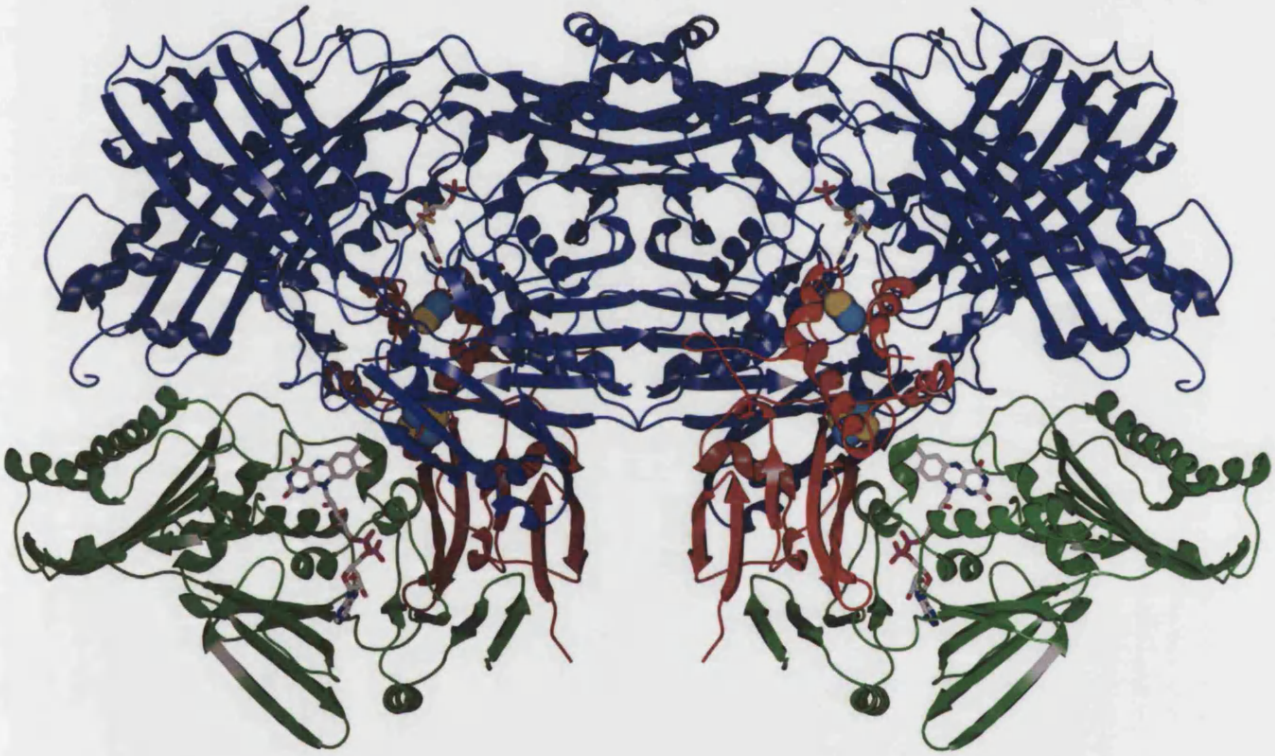

1.2 Enzymology

While there are still no definitive answers as to the pathophysiological function of XOR, our knowledge of the structure and properties of the enzyme has greatly increased in recent years. XOR has been characterized from rat (Ikegami and Nishino, 1986), chicken (Nishino and Nishino, 1989) and turkey (Cleere and Coughlan, 1975) livers and from mouse mammary gland (McManaman *et al*, 1999) as well as from human (Godber, 1998) and bovine (Massey and Harris, 1997) milk. These preparations have demonstrated that the basic properties of the enzyme are generally consistent, no matter what the source.

1.2.1 Substrates

XOR catalyses the oxidation of a wide range of substrates, most notably hypoxanthine and xanthine, generating xanthine and uric acid, respectively, in the process of purine catabolism (see Fig 1.3) (Bray, 1975). It is also capable of oxidising purines, pteridines, aldehydes and various xenobiotics as well as reducing NAD^+, oxygen and methylene blue (Krenitsky *et al,* 1972). The reduction of inorganic nitrites to NO is believed to occur at the molybdenum site with xanthine or NADH being utilised as the reducing substrates (Godber *et al,* 2000).

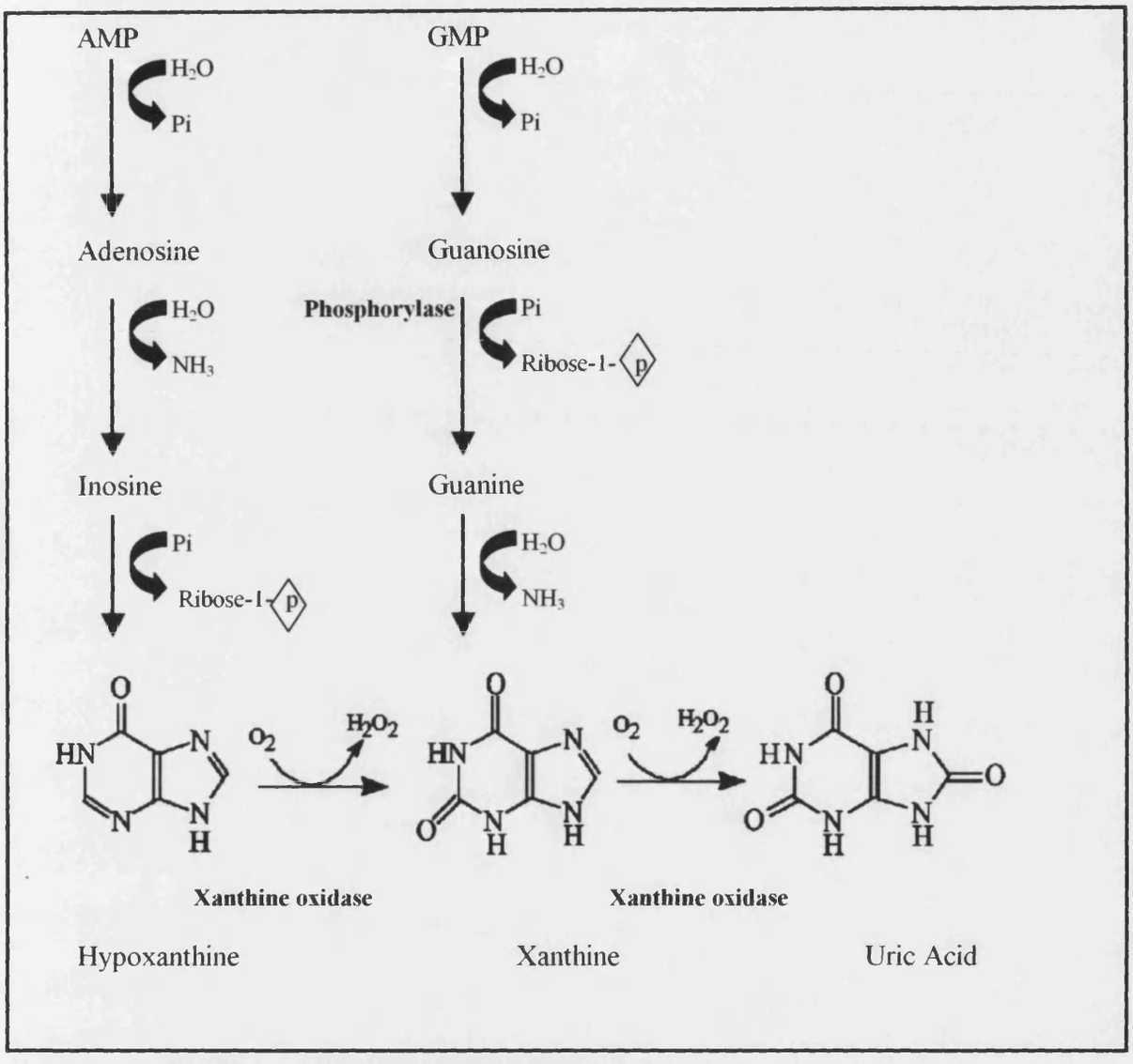

Fig 1.3: *Catabolism of purine nucleotides to uric acid*

Reducing substrates donate electrons at the molybdenum site, except NADH, which is unique in its ability to donate electrons to the FAD site (see Fig 1.4). Electrons are shuttled between the molybdenum, iron-sulphur and FAD sites with the iron-sulphurs maintaining the other centres in the optimum redox state (in general, molybdenum for reducing substrates and FAD for oxidising substrates) by acting as electron resevoirs (Olson *et al,* 1974).

Fig 1.4: *Molecular activity of XOR, purple lines show the flow of substrates to products, white lines show the flow of electrons*

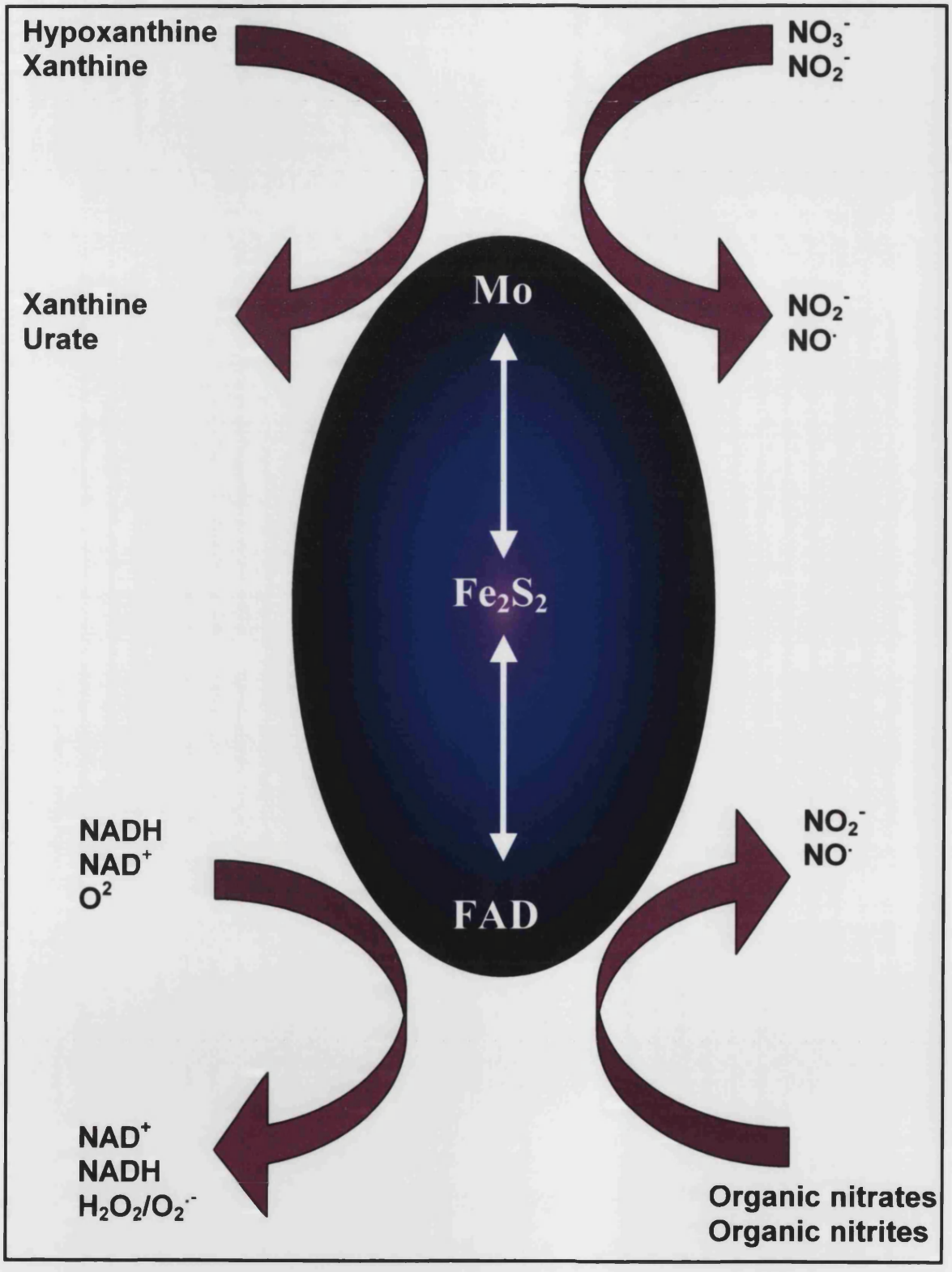

1.2.2 Dehydrogenase and oxidase forms

As previously stated, XOR is a homodimer of 150kDa subunits and exists in two interconvertible forms, xanthine dehydrogenase (XDH) and xanthine oxidase (XO). XDH is the predominant form *in vivo* and the only form observed in avian sources (Bray, 1975). The two forms are interconverted reversibly by sulphide reagents or, irreversibly (XDH to XO) by proteolysis (Della-Corte *et al* 1972).

XDH preferentially reduces NAD^+, whereas XO cannot reduce NAD^+, preferring molecular oxygen. The three dimensional structure of bovine milk XOR has been determined by Enroth *et al* (2000), who showed that XDH to XO conversion involved major changes in the FAD site.

1.2.3 Reactive oxygen species metabolism

Reduction of oxygen leads to superoxide anion and hydrogen peroxide, and it is the potential to generate these reactive oxygen species (ROS) that has led to particular interest in the enzyme as a destructive agent in many instances of ischaemia-reperfusion injury (Sussman and Bulkley, 1990). XOR-derived ROS have also been implicated in the tissue injury and loss of epithelial barrier function associated with clinical disorders resulting from deregulated inflammation (Pfeffer *et al,* 1994). These pathological roles for the enzyme have attracted greater attention following the discovery that corticosteroids and cytokines can regulate the transcriptional activation of the XOR gene (Pfeffer *et al,* 1994). Also of interest is the NADH oxidase activity of XOR, where the enzyme-catalysed oxidation of NADH results in the production of superoxide (Sanders *et al,* 1997). As mentioned earlier, NADH is unique in that it donates its electrons to the FAD reactive site and

thus this activity would not be blocked by the most commonly-used XOR inhibitors, allopurinol and oxypurinol (which inhibit specifically at the molybdenum site). Hence, use of these inhibitors as tools to investigate the enzyme's function may lead to overlooking of the NADH derived ROS.

The production of ROS results in the production of urate (see Fig 1.4), which is in itself a powerful antioxidant. It is noteworthy that, whilst for many years ROS have been viewed as harmful pollutants, growing evidence is now mounting for their involvement in mediating the gene expression in a host of cellular responses including growth, survival and apoptosis (Irani, 2000, Hancock *et al,* 2001). XOR-derived oxygen radicals have also been proposed as potential anti-cancer therapies. One study has shown that VX2 carcinomas are more susceptible to oxygen radicals than the surrounding muscle tissue (Yoshikawa *et al,* 1995) and, more recently, one group has shown the succeful suppression of tumour growth using chemotherapy based on a xanthine oxidase-polymer conjugate (Sawa *et al,* 2000).

1.2.4 Nitric oxide metabolism

The ability of the XOR to produce NO has aroused much interest in recent years. This is a property that is, perhaps, not surprising in view of the enzyme's many similarities with the assimilatory nitrate reductases of fungi, algae and higher plants (Hille, 1996). It is of interest because NO is a widespread signalling molecule involved in the regulation of an impressive spectrum of diverse cellular functions (Kelm *et al,* 1997).

The physiological roles of NO include blood pressure regulation, antimicrobial defence and neuronal communication (Sampath *et al,* 1994). This has been reflected in the near exponential growth of publications relating to NO and NO synthase (Knowles and Moncada, 1994, Alderton *et al,* 2001). Other functions of NO are as a paracrine messenger, regulation of guanylyl cyclase activity, control of neurotransmitter release and acting as a neurotransmitter. NO also has bactericidal and tumoricidal activities, may contribute to the biochemistry underlying memory and is a mediator of vasodilation acting on smooth muscle cells in the blood vessel wall (Moncada *et al,* 1991).

Nitric oxide (NO) synthesis is well-known to result from the oxidation of L-arginine by a family of NO synthases (NOS), which requires oxygen. XOR, on the other hand, reduces nitrite to NO under anaerobic conditions, and could constitute a complementary system to NOS. Indeed, XOR-catalysed production of NO has been shown to fall off as levels of oxygen increase, consistent with the concomitant production of superoxide and interaction of the latter with NO to yield peroxynitrite (Godber *et al,* 2000). An NO synthase-independent generation of NO has also been demonstrated in rat skeletal muscle after ischemia reperfusion injury (Lepore *et al,* 1999). The XOR-catalysed generation of NO may be important in redistribution of blood flow to ischaemic tissue as a supplement to NOS, since both nitrite (Iizuka *et al,* 1999) and NADH (Harrison, 1997) have been shown to be elevated in hypoxic tissue.

1.2.5 Inactive forms

The ability to purify XOR from milk has allowed insight into the enzyme's structure, activity and kinetics (Godber, 1998). One potentially surprising observation is that up to 60% of XOR, purified from bovine milk, is inactive towards conventional reducing substrates such as xanthine (Bray, 1975). Of this 60%, approximately half lacks the Mo (and potentially the molybdopterin), whilst in the other half the Mo=S grouping (essential for catalytic activity) is replaced by Mo=O (Gutteridge *et al*, 1978). These inactive forms are known as demolybdo-XOR and desulpho-XOR respectively.

Enzyme purified from human milk is up to 95% demolybdo-XOR (Godber *et al*, 1997). The physiologic reason for the production of large amounts of inactive enzyme is unclear, but it is possible that the activity of the enzyme may be subject to regulation. Evidence to support this was found from study of the activity of XOR in serial samples of human milk taken during the first month *post partum* (Brown *et al,* 1995). Enzyme activity was observed to peak during the first 15 days and then to decline by as much as 95% back to basal levels. Protein levels remained constant and the variation in activity was attributed to post-translational modification.

1.3 Properties of human XOR

Reports on the tissue specific activity of XOR vary greatly and are discussed in greater depth later, but the consensus would appear to be that, in human tissue, little XOR activity is seen apart from in the liver and small intestine (Parks and Granger, 1986). This tissue specific activity, along with the variation in activity observed in human milk (Brown *et al,* 1995) gives the best evidence for the support of an alternate physiological role for XOR other than that of the generalised house-keeping function of purine catabolism.

One group has reported 'bovine-level' activity from a human source that was purified from human liver (Krenitsky *et al,* 1986). However, recent work has given reason to suspect that this may not be the case *in vivo* and that it is more likely to be the result of a purification procedure that selects for active forms of the enzyme (Choudhury, 2001).

1.4 Tissue and cellular distribution

Immunolocalisation studies using rabbit anti-bovine milk fat globule membrane antibodies demonstrated the presence of XOR in bovine mammary epithelial cells, capillary endothelial cells and liver sinusoidal endothelial cells (Jarasch *et al,* 1981). Subsequent immunolocalisation studies have shown the enzyme to be present in human hepatocytes, epithelial cells of the digestive and respiratory systems and epithelial cells of lactating mammary gland (Moriwaki *et al,* 1996). There is still some debate as to the presence of XOR in cardiac capillaries and smooth muscles cells (Jarasch *et al,* 1981, De Jong *et al,* 1990).

The tissue specific activity of XOR is also a matter of debate. Several groups have demonstrated that enzyme activity can only be detected in trace amount in all organs other than the liver and small intestine (Kooij *et al,* 1992, DeJong *et al,* 1990, Saksela *et al,* 1998)). A particularly contentious issue is that of the presence of XOR activity in the heart. Whilst it is likely that circulating XOR is present in the blood flowing through the heart, only one group has reported significant enzyme activity in the organ (Wajner and Harkness, 1989) and the difficulty experienced in reproducing their results has cast doubt upon them. Indeed, at least one group recently detected no XOR protein in heart tissue (Linder *et al,* 1999).

Also of interest are the reports of localisation and activity of XOR in cancerous tissues and cells. Immunocytochemical localisation revealed an absence of XOR in neoplastic breast epithelium, in contrast to normal breast epithelium, suggesting that expression of the enzyme is reduced to undetectable levels in breast cancer (Cook *et al,* 1997). Furthermore, XOR activity has been shown to be significantly reduced in hepatomas (Pradja *et al,* 1976, Ikegami *et al,* 1986), colon carcinomas (Weber *et al,* 1978)) and renal carcinomas (Prajda *et al,* 1981). Immunohistochemical localisation also failed to detect XOR breast cancer cells metastased to the liver (Moriwaki *et al,* 1996). These studies lead to the conclusion that cancerous cells down-regulate the expression and activity of XOR. If some understanding could be gained as to why this occurs it may well answer the riddle as to the function of the enzyme and simultaneously arm us with a potential therapeutic tool.

The reports of the sub-cellular localization of XOR are perhaps even more confusing, although, as with the tissue localisation, there seems to be an emerging pattern. Immunolocalisation of the enzyme has shown it to be present on the surface of cultured human (Roquette *et al,* 1998), bovine and porcine (Vickers *et al,* 1998) endothelial cells and on the luminal side of the plasma membrane of rat liver sinusoidal endothelial cells (Frederiks *et al,* 1999). In contrast to these observations,

Jarasch and coworkers (1981) observed the enzyme exclusively in the cytosol of bovine endothelial cells. Immunogold labeling in conjunction with electron microscopy also showed that XOR was exclusively cytosolic in rat hepatocytes (Ichikawa *et al,* 1992).

Obtaining accurate data on the tissue, cellular and sub-cellular localization of XOR will undoubtedly aid greatly in discovering the enzyme's true physiological function. However, it would seem that recent attempts to elucidate this information have only served to muddy the waters. The reasons for these apparent discrepancies could be many and undoubtedly include factors such as sample source, preparation and immunolocalisation methodology. But probably by far the largest contributing factor is the lack of high-affinity and high-specificity antibodies to XOR.

1.5 Proposed pathogenic roles

Generation of ROS by XOR has led to the hypothesis of its involvement in ischemia-reperfusion (IR) injury (Granger *et al,* 1981, McCord, 1985). The key events proposed for this mechanism are as follows. During ischemia, cytosolic calcium levels are elevated due to the dissipation of transmembrane ion gradients. This results in the activation of proteases that irreversibly convert XOR from the XDH form to the XO form. Concurrently, hypoxanthine accumulates from the cellular catabolism of ATP. The influx of oxygen on reperfusion causes it to react with XO and hypoxanthine resulting in the generation of superoxide and hydrogen peroxide and the subsequent production of cytotoxic agents such as hydroxyl radicals (Granger *et al,* 1981).

Publication of this hypothesis has resulted in a great deal of debate as to the possibility of this mechanism actually occurring *in vivo* (Wiezorek *et al* 1994, Frederiks *et al,* 1993, Kooij *et al,* 1994, Brass, 1995, Kooij *et al,* 1995, Frederiks and Bosch 1996). Observations in support of the hypothesis include attenuation of damage in experimental animals after the administration of allopurinol, oxypurinol (both specific XOR inhibitors) or a tungsten rich diet resulting in the inactivation of XOR (Kurose and Granger, 1994). However, doubt has been cast upon some of these data in view of the hydroxyl scavenging properties of allopurinol and oxypurinol (Moorhouse *et al,* 1987).

ROS are not the only cellular pathogenic agents. NO, has been shown to have a deleterious effect, mediated in part by peroxynitrite, on intestinal barrier function (Menconi *et al,* 1998). As previously stated, XOR is a potential source of both these molecules and, in an intestinal model using Caco-2 cell monolayers, the breakdown in barrier function could be prevented by the addition of allopurinol, an XOR inhibitor (Menconi *et al,* 1998).

If XOR does have a pathogenic role *in vivo,* it would seem that there are defences already in place to protect the body from damaging effects of circulating XOR. Levels of IgM class anti-human XOR antibodies in human serum have been found to be particular high, representing approximately 3% of total IgM (Benboubetra *et al,* 1997). The majority of these antibodies appeared as immune complexes, suggesting that they were fulfilling a protective role by removing XOR (Benboubetra *et al,* 1997).

1.6 Normal physiological roles

As previously stated, XOR is best known for its role in purine catabolism. Mutations in the XOR gene cause the disease xanthinuria (Rytkonen *et al,* 1995). Hereditary xanthinuria is a rare autosomal recessive disorder in which patients often display renal symptoms because they excrete large amounts of xanthine in their urine (Sumi and Wada, 1996). However, the disease is often asymptomatic and goes largely undetected.

It has been proposed that XOR may be an anti-microbial agent in the neo-natal gut (Brown *et al,* 1995). This idea is supported by the observation that XOR activity in human breast milk shows great variation in the first weeks *post partum*, reaching peak values (as much as 50-fold higher than basal levels) usually within the first 10 days, and falling to basal levels thereafter (Brown *et al,* 1995). This idea was originally based on the enzyme's ability to produce ROS, similar to that of NADPH oxidase which catalyses the 'respiratory burst' in white blood cells. However, not only is XOR capable of generating superoxide, it also catalyses the production of NO, a prerequisite for peroxynitrite generation (Godber *et al,* 2000). All of these molecules have potent microbicidal effects and it has been known for many years that mammalian milk has antibacterial properties (Stevens *et al,* 2000). In support of this hypothesis is the observation that pathogenic bacteria may well bind to epithelial antigens on the milk fat globule membrane in the same manner that they bind to similar antigens on the surface of epithelial cells in the digestive track (Keenan and Patton, 1995). This would bring the bacteria into close contact with XOR. Millimolar levels of nitrite (DeMoss and Hsu, 1991) produced by the bacteria's nitrate reductases (Cole, 1996) would provide substrates for NO generation and it is noteworthy that the K_m value for XOR catalysed nitrite production is in the millimolar range (Godber *et al,* 2000a).

The localisation of XOR to endothelial cells (Jarasch *et al,* 1981, Roquette *et al,* 1998) and its ability to produce NO (Godber *et al,* 2000) has led, as previously stated, to the suggestion that the enzyme may be involved in NO-mediated vasodilation. The vasodilatory action of organic nitrates has been known for over 150 years and they have been widely used to treat a variety of cardiac diseases (Ahlner *et al,* 1991). However, their mode of action remains unclear (Harrison and Bates, 1993). XOR has been shown to catalyse the reduction of one such drug, glyceryl trinitrate (GTN), to NO in the presence of NAD under hypoxic conditions (Millar *et al,* 1998). XOR can also catalyse the reduction of isosorbide dintrate and isosorbide mononitrate (Doel *et al,* 2001). Indeed, it has been demonstrated that, in the presence of GTN, XOR produces sufficient NO *in vitro* to inhibit platelet aggregation (O'Byrne *et al,* 1999). Whilst the majority of this work centers on experimental data gained from purified enzyme, endothelial and smooth muscle cells have also been shown to reduce organic nitrates to NO with comparable efficacy (Feelisch and Kelm, 1991).

The administration of these vasodilating drugs results in a phenomenon known as clinical tolerance, which is believed to reflect the inactivation of the enzyme(s) responsible for their metabolism (Abrams *et al,* 1998). XOR has also been shown to be inactivated when incubated anaerobically with GTN and xanthine (Doel *et al,* 2001). The ability of XOR to produce NO under hypoxic conditions lends itself to the theory that XOR could be an alternative pathway to that of NO synthase, as the production of NO from NOS requires oxygen. Interestingly, it has been shown that hypoxia up-regulates XOR, although the exact mechanisms of pre and posttranslational synthesis of active enzyme remain unclear (Hassoun *et al,* 1994, Poss *et al,* 1996).

The ability of XOR to participate in a broad range of reduction and oxidation activities has led to many theories as to its actual function. A greater understanding of the enzyme at a genetic, molecular and structural level is needed, along with knowledge of its cellular and sub-cellular localisation. It may well be that this intriguing flavoenzyme is merely a partially redundant house keeping enzyme, but the current level of interest suggests that there are many who are unwilling to accept this as the complete story.

2 AIMS

The aims of this project were to investigate the localization of XOR in various cell types in an attempt to gain further understanding of function *in vivo*. The decision to concentrate on mammary and gut epithelial, as well as vascular endothelial cells was based on literature evidence of the likely importance of XOR in these cells. Central to many of the results presented is the use of a highly specific anti- human XOR antibody, a tool that in previous studies had been unavailable.

3 MATERIALS

3.1 Chemicals

Bio-Rad protein assay reagent dye concentrate was obtained from Bio-Rad, Hemel Hemstead, Hertfordshire. All other chemicals were obtained from Sigma, Poole, Dorset, unless otherwise stated.

3.2 Instruments

Centrifugation was carried out in a Beckman TL-100 ultracentrifuge, MSE Centaur 2 benchtop centrifuge and a Sarstedt microcentrifuge. Sonication was performed using an MSE 150Watt ultrasonic disintigrator Mk2. Fluorescent enzyme assays were carried out on a Perkin-Elmer LS-5B luminescence spectrophotometer, and absorbance spectra on a Cecil CE 6600 multimode computing UV spectrophotometer. Nitric Oxide levels were measured using a Sievers 280 nitric oxide analyser. Oxygen levels were measured using a MI-730 oxygen microelectrode from Microelectrodes Incorporated. Confocal microscopy was carried out on a Zeiss Axiovert 100M confocal microscope, and electron microscopy was carried out on a JEOL JEM-1200EX II (JEOL, Tokyo, Japan) EM, funded by 'The Science & Engineering Research Council'. Resin blocks were cut on an Ultracut E Ultramicrotome and samples were preserved by slam freezing in a Leica EMMM80 Freeze-Slamming Device, both of which were supplied by Leica, Wien, Austria.

3.3 Cell culture

Cell culture was carried out in a microflow culture hood. RPMI 1640 media, Dulbecco's Modified Eagle media, M199 media, foetal bovine serum, L-glutamine, penicillin/streptomycin mixture, cholera toxin, trypsin - EDTA solution, hydrocortisone (water soluble), insulin from bovine pancreas, PBS tablets and sigmacote, were all obtained from Sigma, Poole, Dorset. Plasticware was obtained from Helena Biosciences.

3.4 Cells

HB4a (a conditionally immortalised human mammary luminal epithelial cell line) cells were a gift from Dr Kalamati, The Royal Cancer Hospital, Sutton. BRLE (an immortalised buffalo rat liver epithelial cell line) cells were a gift from Dr T. Edwards, Bath University. EA-hy-926 (a permanent human endothelial cell line) cells were a gift from Dr A. George, Hammersmith Hospital, London. ECV-304 (a permanent human endothelial cell line) cells were a gift from Dr R. Hurst, University of The West of England. Caco-2 (a permanent human gut epithelial cell line) cells were a gift from Dr R. Hurst, University of The West of England. CPA (a co-culture of bovine aortic endothelial and smooth muscle permanent cell lines) cells were purchased from the European Collection of Cell Cultures (ECACC).

3.5 Antibodies, apoptotic markers and ELISA

Primary anti-human XOR antibody, 1D9/D1 and XOR ELISA kit were developed and supplied by Eurogenetics, Belgium. All other primary antibodies, TRITC and FITC secondary antibodies and phalloidin-TRITC were obtained from Sigma immunochemicals. Secondary gold antibodies were obtained from British Biocell. The apoptotic cell marker kit, ApoAlert™ DNA Fragmentation Assay Kit, was obtained from Clonetech.

3.6 Electron microscopy reagents

LR White acrylic resin, Epoxy resin (812 Premix Resin Kit) and Gilder Grids (single slot, nickel) were all obtained from Taab Laboratories Equipment Ltd., Aldermaston, Berks, UK. 50 mesh gold grids, glutaraldehyde 25% in ampoules and paraformaldehyde powder were obtained from Agar Scientific, Stansted, Essex, UK. The epoxy tissue stain (used for semi-thin sections) comprised a mixture of Toluidine Blue O and Basic Fuchsin in aqueous alcohol and was obtained from Electron Microscopy Sciences (EMS), Fort Washington, PA, USA.

4 METHODS

4.1 Routine maintenance of cells

Cells were cultured as monolayers in filter capped tissue culture flasks, at 37°C in a humidified incubator with 5% CO_2 (v/v) and 95% air (v/v). The cells were provided with 0.2ml of medium per cm^2, which was discarded every other day and replaced with fresh prewarmed medium. In all cases, an aliquot of the medium was placed in the incubator to check for contamination prior to culture.

4.1.1 Medium for HB4a cells

RPMI-1640 medium (without L-Glutamine) (500ml) was used and supplemented with 10% (v/v) foetal bovine serum (FBS) (50ml), 200mM L-Glutamine (7.5ml), penicillin (10,000units/ml)/streptomycin (10mg/ml) solution (10ml), 5μg/ml insulin (0.5ml), 5μg/ml hydrocortisone (0.5ml) and 100ng/ml cholera toxin (1ml).

4.1.2 Medium for BRLE and Caco-2 cells

Dublecco's Modified Eagle Media M199 (without L-Glutamine) (500ml) was used and supplemented with 10% (v/v) FBS (50ml), 200mM L-Glutamine (7.5ml), penicillin (10,000units/ml)/streptomycin (10mg/ml) solution (10ml).

4.1.3 Medium for ECV-304 and EA-hy-926 cells

RPMI-1640 medium (without L-Glutamine) (500ml) was used and supplemented with 10% (v/v) FBS (50ml), 200mM L-Glutamine (7.5ml), penicillin (10,000units/ml)/streptomycin (10mg/ml) solution (10ml).

4.1.4 Medium for CPA cells.

M199 medium (without L-Glutamine) (500ml) was used and supplemented with 20% (v/v) FBS (100ml), 200mM L-Glutamine (7.5ml), penicillin (10,000units/ml)/streptomycin (10mg/ml) solution (10ml).

4.1.5 Establishing cultures from cryopreserved cells

Cell cultures were initially established from cells preserved by freezing in liquid nitrogen. Appropriate medium for the cell type was warmed for 30min in a 37°C water bath to avoid subjecting the cells to thermal shock. An aliquot of cells stored in a cryopreservation vial were removed from the liquid nitrogen and allowed to thaw rapidly in the water bath. Once thawed, the cells were pipetted into medium (10ml) in a sterile Universal and then centrifuged at 200g for 5min. The supernatant was discarded and warmed medium (5ml) was used to resuspend the cell pellet. This was then transferred into a flask of equal volume to that in which the cells were originally grown. The medium was changed after 24h to remove any remaining DMSO.

4.1.6 Subculture of cells

Cells were subcultured shortly before reaching a confluent monolayer. Appropriate medium and phosphate buffered saline (PBS) were warmed in a water bath at 37°C to avoid subjecting the cells to thermal shock. Medium from the flask was discarded and the monolayer of cells was washed twice with warm PBS. After the second wash the cells were detached from the flask by trypsinisation, using 0.05% (w/v) trypsin/0.02% EDTA (w/v) solution in PBS. BRLE and EA-hy-926 cells started to detach from the flask immediately on addition of the trypsin. HB4a and Caco-2 cells were placed in the incubator for 5-10min to dislodge them from the surface of the flask. Once all the cells were detached from the floor of the flask the reaction was stopped by adding an equal volume of medium. An aliquot of the cell suspension was taken and the cell density and viability checked using the trypan blue exclusion method. The suspension was diluted 1:1 with 0.04% (w/v) trypan blue and the haemocytometer prepared, ensuring that Newton's rings of diffraction were visible on the cover slip. The mixture (10µl) was loaded into the haemocytometer, being careful not to flood the chamber. The number of viable cells (those that do not take up the trypan blue stain) in each of the five large squares was counted. If the number of cells counted in 5 squares is n, the cell count is:

$$[(n/5) \times df] \times 10^4 \text{ cells per ml}$$

where df = dilution factor with trypan blue. If there are too many cells to count or if clumping is seen the sample can be diluted further with trypan blue. Once the cell

viability had been calculated, new tissue culture flasks were seeded at the required cell density.

4.1.7 Cryopreservation of cells

Cell stocks were preserved by freezing in liquid nitrogen. One flask containing a monolayer of confluent cells was trypsinised as described in Section 4.1.6, and transferred into a sterile tube.

The cell suspension was centrifuged at 200g for 5min to obtain a cell pellet. The supernatant was discarded and the pellet resuspended in FBS (0.5ml). The cells were transferred into a cryogenic vial along with appropriate medium (0.4ml) and DMSO (100µl). The cryogenic tubes were stored at -70°C for 24h before being transferred into liquid nitrogen.

4.1.8 Cell harvesting for fluorimetric assay

Cells were grown up for fluorimetric assay as a monolayer in tissue culture flasks as described in Section 4.1. They were then removed from the flasks as described in Section 4.1.6, and a pellet was obtained by centrifuging the cell suspension at 200g for 5min. The supernatant was discarded, the inside of tube allowed to air dry and the pellet resuspended in fluorimetric buffer (1.2ml). This buffer comprised 50mM potassium phosphate (pH 7.4), 0.1mM EDTA, containing 1µg/ml of each of the following antiproteinases: pepstatin A, leupeptin, antipain and aproteinin. The

suspension was then transferred to a 1.5ml Eppendorf tube and kept on ice. The Eppendorf was then placed in a cool box to keep cells at a constant temperature and sonicated using the 3mm probe for 20s at power setting 6.5. The suspension was then ultracentrifuged at 100,000g for 30min at 4°C to give a crude cytosolic fraction that was used in both enzyme assays and protein estimations.

4.1.9 Induction of apoptosis

Apoptosis was induced by the addition of 5mM sodium butyrate to the media, as described by Hara et *al* (2000). Apoptotic morphology (cells rounding up and detaching) could be seen 36 – 48h after the addition of the sodium butyrate. Apoptosis was confirmed by staining with the TUNEL assay (see Section 4.6.2).

4.2 White blood cell preparation

Blood was collected into heparin (1µl/ml) in polypropylene tubes and diluted 1:1 with sterile PBS. This was then layered onto Lymphoprep (specific gravity 1.077g/ml, Nycomed) (15ml) in 50ml polypropylene tubes and centrifuged for 30min at 350g. The white, cloudy, buffy coat (middle layer) was then harvested directly into RPMI + 10% FBS and centrifuged for 10min at 350g. The medium was removed and the pellet was resuspended and washed with warm RPMI. This was repeated several times. This method should yield approximately 1 million cells/ml of blood sample. If the sample was severely contaminated with platelets, another wash step was performed.

4.3 Pterin assay for enzyme activity

The sensitive fluorimetric assay described by Beckman *et al*, (1989), was used to assess the activity of XOR. The assay measures the conversion of pterin (2-amino-4-hydroxy pteridine) to the fluorescent product isoxanthopterin and utilises 10μM pterin as the reducing substrate and 10μM methylene blue as the oxidising substrate.

All the assays were performed at room temperature in quartz cuvettes using the crude cytosolic fraction derived from the cells and cell buffer (made up as described in Section 4.1.9) or sonicated whole cells. Fluorescence was measured at an excitation wavelength of 345nm, an emission wavelength of 390nm and with slit widths of 5nm.

A stable baseline was obtained for the cell fraction diluted in fluorimetric buffer. 10μM pterin and 10μM methylene blue were then added and the reaction rate measured over 10-15min. The reaction was stopped by the addition of 50μM allopurinol (an inhibitor of XOR activity). Sequential additions of isoxanthopterin (4pmol) were added to provide calibration and an internal standard accounting for variations caused by fluorescence quenching and scattering. The final reaction rate was then calculated as pmol isoxanthopterin/min/mg total protein.

4.4 Protein estimations

Protein estimations of the crude cytosolic fraction were estimated by using the method described by Bradford (1976). The standard used was bovine serum albumin (BSA) at a concentration of 0.1mg/ml.

BSA was diluted in phosphate buffer to a total volume of 100µl to give concentrations ranging from 0 to 10 µg/ml. The crude cytosolic fraction was diluted in phosphate buffer to give an approximate concentration that fell within the range of the BSA standards. Bio-Rad reagent (1ml) was added to each sample in a plastic cuvette. The cuvette was inverted several times and left at room temperature for 10min for the colour to develop. The absorbance at 595nm was measured using a spectrophotometer and a standard curve generated from the absorbance readings of the BSA standards. This curve was then used to assess the protein content of the crude cytosolic fraction.

4.5 Nitric oxide assay

Nitric oxide assays were carried out on a Sievers 280 nitric oxide analyser. Oxygen levels were measured using a Microelectrodes Incorporated MI-730 oxygen microelectrode. Oxygen-free nitrogen was passed through the reaction vessel to ensure that the reaction remained anaerobic. pH was maintained throughout by a Radiometer pH stat. Cells were detached from tissue culture flasks using the mechanical method of a cell scraper (there is some concern that trypsin may cleave syndecan bonds that bind XOR to the surface of cells), spun down to form a pellet and resuspended in the

required amount of Hanks buffered saline solution (HBSS). Meanwhile HBSS (pH 7.2) containing 100μM xanthine and 100mM sodium nitrite was allowed to equilibrate in the water-jacketed reaction chamber of the NO analyser until prewarmed to 37°C. Once a steady base line was obtained the cells were added and the rate of NO production measured. The reaction was stopped by the addition of 50μM allopurinol.

4.6 Confocal microscopy

Confocal microscopy is a powerful tool that allows the reconstruction of high-resolution 3D images along with fluorescence labeling and co-localisation.

4.6.1 Preparation of cells

Cells were seeded; either from monolayer culture or cryopreservation, onto heat-sterilised coverslips or Falcon cell culture inserts placed in six well plates. The density of seeding varied and depended on the experiment being performed, although the cells were always allowed a minimum of 24h to adhere.

4.6.2 Staining of cells

Cells grown on coverslips and cells grown on inserts were exposed to the same staining protocol. Cells were washed twice in pre-warmed PBS and then fixed in 4%

(w/v) formaldehyde in PBS for 20min at room temperature. Three more PBS washes were performed before permeabilising the cells in 0.1% (v/v) Triton X-100 in PBS for 30min at room temperature. After anther three PBS washes, the cells were placed in blocking buffer [10% (v/v) horse serum, 6% (w/v) bovine serum albumin, made up in PBS] at room temperature for 1h. A further 6 PBS washes were performed before exposing the samples to the primary antibody (see Table 4.1) for 2h. The cells were then washed another 6 times in PBS after which, if the primary antibody had no fluorescent conjugate, a secondary antibody (diluted 1/200 in blocking buffer) with a fluorescent conjugate was applied to the cells at room temperature for 1h. A final 6 PBS washes completed the process. For co-localisation a second primary and secondary antibody, with a differently coloured fluorescent tag, was applied in the same manner. Once the staining process was completed, the coverslips were mounted, cell side down, in a drop of Vectorshield (Vector Laboratories, California, USA) on a clean microscope slide. The edges of the coverslip were sealed with clear nail varnish and allowed to dry.

Target	**Name**	**Type**	**Tag?**	**Working dilution**
XOR	1D9/D1	Mouse anti-human IgG	No	1/1000
Actin	Phalloidin	Fungal toxin	Yes – red (TRITC)	0.3μM
Apoptotic nuclei	TUNEL	Chemical labelling	Yes - green	As supplied protocol
Plasmalema	Annexin II	Mouse anti-human IgG	No	1/5000
Zonula Adherans	β-Catenin	Mouse anti-human IgG	No	1/500
Gap Junctions	Connexin-43	Mouse anti-human IgG	No	1/250
Focal Contacts	Paxillin	Mouse anti-human IgG	No	1/10,000
Zonula Occludens	ZO-1	Mouse anti-human IgG	No	1/250
Plasma Membrane	VLA-2α	Mouse anti-human IgG	No	1/250

Table 4.1: *Labels used in cell staining for confocal microscopy.*

4.6.3 Image collection

Sample images were collected on a Zeiss Axiovert 100M confocal microscope. Images were taken under oil for both transmitted light and with the appropriate lasers and filters for the fluorescent tag. Serial z-sections were taken of some samples, allowing the generation of 3D images. Light transmitted and fluorescent images were overlaid allowing the fluorescence localisation to be related to the cell monolayer. The fluorescent tags used generated either a green colour (FITC) or a red colour (TRITC). Where the two overlaid a yellow colour was generated. Prolonged exposure to any light source was kept to a minimum to avoid fluorescence quenching of the tag.

4.7 Electron microscopy

Electron microscopy allows high-resolution 2D imaging of cells. Depending on the fixing process and the resin used, structures such as the Golgi apparatus, endoplasmic reticulum and ribosomes can be seen. Labeling is achieved in a similar fashion to confocal microscopy, but a gold tag is used instead of fluorescence, thus avoiding the inherent problem of quenching associated with confocal microscopy.

4.7.1 Pre-embedding labelling

Cells were grown on inserts, as described in Section 4.1.6, until they reached the required density. They were initially washed twice in pre-warmed PBS and then fixed

in 4% (w/v) formaldehyde in PBS for 20min at room temperature. No permeabilisation step was performed in an attempt to visualise localization on the cell surface. Three more PBS washes were completed after which the cells were placed in blocking buffer [10% (v/v) horse serum, 6% (w/v) bovine serum albumin made up in PBS] at room temperature for 1h. A further 6 PBS washes were performed before exposing the samples to the primary antibody for 2h. The cells were then washed a further 6 times in PBS after which they were embedded in resin as described in Section 4.7.2. After embedding, the cells were labelled with a secondary antibody conjugated to a 10nm gold tag.

The secondary antibody was an anti-IgG antibody conjugated to 10nm gold particles. The antibody mix was made up at a concentration of 1/50 in blocking buffer and polyethylene glycol [10% (v/v) horse serum, 6% (w/v) bovine serum albumin made up in PBS] and the samples were incubated, section side down, on a drop of the mix for at least 2h.

The samples were then washed 6 times, each wash lasting at least 5min, in TBS as previously described. This was followed by a 5min wash in PBS, and then a 2min incubation of 2% (v/v) gluteraldehyde in PBS. Finally the grids were washed 6 times, 5min each wash, in distilled water and dried in warm air.

4.7.2 Embedding cell samples

Cells were seeded; either from monolayer culture or cryopreservation, onto Falcon cell culture inserts (suitable for electron microscopy) placed in six well plates. The density of seeding varied and depended on the experiment being performed, although the cells were always allowed a minimum of 24h to adhere.

The cells were removed from the medium and three gentle PBS washes were completed after which the cells were placed in blocking buffer [10% (v/v) horse serum, 6% (w/v) bovine serum albumin made up in PBS] at room temperature for 1h. A further 6 PBS washes were performed, at which point the samples were treated differently according to the resin in which they were to be embedded.

For epoxy resin, the samples were fixed in 2% glutaraldehyde in PBS at room temperature for 1h. They were then washed 3 times, each wash lasting 10min, in PBS. Cell ultrastructure was then further preserved by incubating the cells in 1% osmium, made up in PBS, for 30min at room temperature. This was followed by another three 10min washes in distilled water. The samples were then dehydrated by incubation in gradually increasing concentrations of acetone. Initially the samples were submerged in 50% acetone for 10min. This was then removed by aspiration and replaced by fresh 50% acetone. The process was repeated with 70, 80, 90, 95 and 100% acetone, effectively removing all water from the cell samples. Cells were then submerged in a 1:3 (v/v) epoxy resin and acetone mix and incubated at room temperature for 30min. This was poured off and replaced with a 1:1 (v/v) epoxy resin and acetone mix and again incubated at room temperature for 30min. The resin mix was removed and

replaced with pure epoxy resin, in which the samples were allowed to stand for 1h, after which the resin was replaced with fresh resin and left to stand overnight. Complete resin infiltration of the samples was achieved by a further change of resin, which was left at room temperature for 6h. The resin was then polymerised by heating to 60°C for 24h.

Samples to be embedded in LR White resin were fixed by slam freezing in an attempt to avoid the antigenic damage done to the cells by harsher chemical fixing methods. However, a weak chemical fixing step was still required, and this was achieved by incubating the cells in 4% paraformaldehyde and 0.1% glutaraldehyde, made up in PBS, for 1h at room temperature. The samples were then given 3 x 10min washes in PBS. The cells were cryoprotected by exposing them to increasing concentrations of sucrose. First, they were immersed in 0.5M sucrose for 30min. This was removed and successively replaced by 1M sucrose for 30min, then 1.5M sucrose for 45min and finally 2M sucrose for 1h. Samples were then slam frozen in a Leica EMMM80 freeze-slamming device, force setting 1, thickness 2 and speed 1. Once frozen, the samples were transferred into methanol that had been allowed to chill in dry ice and incubated at -40°C overnight. This was followed by an overnight incubation in 0.5% uranyl acetate in methanol at -40°C to further preserve cell ultrastructure. The samples were washed 4 times, each wash lasting 2h, in 100% methanol. During the washes the temperature was raised from -40°C to -14°C, after which the samples were infiltrated with resin. Infiltration was initiated by submerging in the samples in a 1:1 (v/v) mix of methanol and LR White resin and incubated, on ice, for 1h. This was removed and replaced by a 1:2 (v/v) mix of methanol and LR White resin for a further 1h. Infiltration was achieved by incubating the samples in 100% LR White resin overnight,

during which the temperature was raised to 0°C. The resin was then polymerised at 50°C for 24h.

4.7.3 Sectioning

After the samples were embedded in resin, as described in the previous Section, they were then sectioned. The resin block was first trimmed with a razor blade under a microtome until the filters, upon which the monolayer of cells were grown, could be seen. The resin surrounding the filter was trimmed away with a razor to leave a small surface area of resin surrounding the filter. This was then sectioned on the microtome, using a glass knife, until smooth. Semi-thin sections of approximately 0.5μm were taken and floated on a water boat incorporated onto the glass knife. The semi-thin sections were then stained with epoxy tissue stain and viewed under a light microscope to check that the cells looked healthy (i.e. intact membranes, normal nuclei etc.) and, in the case of Caco-2 cells, to look for dome formation.

Once an area of interest had been established, the resin was further trimmed around the filter, using a glass knife, until the surface area was reduced as much as possible. Thin sections of 100nm were then floated into a water boat, incorporated on a diamond knife, and secured onto either nickel slot grids or gold mesh grids. Once dried, the grids were ready for staining and viewing. The grids were prepared for the section by Pioloform powder. A solution of 1% pioloform in chloroform was used to coat the grids by casting a pioloform film onto a glass slide using a 'Film Casting apparatus' and then floating the film off the slide onto the surface of water in a large dish. Grids

were then dropped matt side down onto the surface of the pioloform film and grids plus film were picked up off the water surface with a piece of Parafilm.

4.7.4 Post-embedding labelling

Once on the grids, the samples were ready for labelling via immunocytochemistry. All reagents, excepting those containing antibody, were filtered through a 0.22μm filter unit to remove impurities.

The first step in this process was to etch the resin away from the samples to achieve exposure of antigenic structure. This was accomplished by floating the grids, section side down, on a drop of 1% periodic acid for 10min at room temperature. They were then washed by floating them, section side down, in a drop of distilled water for 5min. This step was repeated 6 times. The grids were finally floated on a drop of 1% sodium metaperiodate for 10min to complete the etching process. The etching process is not necessary for samples embedded in LR White resin and was only performed on samples embedded in epoxy resin.

The samples were then washed, as previously described, by floating on a drop of distilled water. Again, this step was repeated 6 times, followed by another two 5 minute washes in TBS (Tris buffered saline). After this, the samples were floated on a drop of blocking buffer [10% (v/v) horse serum, 6% (w/v) bovine serum albumin made up in PBS] for 30min at room temperature.

The primary antibody was made up in blocking buffer [10% (v/v) horse serum, 6% (w/v) bovine serum albumin made up in PBS] with concentrations of 1D9/D1 (anti-XOR antibody) varying from 1/50 to 1/1000 and the control monoclonal anti-Golgi apparatus antibody ranging from 1/25 to 1/100. The grids were taken from the blocking buffer and floated, section side down, in a drop of the primary antibody mix overnight. The samples were then washed twice, as described previously, in TBS for 10min before being returned to blocking buffer for another 10min.

The secondary antibody was an anti-IgG antibody conjugated to 10nm gold particles. The antibody mix was made up at a concentration of 1/50 in blocking buffer and polyethylene glycol [10% (v/v) horse serum, 6% (w/v) bovine serum albumin made up in PBS] and the samples were incubated, section side down, on a drop of the mix for at least 2h.

The samples were then washed 6 times, each wash lasting at least 5min, in TBS as previously described. This was followed by a 5min wash in PBS, and then a 2min incubation of 2% (v/v) glutaraldehyde in PBS. Finally the grids were washed 6 times, 5min each wash, in distilled water and dried in warm air.

4.7.5 Staining grids for viewing under a transmission electron microscope

The samples were counterstained to improve contrast when viewed under the electron microscope. Firstly the grids were washed several times in distilled water. This was then followed by a 10min incubation in filtered uranyl acetate, conducted in the dark due to the photoinstability of the chemical. The grids were washed 5 more times by

submerging them in distilled water. Counterstaining was completed by incubating the samples in filtered lead citrate for 5min. The grids were washed a further 5 times in distilled water and then dried using warm air.

4.7.6 Data collection

Images were collected on a JEOL JEM-1200EX II (JEOL, Tokyo, Japan) EM, funded by The Science & Engineering Research Council. Photographic records were taken of areas of interest along with random samples for statistical analysis.

4.8 Western blot analysis.

The anti-XOR monoclonal antibody, 1D9/D1, was utilised in Western blotting in order to localise XOR to cell compartments.

4.8.1 Nuclear preparation

Cells were grown to confluence and then detached from tissue culture flasks using the mechanical method of a cell scraper, spun down to form a pellet and resuspended in lysis buffer (1.5ml). Lysis buffer comprised 10mM Tris, 10mM NaCl, 10mM $MgCl_2$, 1% (v/v) Triton. The cells were then spun down, for 3min at 3000g in a desktop microfuge. The resulting pellet formed a crude nuclear fraction and the supernantant a crude cytosolic fraction. The pellet was resuspended in nuclease free water (1ml).

4.8.2 SDS-PAGE

A 7.5% SDS-PAGE gel was made up as described in Table 4.2. The separating gel was flattened by the addition of water-saturated butanol (20µl) and allowed to set first before the stacking gel was poured. The cell fractions were mixed 1:1 (v/v) with reducing sample buffer [distilled water (4ml), 0.5M Tris (1ml), glycerol (0.8ml), 10% (w/v) SDS (1.6ml), 2-βmercaptoethanol (0.4ml), 0.05% (w/v) bromophenol blue (0.2ml)] together with SDS high colour markers and boiled for 3min to reduce disulphide bonds. The gel was immersed in running buffer [Tris base (30g), glycine (144g), SDS (10g) made up to 1l with distilled water, pH 8.3 then diluted 1:10 with distilled water] and each sample (25µl) and markers were loaded into the wells. The gel was initially run at 100V until the dye front had passed through the stacking gel. Then the voltage was increased to 200V and the samples run through until the dye front came off the bottom of the gel. At this point the gel was ready for probing by Western blot analysis.

	Separating Gel (7.5%)	Stacking Gel (5%)
Acrylamide	2.5ml	0.67ml
Distilled water	4.85ml	2.7ml
1.5M Tris, pH 8.8	2.5ml	-
1M Tris, pH 6.8	-	0.5ml
10% Lauryl sulphate (w/v)	100µl	40µl
10% Ammonium Persulfate (w/v)	50µl	40µl
TEMED	4µl	4µl

Table 4.2: *Recipe for SDS stacking and separating gel.*

4.8.3 Western blot

4 Thick filter papers, designed for Western blot transfer, were soaked in transfer buffer [Tris (5.8g), glycine (29g), SDS (1g), methanol (200ml), made up to 1l with distilled water] and used to form the outside of a sandwich with the SDS gel and a sheet of nitrocellulose in the centre. The transfer apparatus was dampened with transfer buffer and any air bubbles removed from the stack by the application of gentle pressure. The current on the transfer apparatus was set using the following equation:

$$current\ (mA) = length\ of\ gel\ (cm) \times width\ of\ gel\ (cm) \times 0.8$$

The transfer took approximately 2h, the colour markers becoming visible on the nitrocellulose membrane when transfer was complete. The nitrocellulose was carefully removed from the stack and washed firstly in distilled water and then in TBS. Blocking was then achieved by incubation overnight, at 4°C in 2% (w/v) BSA made up in TBS. The membrane was then washed in 0.05% (v/v) Tween, made up in TBS. The primary anti-XOR monoclonal antibody was made up at a dilution of 1/200 in 1% BSA, 0.05% Tween in TBS. Enough of the antibody mix was added to submerge the membrane, which was then placed on a shaker at room temperature for 2h.

After incubation with the primary antibody, the membrane was washed 3 times in 0.05% (v/v) Tween in TBS. The secondary antibody (anti-mouse IgG peroxidase conjugate) was made up in the same manner and dilution as the primary antibody and enough was added to the membrane to submerge it. The membrane was incubated with

the secondary antibody on a shaker, at room temperature, for 1h and then washed a further three times in 0.05% (v/v) Tween in TBS.

Visualisation was achieved by the addition of 4-chloro-naphthal [one tablet dissolved in methanol (2ml) and made up to 17ml with TBS]. The blue-black colour developed after several minutes and the reaction was stopped by washing the membrane with distilled water. The membrane was then allowed to dry.

5 ACTIVITY AND LOCALISATION OF XOR IN ENDOTHELIAL CELLS

Endothelial cells are cells that line blood and lymphatic vessels. Nitric oxide is continuously produced by these cells for the purpose of vascular homeostasis, including modulation of vascular tone. Previous work has indicated a role for XOR in the reduction of inorganic and organic nitrates and nitrites (Godber *et al,* 2000a, Doel *et al,* 2000; 2001) and it was with this in mind, coupled with the observation that endothelial cells can also reduce organic nitrates to NO (Feelisch and Kelm, 1991), that it was decided to investigate the localisation and activity of XOR in endothelial cells.

Two cell lines, EA-hy-926 and ECV-304, were used as models. EA-hy-926 is a permanent endothelial cell line created by hybridisation of human umbilical vein endothelial cells (HUVEC) with a permanent cell line derived from a human lung carcinoma (A549), whereas ECV-304 spontaneously immortalised. There is some controversy over which is the better model, or if indeed either truly represents endothelial cells. However, recent work has demonstrated that, whilst ECV-304 may not be ideal, it is still an appropriate choice for the study of endothelial cells (Tan *et al,* 2001). EA-hy-926 cells, for their part, have been shown to display at least one highly differentiated function of vascular endothelium, factor VIII-related antigen, with the same morphological distribution as primary endothelial cells (Edgell *et al,* 1983). In this project, both cell lines were used in order to allow comparisons between the two and to minimise artifacts caused by using individual cell lines.

5.1 Growth curve and pterin-dependent XOR activity

EA-hy-926 cells were seeded at the same density in multiple flasks and, as described in Section 4.1, harvested at set intervals for fluorimetric assay. Assays were performed on samples from three flasks and all assays were done in duplicate. The pterin assay was performed, as described in Section 4.3, with appropriate controls.

The growth curve for pterin-dependent XOR activity versus cell number is shown in Fig 5.1. XOR activity only appears on day 11, after the cells have reached confluence. It rises to plateau values by day 13 and maintains these levels until day 17 when it rises to a further peak. At this point, cells are starting to overgrow and detach and many more non-viable cells are seen, presumably because of overcrowding, acidification of the growth media and competition for resources. The peak in XOR activity under these circumstances could imply that the enzyme has a role to play in the apoptotic pathway.

Similar data were obtained for the ECV-304 cell line (data not shown). However, the activity of these cells frequently borders on the lowest level of detection of the pterin assay and therefore can cause problems with reproducibility.

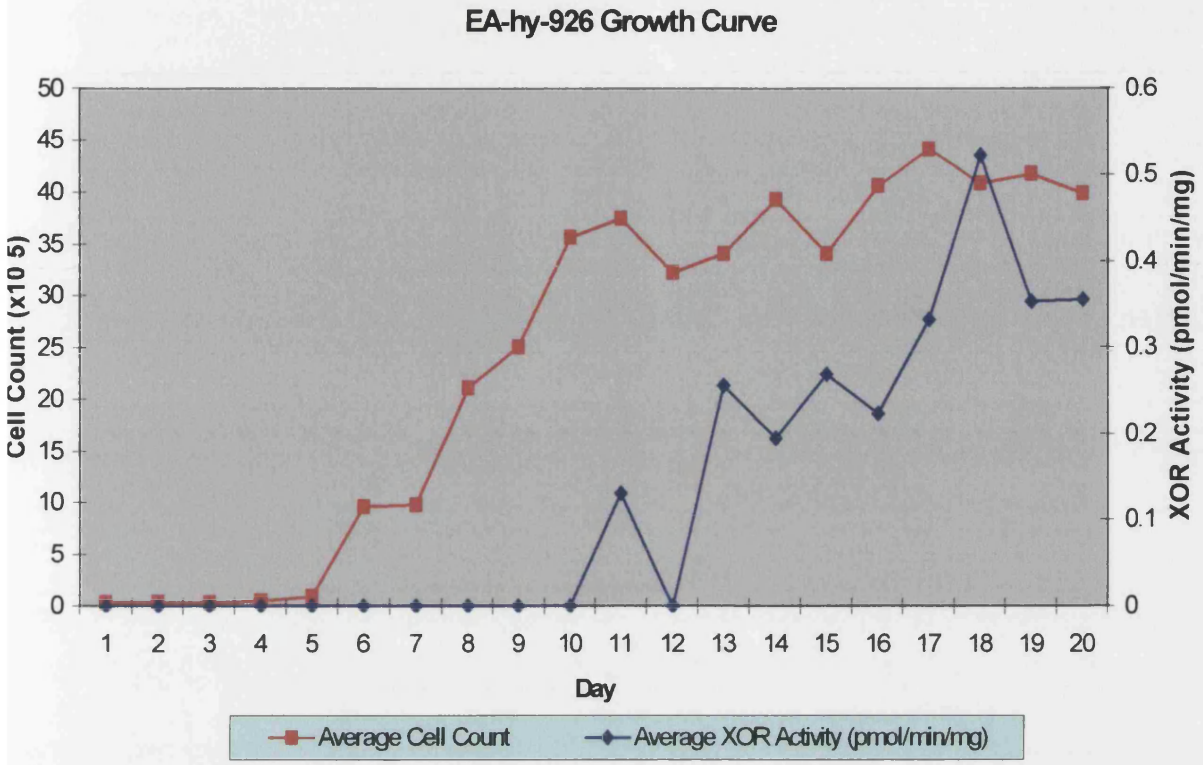

Fig 5.1: *Changes in cell count and XOR activity over a time course of 20 days*

5.2 Nitric oxide generation

Nitric oxide levels were measured as stated in Section 4.5. However, results were unpredictable and difficult to reproduce. Xanthine, hypoxanthine and NADH were all used as electron donors, along with various combinations of inorganic and organic nitrates and nitrites in attempts to optimise the assay. Fig 5.2 shows NO generation observed with EA-hy-926 cells in the presence of 100μM xanthine and 100mM sodium nitrite. The pH was maintained at 7.2, using a pH stat to avoid the acidification of nitrites and consequent production of NO. Ideally, had the results been

more predictable, an XOR inhibitor would have been added at the end of the assay, but this was made difficult by the lack of reproducibility of the data. The only evidence that XOR is the enzyme responsible for this NO production is the observation that NO was not detected in the absence of XOR substrates.

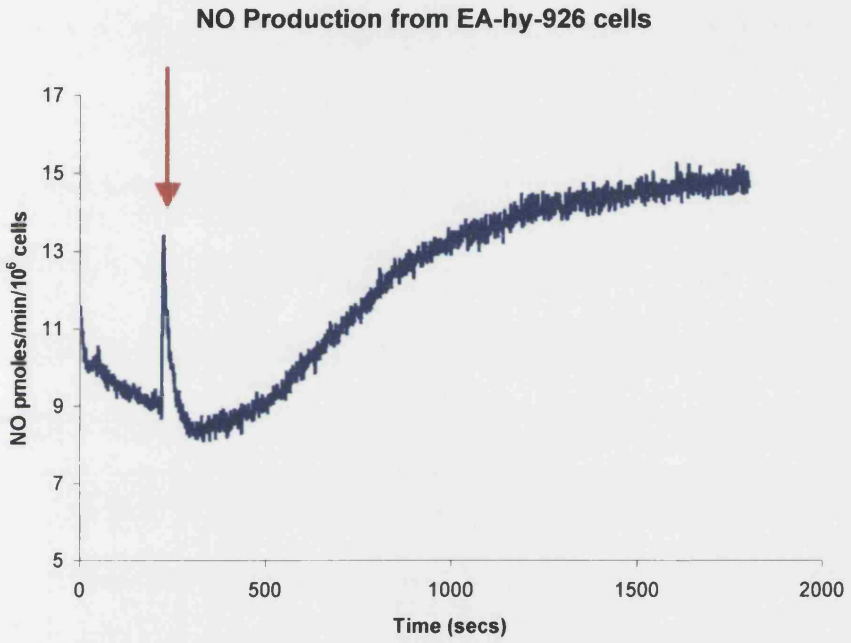

Fig 5.2: *NO production from the endothelial cell line EA-hy-926. Buffer containing 100μM xanthine and 100mM sodium nitrite was allowed to equilibrate in the reaction chamber for several minutes. The reaction was started (indicated by a red arrow) by the addition of between 10^6 and 20^6 cells that had been pelleted, washed and resuspended in reaction buffer (1ml) .*

5.3 Localisation of XOR in endothelial cells by electron microscopy

Electron microscopy was carried out as detailed in Section 4.7. All 'secondary antibody only' controls show very low levels of non-specific staining. Cells were either embedded in epoxy or LR White resin and samples were preserved either chemically or by slam freezing.

5.3.1 Cell morphology

Cells were observed at approximately 80% confluence. EA-hy-926 cells grew as a monolayer, with some cells 'piling' up and appearing cuboidal, as seen in Fig 5.3. Limited microvilli could also be seen.

No good sections of ECV-304 cells were obtained. Despite repeated attempts to optimise the protocol, the cells were sparse and showed few of the signs of 'healthy' cells, such as Golgi apparatus, mitochondria and vesicular activity. Therefore, the electron microscopy results in this Chapter are from EA-hy-926 cells only.

5.3.2 Localisation of XOR in cells embedded in LR White resin

LR White resin often gives better levels of labelling than does epoxy resin, because it can be polymerised by heat or UV light, whereas epoxy resin can only be polymerised by heat. Also, LR White sections are hydrophilic, resulting in better penetration of probes into the sample, with superior results for post-embedding immunogold labelling (Hayat, 1989). LR White resin also lends itself to fixing of the sample by slam freezing. This combination was shown to give the best results with EA-hy-926 cells, although the cell ultrastructure is less well preserved than for samples embedded in epoxy resin.

XOR labelling could be seen in defined areas of the cell and in certain organelles. Figs 5.4 and 5.5 show packets of gold, potentially indicating vesicular transport of the enzyme. The nuclear membrane is also labelled, suggesting that the enzyme is either bound to the inside of the membrane itself or attached to nuclear pores. The labelling is particularly hard to see in Fig 5.4 due to the low magnification, but it gives an indication of the distribution of the clusters of gold.

The edges of two neighbouring cells can be seen in Fig 5.6. This concentration of XOR, in the area where two cells abut, was frequently observed and is supported by the later confocal localisation.

Statistical analysis of the labelling (see Appendix) showed high levels of staining in the area where cells abut. High levels of gold were also seen clustered in small 'packets'. Very little of the labelling appeared to be solely cytosolic.

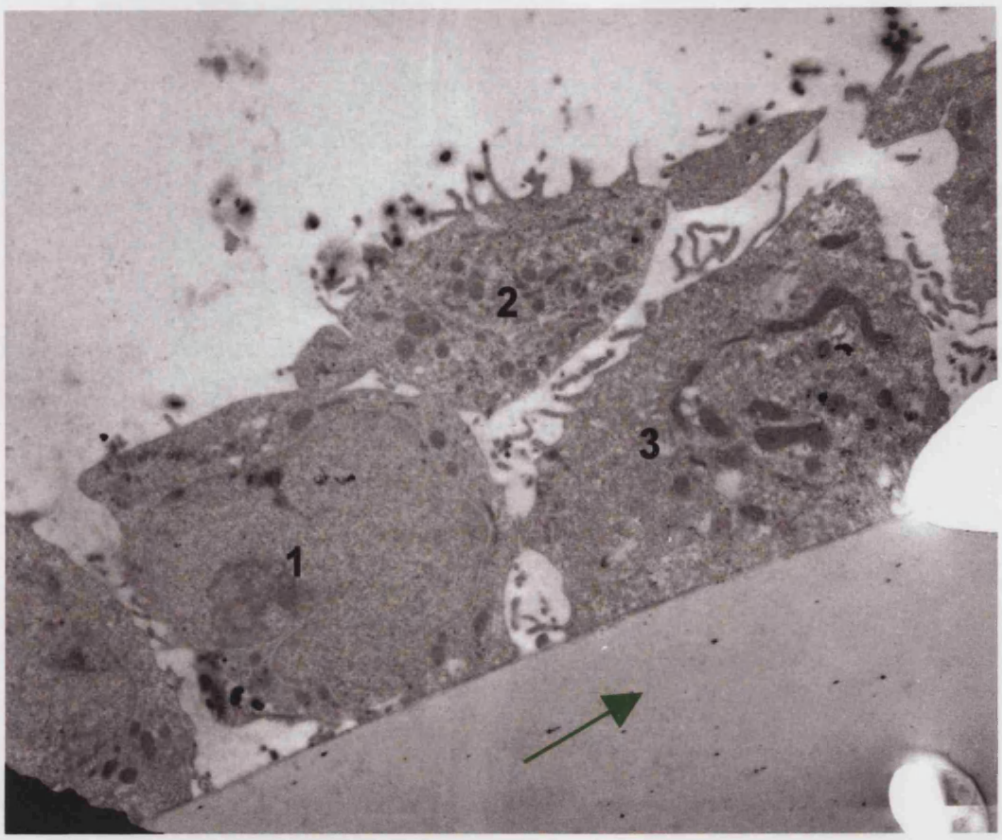

Fig 5.3: *This image shows a low magnification overview of EA-hy-926 cells. The green arrow indicates the film the cells are grown upon. Three whole cells can be seen in this image. Cells 2 and 3 display microvilli on their apical surface, unlike cell 1. The ultrastructure is poor due to the method of fixing used on samples embedded in LR White resin. No gold labelling can be seen at this magnification. (Magnification x6000).*

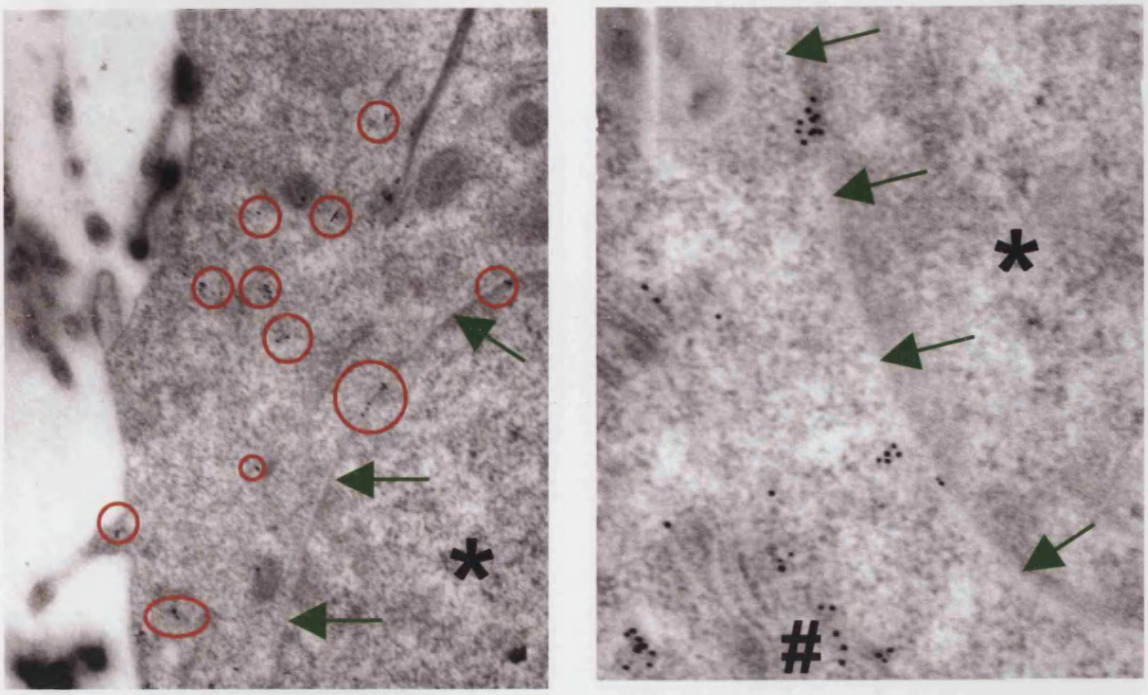

Fig 5.4 and 5.5: *Gold labelling in 'packets' and within the nuclear membrane in LR White embedded endothelial cells. The nuclear membrane is highlighted in several places in each image with green arrows and the nucleus itself indicated by a star. To make the clusters of gold in Fig 5.4 easier to identify a red circle indicates them. The gold labelling can clearly be seen in Fig 5.5 as near perfectly spherical black dots. There appears to be some localisation with a membrane, shown by a #, but the quality of the ultrastructure makes it impossible to tell what organelle, if any, this is. (Magnification x30,000 and x75,000 respectively)*

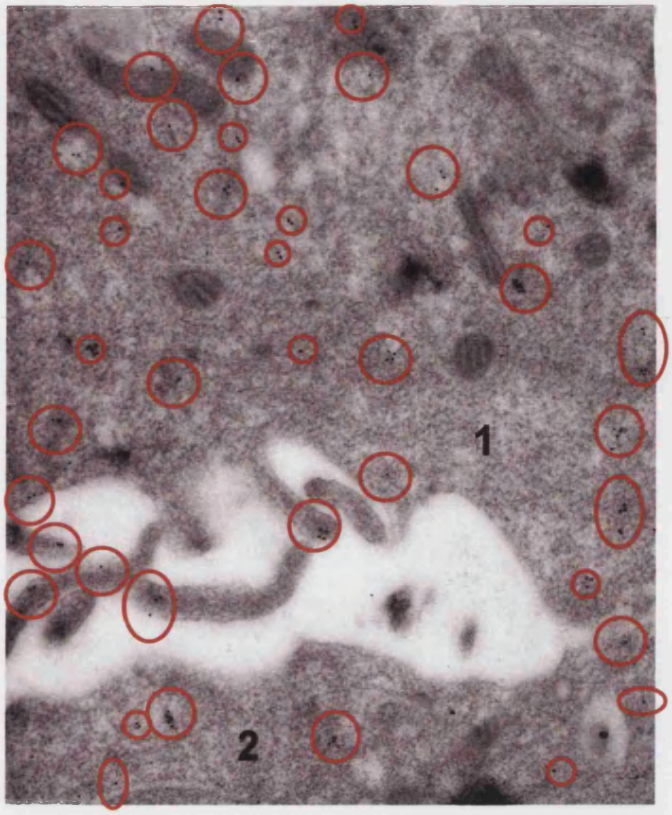

Fig 5.6: *Localisation of XOR in two neighbouring endothelial cells. The gap between the cells shows up on the image as white with a few microvilli reaching into the space. The cells are numbered 1 and 2 with the gold being highlighted by red circles. (Magnification x25,000)*

5.3.3 Localisation of XOR in cells embedded in epoxy resin

Low levels of staining were observed when compared to the levels of staining seen in LR White embedded samples. Although staining levels were low, the results were reproducible and seemed independent of the etching process used. It is not unexpected to obtain lower levels of staining in epoxy resin. However, provided that the staining correlates with that seen in LR White resin, epoxy resin can be useful in aiding localisation because of the higher quality of ultrastructure achieved. Both the lower levels of labelling and the higher quality of the ultrastructure are a reflection of the polymerisation and fixing procedures used in conjunction with epoxy resin. In all the images referred to in this Section, a purple arrow highlights the gold labelling as the low abundance of labelling makes it less easy to recognise.

Fig 5.7 clearly shows localisation of XOR to the inside of a vesicle near the apical surface of an endothelial cell. The clarity of the image leaves little room for doubt and supports the localisation in LR White resin. Furthermore, in Fig 5.8 the enzyme can be seen within the Golgi apparatus and associated vesicles. This result was particularly convincing as labelling was seen in this specific organelle on several serial sections, making the probability that it was non-specific labelling very unlikely.

The nuclear staining seen in the previous Section is further verified by the localisation seen in Fig 5.9. In this image a cluster of gold can be seen at the nuclear membrane and, once again, it would seem to be lodged in a nuclear pore. Fig 5.10 is an image of two abutting cells. Despite the low levels of labelling seen using this technique, the

Fig 5.7: *Localisation of XOR to a vesicle near the basal surface of an endothelial cell. The gold can clearly be seen as black spheres in close proximity to the vesicular membrane. (Magnification x75,000)*

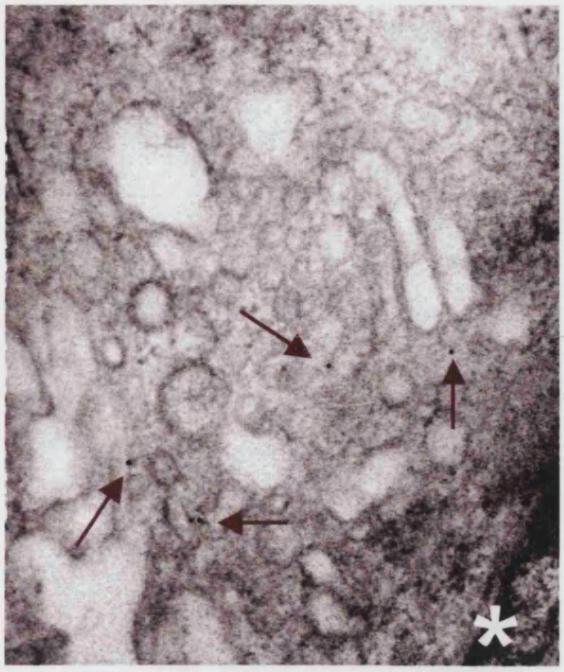

Fig 5.8: *Labelling for XOR within the Golgi apparatus and associated vesicles of an endothelial cell. The bulbous Golgi cisterne are seen close to the nucleus, just visible in the bottom right and denoted by a star. (Magnification x40,000)*

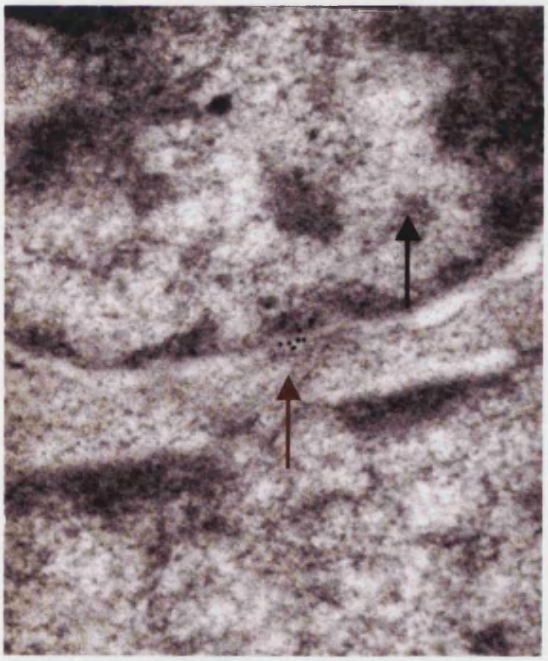

Fig 5.9: *XOR is shown to be localised to the nuclear membrane. A black arrow indicates the nucleus. (Magnification x75,000)*

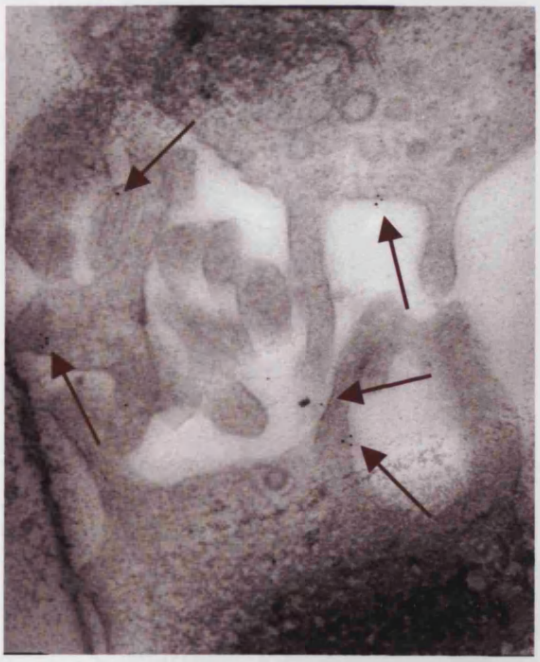

Fig 5.10: *Localisation of XOR in the periphery of neighbouring cells. The area between the cells shows as white with microvilli intruding from each cell. (Magnification x40,000)*

labelling was noticeably higher in these areas, once again supporting observations from the previous Section.

The results from cell samples embedded in epoxy resin supported all those obtained for samples embedded in LR White resin. This is a strong indication that the labelling is specific and not an artefact of experimental protocol.

5.3.4 Controls

Two staining controls were used (see Appendix for results). For each batch of staining a 'secondary only' control was performed, where secondary antibody (10nm gold conjugate) was added, but no primary antibody was used. This demonstrated no non-specific binding of the secondary antibody. In all samples this was negligible.

A monoclonal IgG antibody to the peripheral Golgi membrane 58kD protein was used as another control. While this monoclonal could clearly be seen to label the Golgi apparatus, its staining pattern differed completely from those of 1D9/D1. This demonstrated that the staining seen by the 1D9/D1 monoclonal IgG antibody was specific and not non-specific binding of binding of this isotype of antibody.

5.4 Localisation by confocal microscopy

Staining was carried out as described in Section 4.6. The results were consistent and reproducible, with all negative controls showing very little non-specific staining (see Appendix). It was found that fixing with paraformaldehyde caused a degree of permeabilisation. Therefore all data shown are from permeabilised cells.

5.4.1 Localisation of XOR in primary and permanent endothelial cells

Staining in permanent and primary endothelial cells showed a consistent pattern. Fig 5.11 shows the punctate staining seen routinely in the cells before they reach confluence (shown in the permanent cell line ECV-304). The staining was broadly cytosolic with some concentration seen where cells abut. A similar pattern was seen in human umbilical vein endothelial cells (HUVECs), as shown in Fig 5.12, although the staining is less punctate and does not extend to the very edge of the cells.

Figs 5.13 and 5.14 demonstrate an alternative localisation pattern occasionally seen in sub-confluent cells. Here, much larger punctate staining was seen which seems to be associated with a putative vesicle or membrane-bound body, which can be observed in the light-transmitted image (some of these structures can be seen unlabelled in the overlay, Fig 5.13). This pattern of staining was seen less frequently to that mentioned previously and its occurrence appeared to be random. Attempts to find the conditions required to promote this phenomenon were unsuccessful (cells were grown in the

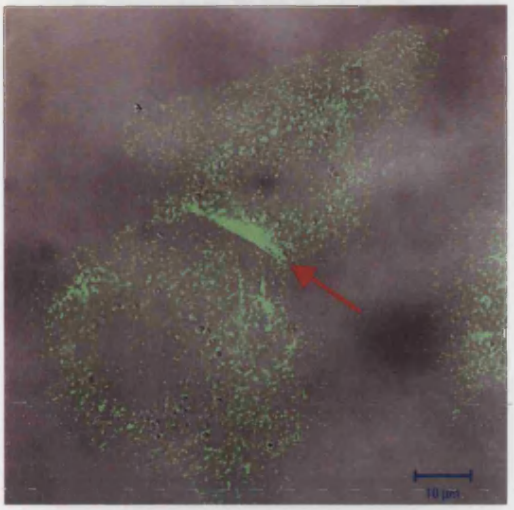

Fig 5.11: *Localisation of XOR in two ECV-304 cells. The boundary between the cells is shown by a red arrow and punctate staining extends to the periphery of the cells.*

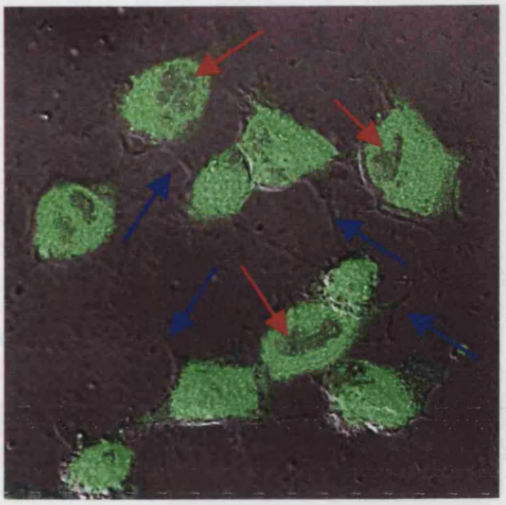

Fig 5.12: *Localisation of XOR in HUVECs. The nuclei appear free of fluorescence (red arrows) with the concentration of staining being perinuclear. Unstained cell process' are shown by a blue arrow.*

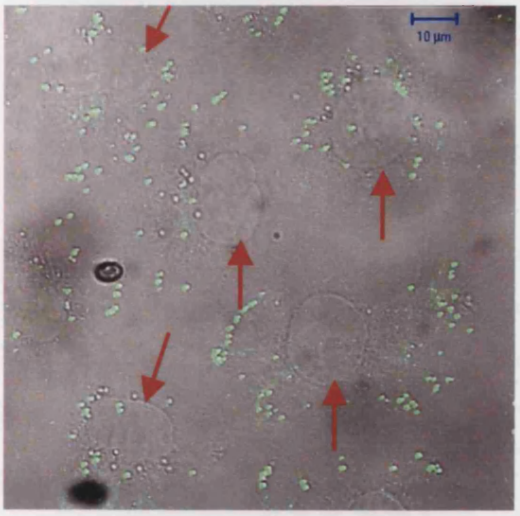

Fig 5.13: *Localisation of XOR in ECV-304 cells. Nuclei are indicated by red arrows and the cytosol can be seen as faint 'dimpling' around the nucleus.*

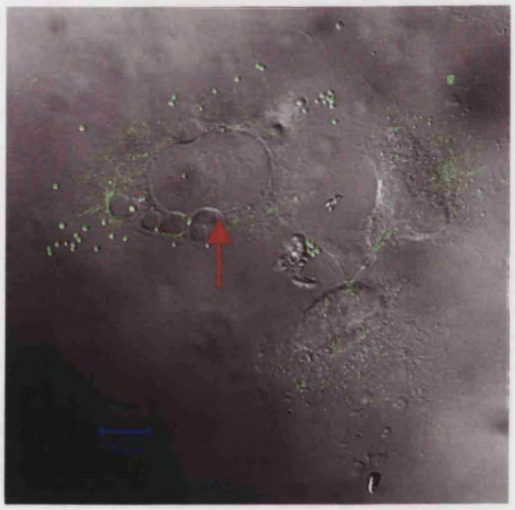

Fig 5.14: *Localisation of XOR in ECV-304 cells. One cell in this image shows the larger punctate staining. Again the nucleus is indicated by a red arrow.*

presence of XOR inhibitors, calcium ionophores, molybdenum trioxide as well as being incubated at 4°C before staining).

Confluent and post-confluent cells show less punctate staining. Nuclear staining was seen on many occasions, as shown in Fig 5.15. When present, the staining in the nucleus was more intense than any cytosolic staining seen in the same sample. Nucleosomes were always visible as unstained portions of the nucleus. Nuclear staining as also seen in sub-confluent cells, but seldom with te intensity and frequency of that seen in confluent and post-confluent cells. To eliminate the possibility of non-specific staining in the nucleus, a nuclear preparation of post confluent cells was subjected to Western blot analysis (as described in Section 5.8). This confirmed the presence of XOR in the nucleus (results not shown because of difficulties encountered scanning the blots).

5.4.2 Localisation of XOR in barrier-positive and barrier-negative endothelial cells

ECV-304 cells grown on cell culture inserts were provided, ready fixed, by Dr Roger Hurst from the University of the West of England, Bristol. The endothelial cells were grown in co-culture with a monolayer of glial cells. Endothelial cells grown in this manner form tight junctional complexes, and develop a permeability barrier having a high transcellular electrical resistance (Hurst and Fritz, 1996). Both barrier-positive (grown in co-culture with glial cells) and barrier-negative (grown in the absence of glial cells) samples were provided. Localisation of XOR was carried out as described in Section 4.6.

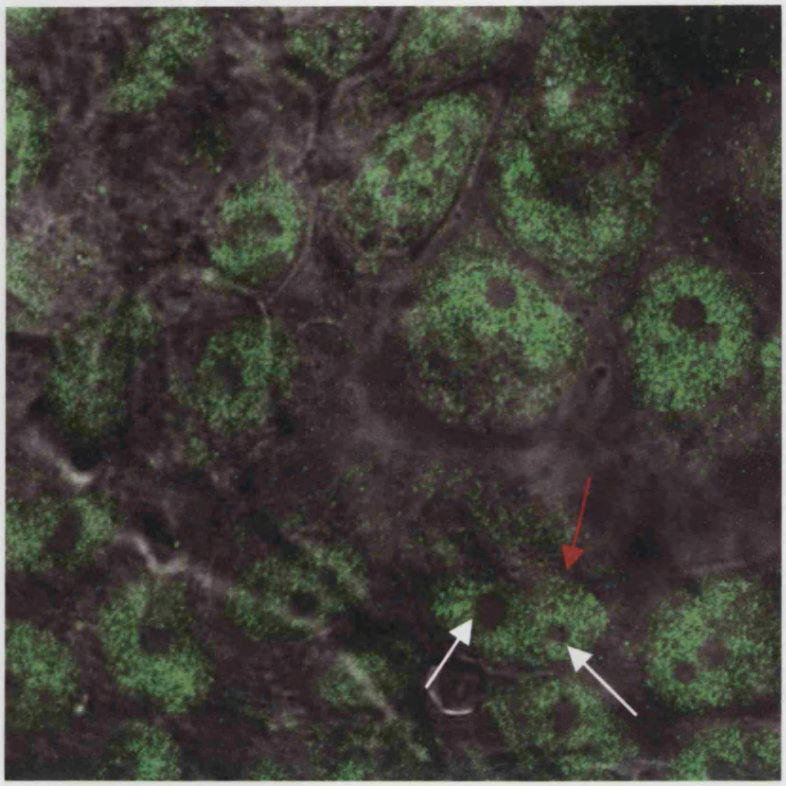

Fig 5.15: *Localisation of XOR in post confluent EA-hy-926 cells. Intense staining can be seen in the nucleus, an example of which is indicated by a red arrow. The nucleosomes are devoid of fluorescence and are indicated in the example by white arrows. The quality of the transmitted light image makes it difficult to identify the edges of the cells.*

Figs 5.16 and 5.17 show the localisation seen in barrier-positive samples. Again, intense nuclear staining was seen with an absence of staining in the nucleosomes. This was accompanied by punctate cytosolic staining that was much less intense. This pattern of staining is similar to that shown previously in post-confluent endothelial cells (see Fig 5.15).

A similar pattern of staining was seen in barrier-negative cells, except that the staining was weaker and the nucleosomes were less pronounced, (Figs 5.18, 5.19).

5.4.3 Localisation of XOR in apoptotic endothelial cells

Previous work (Holt 2000) had shown intense XOR staining in apoptotic cells. The staining appeared to co-localise with TUNEL staining (Holt 2000). This work was reinvestigated and the cells were driven into apoptosis as described in Section 4.1.9. Fig 5.20 shows XOR localisation (red) in EA-hy-926 cells driven into apoptosis by sodium butyrate. The cells were also stained with TUNEL (green). It can be seen that, whilst XOR is present in these cells, it does not seem to exhibit a different staining pattern to that observed in normal confluent cells, except that there appears to be less staining for XOR. There was some concern that the TUNEL labelling may have interfered with the detection of XOR, as cells treated in the same manner but not subjected to TUNEL labelling, showed comparable levels of XOR to those seen previously (see Section 5.4.1). There is no co-localisation between XOR and TUNEL.

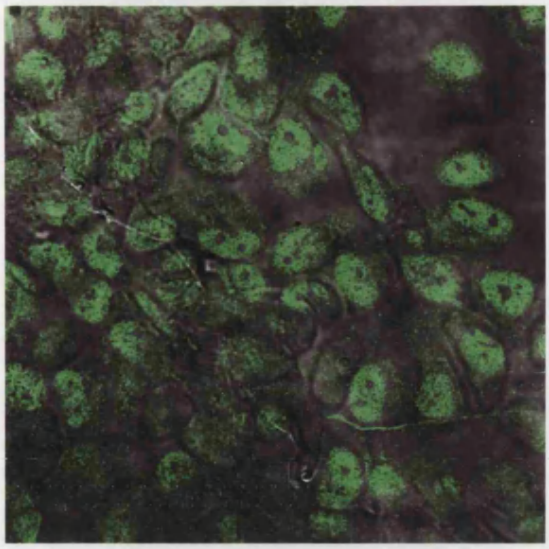

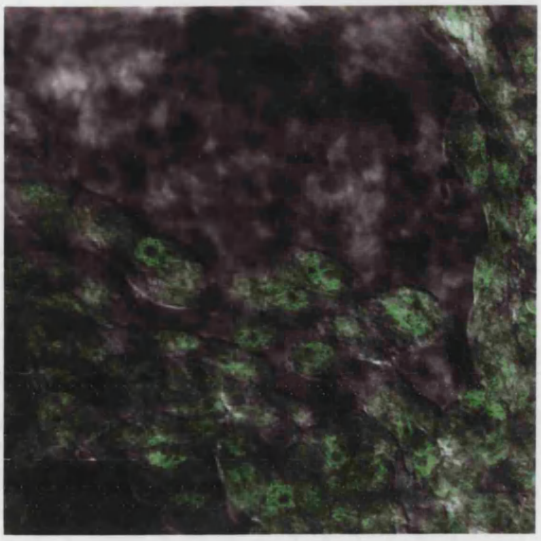

Fig 5.16 and 5.17: *Localisation of XOR in barrier-positive ECV-304 cells. Nuclei show up as areas of more intense staining with the nucleosomes devoid of staining.*

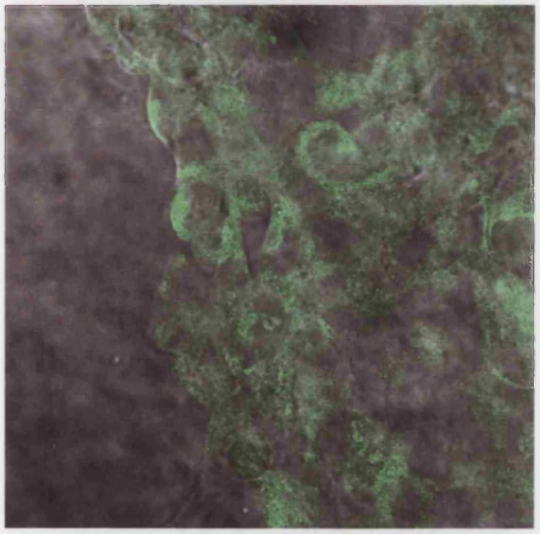

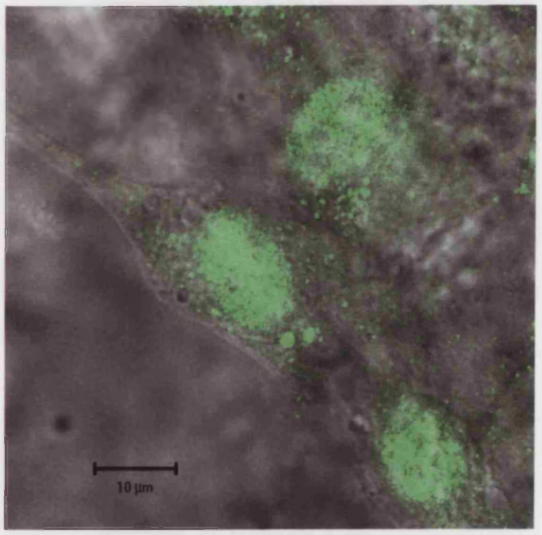

Fig 5.18 and 5.19: *Localisation of XOR in barrier-negative ECV-304 cells. Individual cells are more difficult to identify, as less nuclear staining is present. In Fig 5.19 slightly more nuclear staining is seen and the greater magnification allows three individual cells to be identified.*

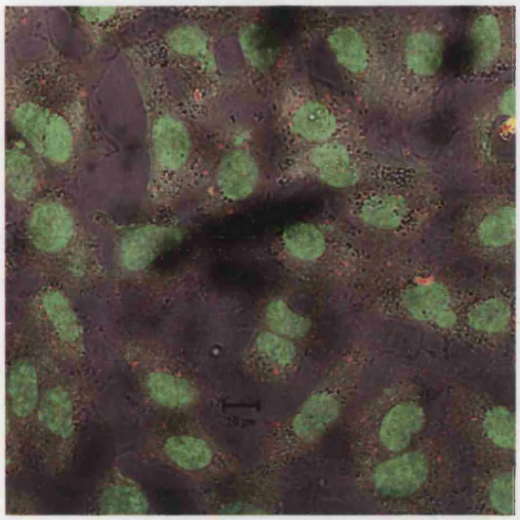

Fig 5.20: *Localisation of XOR (red) and TUNEL (green) in apoptotic EA-hy-926 cells. The TUNEL stain makes the nuclei of apoptotic cells appear bright green.*

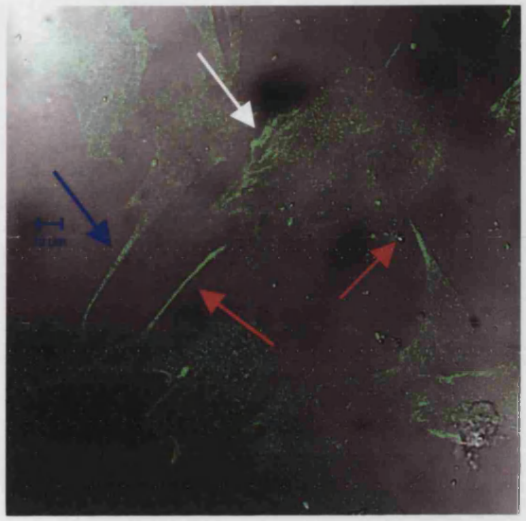

Fig 5.21: *Localisation of XOR in CPA cells. Two endothelial cell processes are shown by red arrows and a smooth muscle cell by a white arrow. The blue arrow indicates an endothelial cell process approaching another endothelial cell.*

5.4.4 Localisation of XOR in CPA co-culture

CPA cells are a co-culture of bovine aortic endothelial and smooth muscle cells. XOR was localised as described in Section 4.6. XOR can be seen in the processes of endothelial cells (highlighted in Fig 5.21 by red arrows) directed towards smooth muscle cells (highlighted in Fig 5.21 by a white arrow).

5.4.5 Localisation of XOR and actin

ECV-304 and EA-hy-926 cells were probed with a monoclonal antibody against XOR, as described in Section 4.62. They were then stained with phalloidin toxin, which binds to actin, as described in Section 4.63.

ECV-304 cells are shown in Figs 5.22 and 5.23. EA-hy-926 cells are shown in Figs 5.24 - 5.26. In both cell lines, the staining is very similar. Once again, clear punctate staining can be seen. This appears to be particularly concentrated in the nuclear and/or perinuclear region. Actin filaments can be clearly seen but no co-localisation between actin and XOR is evident.

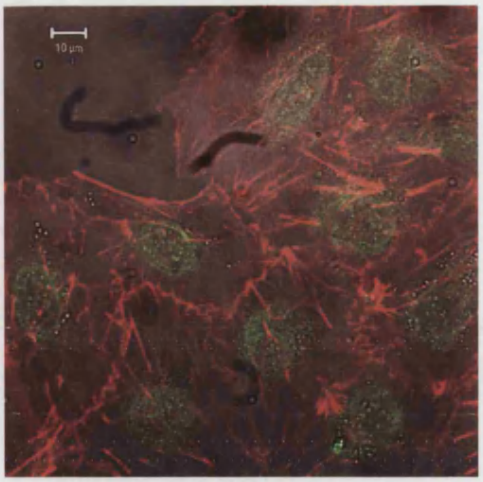

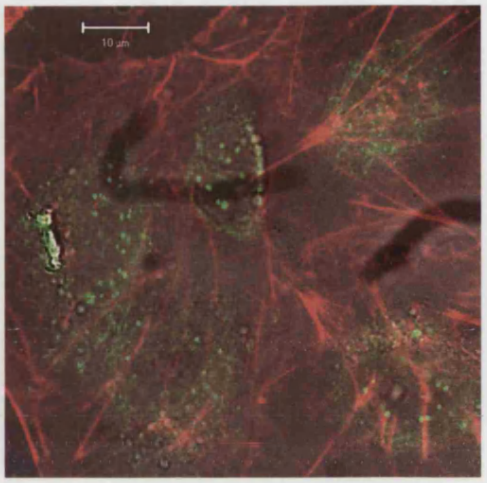

Fig 5.22 and 5.23: *Co-localisation of XOR (green) and actin (red) in ECV-304 cells.*

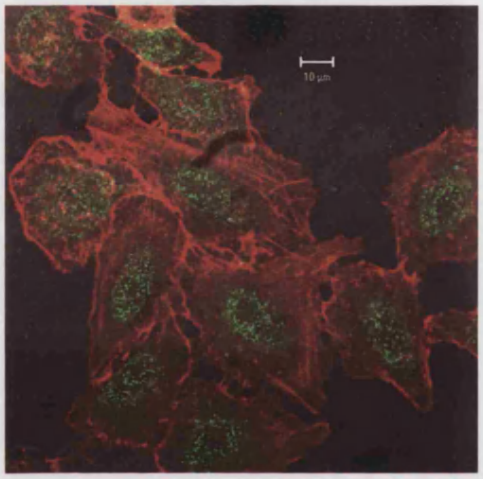

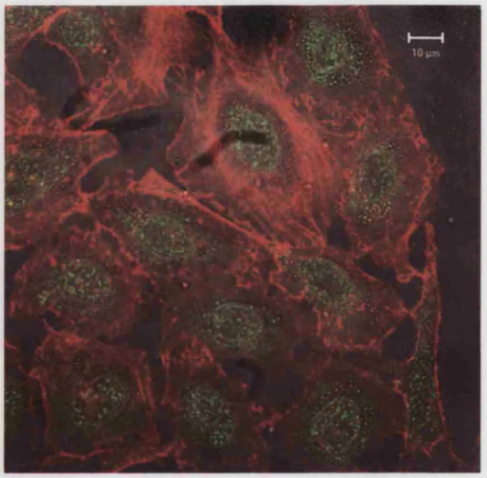

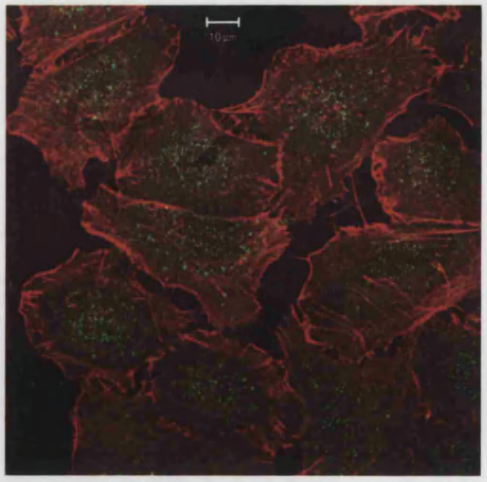

Fig 5.24, 5.25 and 5.26: *Co-localisation of XOR (green) and actin (red) in EA-hy-926 cells. In all the images on this page the actin can be seen as long red filaments within the cell and marking the edge of each cell. XOR staining appears as punctate nuclear and/or perinuclear staining.*

5.5 Discussion

Levels of XOR activity, detected by the pterin assay (Beckman *et al,* 1989), as described in Section 4.3, were low for the EA-hy-926 cell line and on the limit of detection for the ECV-304 cell line. However, the growth curve (Fig 5.1) shows a clear trend in activity of XOR with cell numbers. The initial plateau of activity corresponds with the cells' becoming confluent. It is possible that XOR-derived ROS facilitate cell-to-cell signalling as the monolayer is formed (Rouquette *et al,* 1998).

The second plateau of pterin-dependent XOR activity is seen as the cell numbers further increase (Fig 5.1), causing crowding, competition for resources and cell death, as judged by permeability to Trypan Blue. The ROS produced by XOR may have another role to play at this stage, in the apoptotic pathway (Hancock *et al,* 2001).

NO production from EA-hy-926 and ECV-304 cells was measured as described in Section 4.5. It is well documented that NO can be produced from the acidification of nitrites, as shown in the equations below (Weitzberg and Lundberg, 1998). As cells constantly produce acid in anoxic conditions, it was important to maintain constant pH levels within the reaction. This was achieved by the use of a pH stat.

$$NO_2^- + H^+ \rightleftharpoons HNO_2$$

$$2HNO_2 \rightleftharpoons N_2O_3 + H_2O$$

$$N_2O_3 \rightleftharpoons NO + NO_2$$

$$2NO + O_2 \longrightarrow 2NO_2$$

NO production could be demonstrated, but not consistently. While Fig 5.2 represents one positive result, several runs were negative or inconclusive. The only evidence that XOR was responsible for the production of NO was the observation that apparent NO production was dependent on XOR substrates. Use of XOR inhibitors was complicated by pH effects, in that all those available need to be dissolved in NaOH. The pH stat can only compensate in one direction and was unable to deal with the addition of NaOH as it was programmed to compensate for the production of acid by the cells. The anoxic state of the reaction vessel should rule out the production of NO by NOS, as NOS requires oxygen as a substrate.

The lack of reproducibility of the data probably reflects the complications of running an assay with a whole cell system. The physiological state of the cells could be altered by something as simple as mechanical shock, e.g. knocking the flask in which they were growing. Also the amount of free radical scavengers within the cells was an unknown commodity.

It is likely that one of the reasons that XOR-derived NO was so difficult to detect was the intrinsically low level of XOR activity within these cells (Fig 5.1). Currently, the only way to circumvent this problem would be to use a cell line that had been

engineered to express more active XOR. This is, however, not only difficult and time consuming, but introduces further uncertainties regarding the relevance of observed data to normal cells.

The localisation of XOR via electron microscopy showed a consistent pattern of labelling, despite wide variation in experimental protocols. Such changes included varying the preservation of the cells (both chemical preservation and cryopreservation were used), varying the resin and conditions for its polymerisation, and using different concentrations of both primary and secondary antibodies. However, the levels of labelling remained relatively low. This could reflect the use of a monoclonal antibody, which, unlike polyclonal antibodies, recognises a single epitope. Fewer relevant sites are accordingly available and the signal is correspondingly weaker (Lin *et al,* 1983).

Higher levels of gold labelling were observed in cells embedded in LR White samples rather than in epoxy resin. This is a common phenomenon and is a result of the fixing and polymerisation methods that are used in the different resins. The two resins are often used in conjunction as, whereas LR White resin gives higher levels of labelling, it is at the cost of poorly preserved ultrastructure. In epoxy resin, the membrane components of the cells show far better preservation.

The labelling seen via electron microscopy gave some evidence of vesicular transport of the enzyme. XOR appeared to be localised in discrete 'circles' at high magnification and in 'packets' or 'bundles' at lower magnification. This was confirmed by samples embedded in epoxy resin, where the higher quality of ultrastructure allowed the visualisation of labelling within a vesicle. By means of the

same protocol the enzyme was localised to the Golgi apparatus and associated vesicles. XOR also showed consistent localisation with either the nuclear membrane or the nuclear pore, suggesting a cell signalling function.

Statistical analysis (see Appendix) of the labelling showed high levels of XOR in the areas where neighbouring cells abut. This phenomenon has been observed previously (Rouquette *et al,* 1998) and supports an intercellular signalling role for the enzyme. A high association with small 'packets', shown by epoxy resin-embedded samples to resemble vesicles, was also statistically shown.

In confocal microscopy, XOR showed discrete punctate staining (see Fig 5.11). On several occasions, particularly large vesicle-like structures could be seen on the light-transmitted image that co-localised with the fluorescent labelling for XOR (see Figs 5.13, 5.14). This pattern of labelling was observed in both ECV-304 and EA-hy-926 cells. Attempts were made to define the conditions needed to produce this localisation, but despite the use of ionophores, molybdenum trioxide, XOR inhibitors and additional FBS in the media, the cause of the production these large vesicular structures could not be ascertained and the pattern of localisation could not be reproduced systematically.

It is possible that, under certain conditions, XOR localises to endosomes and previous work, using Lucifer Yellow as a fluid phase marker (Holt, 2000) did indeed show a degree of co-localisation. Nevertheless, not all the structures labelled for XOR appeared to be endosomes. ELISA of the media showed that it contained low levels of XOR (<0.6ng/ml) (Igor Bondarenko, personnel communication), and it is possible

that the cells were endocytosing small quantities of the enzyme. However, this is unlikely to account for all the labelling. In an attempt to clarify this issue, labelling of live cells was attempted. It was hoped that incubation at 37°C or 4°C would show differential labelling, reflecting endocytosis or none, respectively. However, no labelling was observed at either temperature (data not shown), most probably because the monoclonal antibody epitope was not accessible in un-fixed cells. One hypothesis for the labelling of these large vesicular like structures is that they act as a storage facility for XOR and, when the cells are subjected to a certain stimulus, the XOR is released and the more reproducible, smaller punctate staining is seen.

The smaller punctate staining pattern was far more consistent. It was seen in all samples and all endothelial cells examined, including primary HUVEC's (see Figs 5.11 - 5.14). That this represented vesicular localisation was supported by electron microscopy. The intensity of the staining is higher where cells meet, suggested transport to the cell surface or even to the junction between neighbouring cells. Previous work has shown XOR to be localised on the outer surface of endothelial cells (Rouquette *et al,* 1998) but attempts to demonstrate this were unsuccessful, largely because of the fact that the fixing process also permeabilised the cells. The concentration of paraformaldehyde was lowered, as was the temperature at which the cells were fixed, but still antibody was able to gain access to the cytosol.

A high level of labelling for XOR was observed in the nuclei of post-confluent cells (Fig 5.15). Whilst nuclear labelling was evident in sub-confluent cells, it was seldom as intense as that seen in post-confluent cells. Nuclear staining could be distinguished from intense perinuclear staining by the presence of obvious nucleosomes and by the

microscopes' ability to image the cell in 3D. When a cell nucleus is stained it appears as the yolk in an egg when thin slices are taken. In the upper sections the staining is not visible, but as the focal plane moves down, the nucleus begins to appear. Cells displaying this staining were at the same density as those at the end of the growth curve (Fig 5.1, days 17-20). It is possible that the nuclear staining reflects induction of the apoptotic pathway, initiated as the cells become crowded and competition for resources increases. This was further explored by driving the cells into apoptosis by addition of sodium butyrate, and then measuring XOR activity via the pterin assay. However, levels of XOR activity within these cells are on the lower limit of detection of the pterin assay and the results proved inconclusive.

Barrier-positive is the shorthand for endothelial cells grown in co-culture with glial cells; barrier-negative cells have not been grown in co-culture. This method of inducing endothelial cells to form tight junction complexes and develop permeability barriers was designed as a model for investigating the blood-brain barrier (BBB) (Hurst and Fritz, 1996). It has previously been shown that the BBB model is sensitive to oxidative stress (Hurst *et al,* 1998) and, given the ability of XOR to produce ROS (Sussman and Bulkley, 1990), it seemed appropriate to investigate the localisation of XOR in these endothelial cells. The only recognisable difference between barrier-positive and barrier-negative cells was a less intense nuclear staining in the latter. It is unclear if this difference is caused by the presence of a permeability barrier in the cells grown in co-culture with glial cells, or if it is merely a reflection of how confluent the cells were. It proved difficult to determine the precise cell density before labelling as the matrix upon which the cells were grown made identification of single

cells difficult. Whilst individual cells that had been labelled can be seen, it is difficult to judge if any cells have been dislodged by the fixing and staining process.

In order to investigate further the possibility that XOR is involved in the apoptotic pathway, apoptotic cells were stained for both XOR and TUNEL. TUNEL staining labels fragmented DNA and is an early marker of apoptosis. Cells driven into apoptosis by sodium butyrate did not demonstrate elevated levels of labelling for XOR, nor did the labelling co-localise with TUNEL (see Fig 5.20), once again providing no conclusive evidence as to the enzymes involvement in the apoptotic pathway.

As mentioned previously, a potential function of XOR in endothelial cells would be to facilitate vasodilation by the production of NO. NO works as a paracrine messenger that is released from endothelial cells and acts on smooth muscle cells (Moncada *et al,* 1991). With this in mind, the localisation of XOR was studied, by means of confocal microscopy, in CPA cells. CPA cells are commercially available from the European Collection of Cell Cultures (ECACC) and comprise a mixture of bovine aortic endothelial and smooth muscle cells. The smooth muscle cells appear as large and striated (see Fig 5.21, white arrow), whereas the endothelial cells are small and triangular. The red arrows in Fig 5.21 indicate processes reaching out from the endothelial cells towards a smooth muscle cell. These processes show relatively high levels of XOR labelling, along with the usual punctate staining that can be seen in both cell types. Thus XOR does appear to be localised in specific areas of endothelial cells directed towards smooth muscles cells, as expected for an enzyme producing a paracrine messenger. The blue arrow indicates a process from one endothelial cell

approaching another endothelial cell. This suggests that the enzyme is signalling not just to the smooth muscle cells, but also to cells of its own kind.

XOR localisation was performed in conjunction with actin labelling in both ECV-304 and EA-hy-926 cells. The question was asked as to whether the punctate labelling for XOR would be seen to co-localise with actin, consistent with vesicular movement of the enzyme along the cytoskeleton. However, whereas punctate staining can be seen in all the samples (see Figs 5.22 - 5.26), no co-localisation with actin can be seen. The majority of the XOR labelling appears to be in the nuclear and/or perinuclear region. This does not rule out vesicular transport of the enzyme to the cell periphery, but it does eliminate cytoskeletal-facilitated vesicular transport.

6 ACTIVITY AND LOCALISATION OF XOR IN MAMMARY EPITHELIAL CELLS

There is increasing evidence for a physiological role for XOR in human breast milk. XOR is a major protein component of the milk fat globule membrane (Patton and Keenan, 1975) and the enzyme appears to have an increased specific activity for approximately 3 weeks *post partum* (Brown *et al,* 1995). In this Chapter the localisation and activity of XOR in mammary epithelial cells was investigated in order to clarify the enzyme's function within these cells.

6.1 Growth curve and pterin-dependent XOR activity

HB4a cells are a conditionally-immortalised (SV40) human mammary epithelial cell line, showing low levels of XOR activity. Cells were seeded at the same density in multiple flasks and, as described in Section 4.1, harvested at set intervals for the fluorimetric pterin assay. The cell number and pterin-dependent XOR activity were monitored from cells seeded at low density up until post-confluence, where the cell culture became unviable. Assays were performed on samples from three flasks and all assays were done in duplicate. The pterin assay was performed as described in Section 4.3.

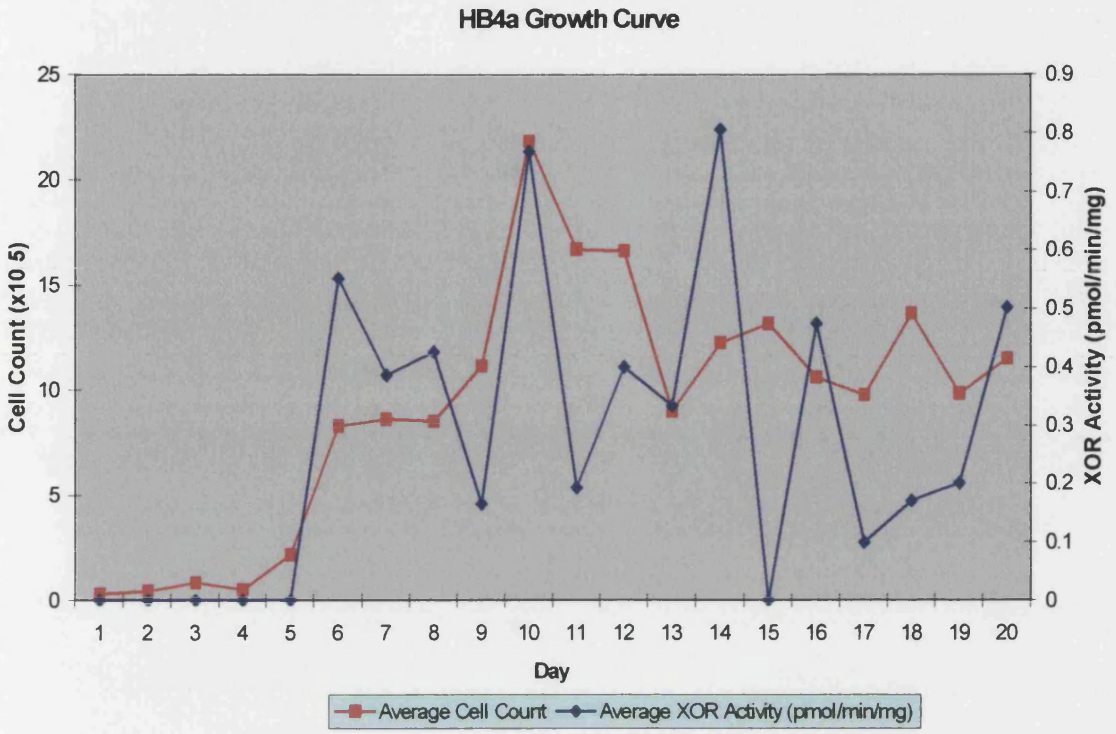

Fig 6.1: *Changes in cell count and XOR activity over a time course of 20 days*

A peak in XOR activity can be seen shortly after the cells reach confluence on day 10. However, the activity of the cells seemed dependent on the addition of fresh medium. Activity clearly falls when the medium is exhausted and in need of changing (every odd numbered day). Overall, the assays were not very satisfactory in that the low levels of activity were at the limit of detection of the pterin assay. Attempts to improve matters by increasing the sample size resulted in increased light scattering and noise, making calibration difficult.

6.2 Nitric oxide activity

NO assays were carried out as stated in Section 4.5. Despite numerous attempts under different conditions, no NO was detected from this cell line. HB4a cells show very low levels of XOR activity and it is possible that this, along with the inherent problems of using a whole cell system, resulted in the failure to detect NO production. The cells were still viable at the end of the 30 min assays, as ascertained by the Trypan Blue exclusion test. When the cells were transferred back into a flask at the end of the assay they continued to multiply and display normal cell morphology, indicating that the inability to detect activity was not a result of cell death during the assay.

6.3 Localisation of XOR by electron microscopy

Electron microscopy was carried out as detailed in Section 4.7. Using samples embedded in both LR White and epoxy resin. As noted in Chapter 5, the procedures used for fixing and embedding cells in LR White resin and epoxy resin result in higher labelling levels in the former and superior preservation of the cell ultrastructure in the latter.

6.3.1 Cell morphology

Hb4a cells were observed at approximately 80% confluence. They grew as a monolayer and appeared elongated and cuboidal with a small number of microvilli on the surface, as seen in Figs 6.2 and 6.3.

6.3.2 Localisation of XOR in cells embedded in LR White resin

The images referred to in this Section were all fixed by freeze slamming.

Whereas the procedures used resulted in poorer visible ultrastructure than that observed in epoxy resin embedded samples, labelling for XOR could nevertheless be pinpointed to areas within the cells. Clear 'packets' of gold could be seen, as demonstrated in Figs 6.4 and 6.5, and there was often higher concentration of these clusters in the apical area of the cell. The uppermost gold packet in Fig 6.5 seems to show localisation to a membrane, seen in the image as a stripe slightly lighter in colour than the main body of the cell. It is possible that this could reflect association with the Golgi apparatus or endoplasmic reticulum. Such a conclusion could not, however, be based on this image alone.

More 'packets' of gold can be seen in Fig 6.6, along with an unlabelled mitochondrion. No mitochondrial staining was observed in any of the cells studied, ruling out any possible function for XOR within this organelle.

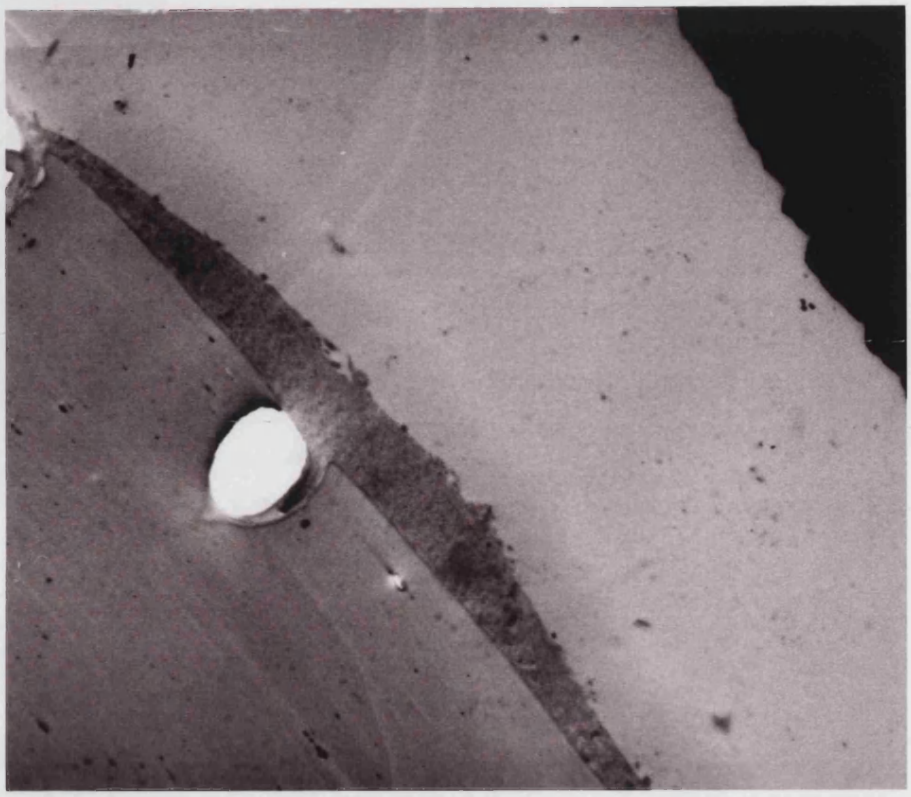

Fig 6.2 and 6.3: *Overview of HB4a cells as seen under electron microscopy. In each image a single cell can be seen. The cells are in the correct orientation with the apical side uppermost in the image. The cells are thickest in the centre and narrow down at either end. No gold labelling or cell ultrastructure can be seen due to the low level of magnification. (Magnification x4000 and x6000 respectively)*

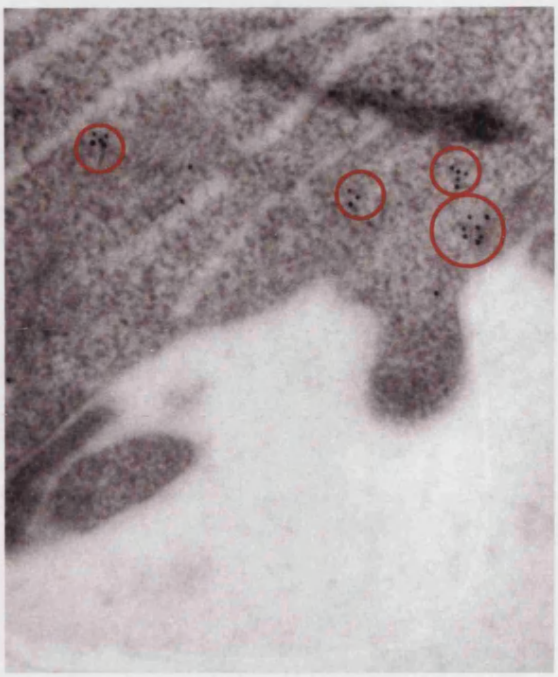

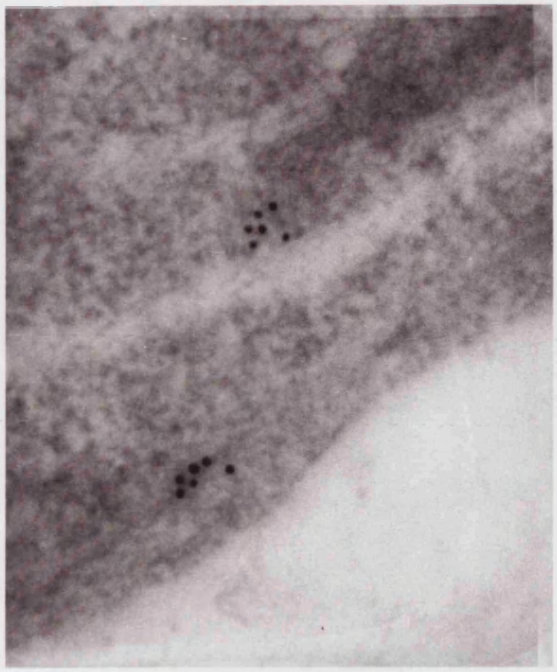

Fig 6.4 and 6.5: *Localisation of XOR in distinct 'packets' at the apical surface of the cell. In both images the cells appear 'upside down' with the apical membrane towards the bottom of the page. The gold 'packets' are highlighted in Figure 6.4 by red circles. (Magnification x20,000 and x60,000 respectively)*

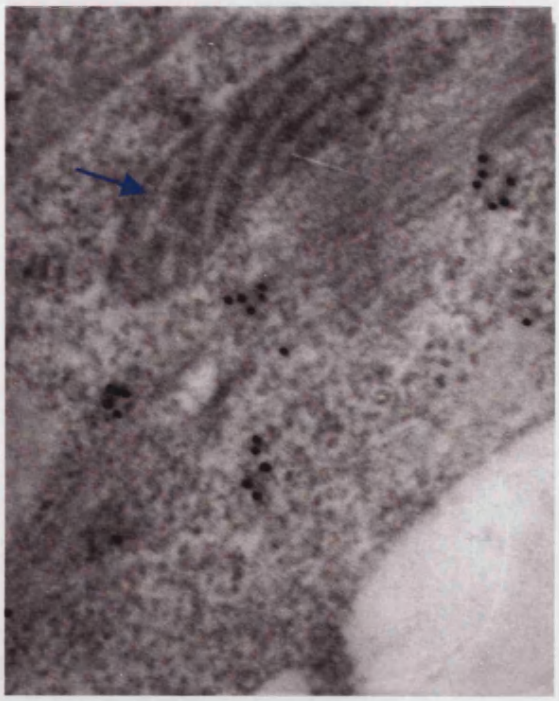

Fig 6.6: *More bundles of gold, with the occasional single particle. An unlabelled mitochondrion is indicated by a blue arrow. (Magnification x100,000)*

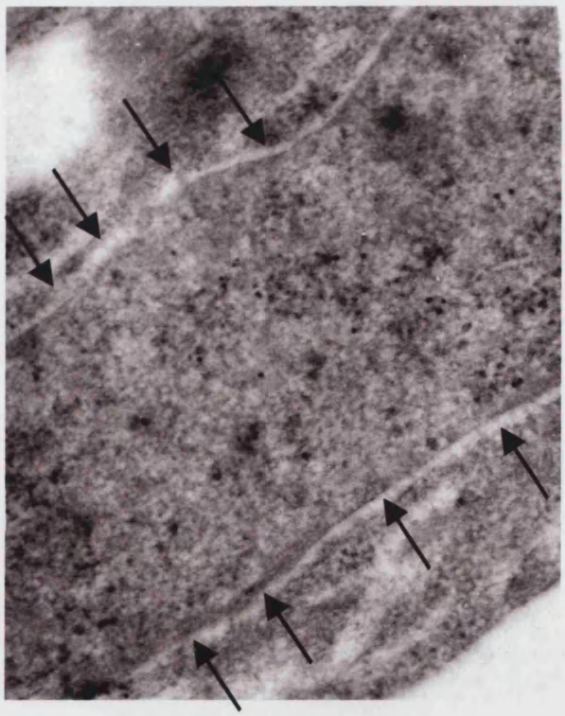

Fig 6.7: *Labelling seen within the cell nucleus. The nuclear membrane is indicated by black arrows. The nucleus appears grainy with the nuclear membrane and other cytoplasmic membranes appearing as light stripes. (Magnification x60,000)*

Fig 6.7 shows localisation of XOR to the nucleus of the cell. There appeared to be a greater concentration of nuclear gold labelling in these cells when compared to the endothelial cell lines studied, where the nuclear labelling could be more sporadic and appeared largely dependent on the cell density. The nuclear membrane can be seen as a lighter band running around the outside of the nucleus, which is grainy in appearance.

Statistical analysis of the staining (see Appendix) demonstrated high levels of labelling in the apical area of the cells, as well as high levels of gold in small 'packets' and the nucleus.

6.3.3 Localisation of XOR in cells embedded in epoxy resin

As previously stated the advantage of using epoxy resin is better preservation of cell ultrastructure than in LR White resin. Thus the use of both methods, gives a more accurate picture of localisation than the use of one method alone. In all the images referred to in this Section, a purple arrow highlights the gold labelling, as the low abundance of labelling makes it less obvious.

Fig 6.8 shows localisation of XOR to a putative vesicle. The two gold particles appeared to be almost on the outside of the vesicular membrane. However, the very nature of labelling with first a primary antibody and then a secondary gold-conjugated antibody means that the gold particle is not in directly the same place as the enzyme but rather adjacent to it (the gold particle alone has a diameter of 10nm). Therefore

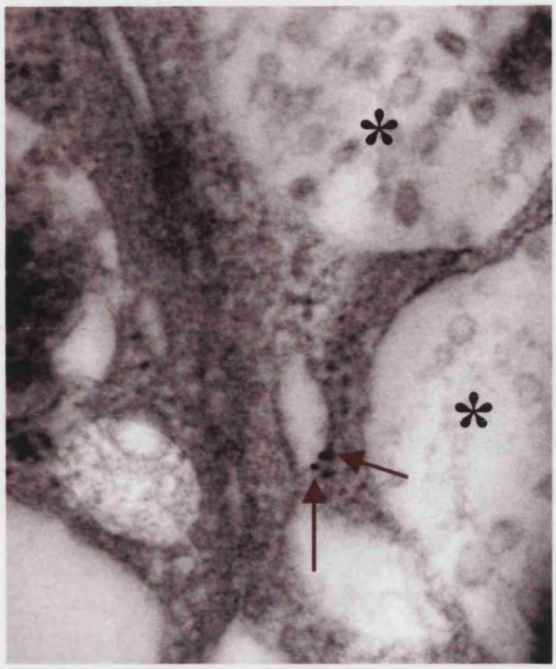

Fig 6.8: *Localisation of XOR to a putative vesicle. Two large lysosomes can be seen to the right of the labelling, indicated by a *, with another, seemingly empty vesicle in the bottom left hand corner of the image. (Magnification x100,000)*

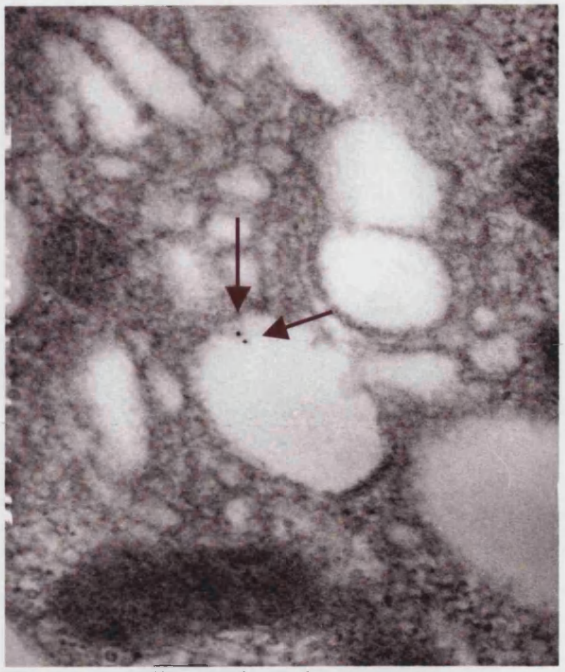

Fig 6.9: *Labelling in the Golgi apparatus. The Golgi lumen appear as white globules within the cytoplasm and the crescent shaped distribution of the Golgi body can clearly be seen under lower magnification. (Magnification x75,000)*

Fig 6.10: *Four gold particles in a vesicle budding of the Golgi apparatus. The rough Endoplasmic Reticulum is indicated by a red arrow. (Magnification x75,000)*

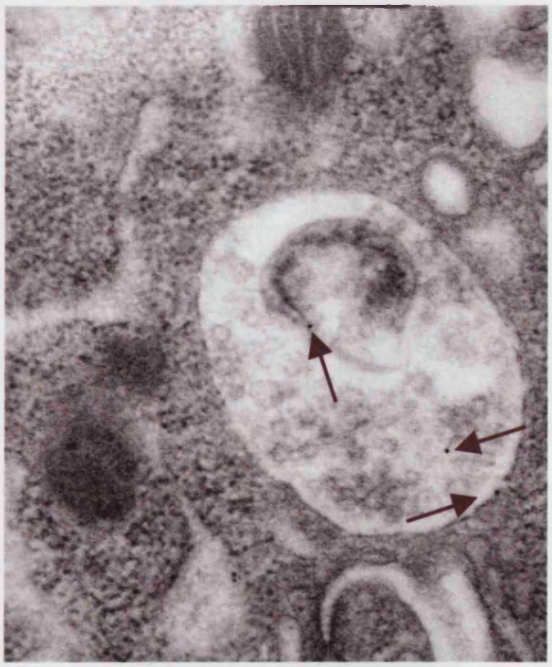

Fig 6.11: *Localisation of XOR in a putative lysosome or endosome. (Magnification x 60,000)*

this result clearly shows association of XOR with a vesicular structure and does not rule out localisation the enzyme to the luminal side of the vesicular membrane. This supports the hypothesis that the 'packets' of gold seen in the LR White sections are vesicle-associated.

The bulbous appearance of the Golgi apparatus is apparent in Fig 6.9. Under these experimental conditions the organelle can be seen quite clearly with localisation of XOR to the inside. The Golgi apparatus can again be observed in Fig 6.10. Here four gold particles can be seen in a vesicle that appears to have budded from the Golgi apparatus, suggesting that the enzyme is being transported from the Golgi apparatus. A Golgi stack to the right of the labelling has membrane bound bodies apparently budding off, giving the appearance of peas popping out of a pod. Once again, the higher quality of ultrastructure achieved by utilising this methodology is apparent. It is even possible to see the ribosomes on the rough endoplasmic reticulum (rER) to the left of the Golgi.

Fig 6.11 shows localisation of XOR to a large granular membrane-bound body, potentially an endosome or lysosome. This observation was rare and was not seen at all in the LR White sections, possibly because of destruction of membrane in the latter, resulting in the loss of many such structures.

Nuclear labelling was observed in both LR White and in epoxy resins. XOR appeared to be membrane bound or lodged in nuclear pores. This can be readily observed in Figs 6.12 and 6.13. Although labelling of the nuclear membrane itself was not seen in

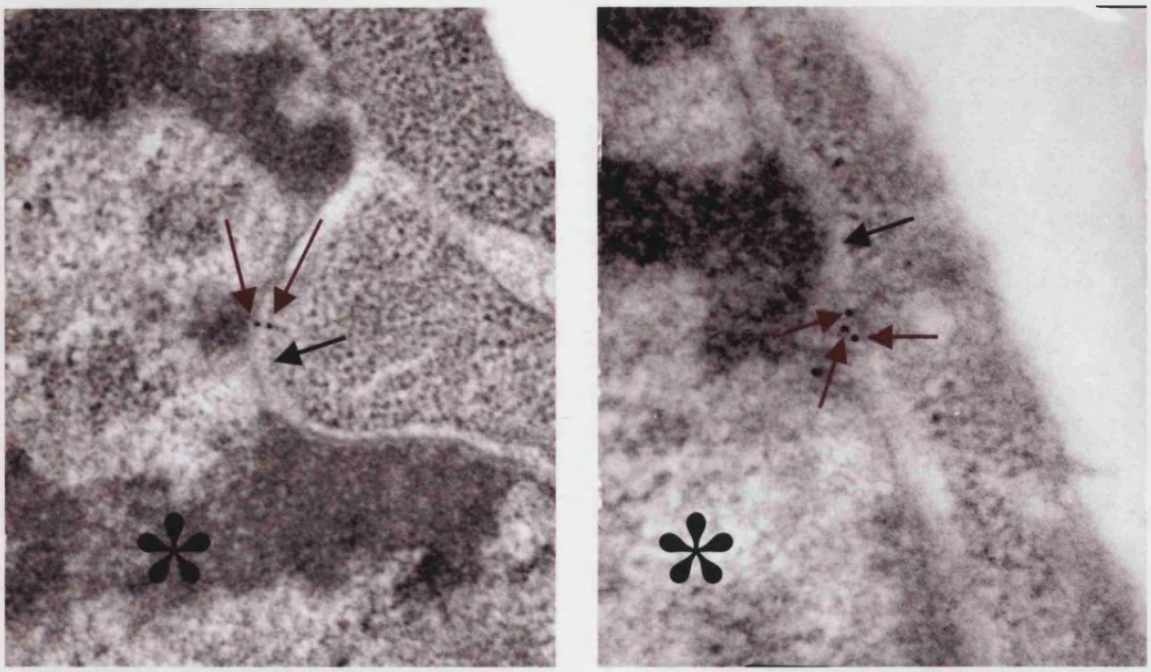

Fig 6.12 and 6.13: *Localisation of XOR to the nuclear membrane – in both instances the nuclear membrane is indicated by a black arrow. A star indicates the nuclear side of the membrane. (Magnification x75,00 and x100,00 respectively)*

the LR White sections for this cell line, this may simply reflect the limited number of samples analysed.

6.3.4 Controls

Two staining controls were used (see Appendix) as described for endothelial cells in Section 5.3.4. Once again, the controls indicated that the labelling observed was neither non-specific nor a result of non-antigenic binding of the primary antibody.

6.4 Localisation by confocal microscopy

Immunofluorescent localisation of XOR was carried out as described in Section 4.6. The results were consistent and reproducible, with all negative controls (labelling in the absence of primary antibody) showing very little non-specific staining (see Appendix). It was found, as mentioned previously, that fixing with paraformaldehyde caused a degree of permeabilisation. Therefore, all pictures and results are from permeabilised cells.

6.4.1 Localisation of XOR in HB4a mammary epithelial cells

Fig 6.14 shows several stained cells. Punctate perinuclear staining is seen along with intense nuclear staining. The nuclear staining seems to be more prevalent in the mammary epithelial cells than in the endothelial cells and is less dependent on cell density.

Fig 6.15 shows a higher magnification of a single cell. Nuclear staining can be seen, with the nucleosomes showing up due to their lack of staining. Both Figs 6.14 and 6.15 show the larger cytoplasmic 'vesicular' staining that was observed with endothelial cells in Chapter 5. Fig 6.16 is another close up of a single cell where punctate perinuclear staining can be clearly seen, although the cytoplasmic labeling is more diffuse than in the previous two images and lacks the larger punctate staining.

6.4.2 Localisation of XOR in apoptotic cells

Fig 6.17 is an example of normal HB4a cells stained with the monoclonal antibody against XOR (conjugated with a red fluorescent tag) and the green fluorescent TUNEL reaction, which marks fragmented DNA and is used as a marker for apoptosis. There is little TUNEL staining and the only co-localisation between TUNEL and the anti-XOR antibody are in areas of cell blebbing. The staining could be accounted for by non-specific aggregation of antibodies and stain in the dead cell body.

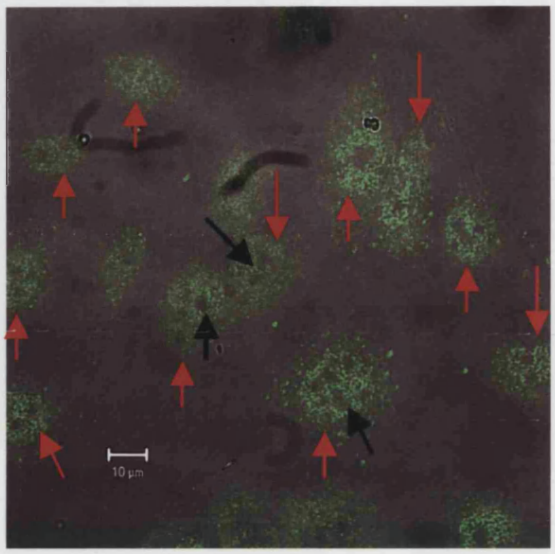

Fig 6.14: *Localisation of XOR in HB4a cells. The nuclei, indicated by red arrows, appear to have the most labelling with a notable absence in the nucleosomes (indicated by black arrows).*

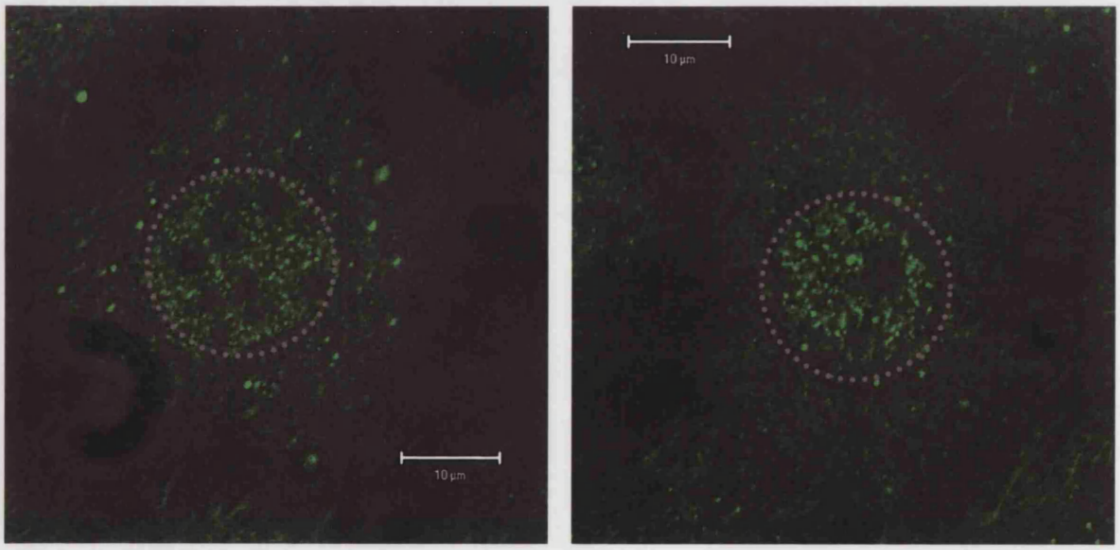

Fig 6.15 and 6.16: *Localisation of XOR in a single HB4a cell. In both cases the nuclei are ringed by a grey dotted line. The cytoplasm extends beyond the nucleus and is slightly easier to visualise in Fig 6.16 due to its 'rough' appearance.*

Fig 6.18 shows the same staining in HB4a cells driven into apoptosis by 5mM sodium butyrate, as described in Section 4.1.9. Here far more green nuclear TUNEL staining can be seen, which seems to co-localise with nuclear XOR staining. Where both are present it shows up on the image as a yellow colour. However, the XOR staining in general was much weaker and more diffuse in these cells, suggesting that either apoptosis had reduced the enzyme level or that the XOR labelling was only partially successful.

6.4.3 Localisation of XOR and actin

Staining was performed on HB4a cells to label XOR, utilizing the monoclonal antibody conjugated to a green fluorescent tag, and actin, utilising the phalloidin toxin conjugated to a red fluorescent tag, as described in Section 4.62.

Figs 6.19-6.21 show punctate nuclear and perinuclear staining for XOR in all the cells. The bundles of actin filaments show up clearly, particularly in the top left hand corner of Fig 6.21. There is no co-localisation between actin and XOR.

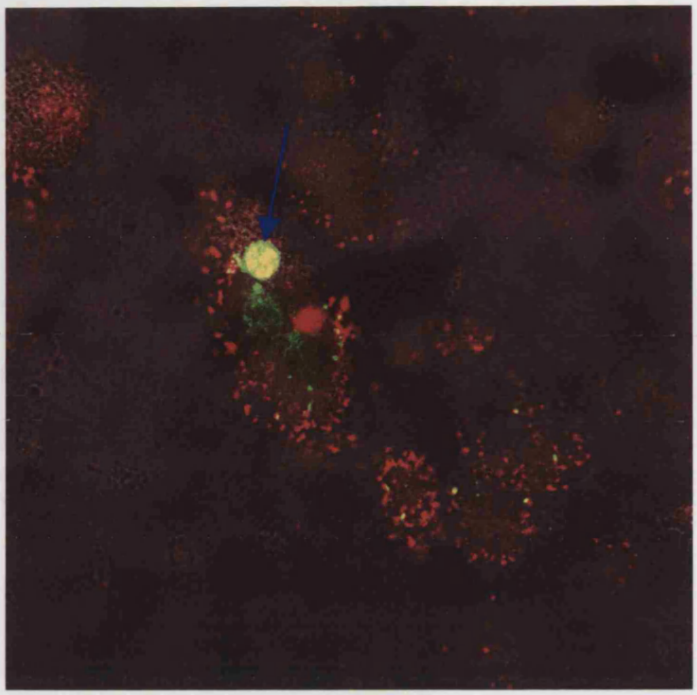

Fig 6.17: *Localisation of XOR (red) and TUNEL (green) in apoptotic HB4a cells before treatment with sodium butyrate. The usual punctate staining for XOR can be observed, and the slight green colour of the nucleus in centre view may indicate that it is apoptotic. However, the yellow 'blob' (where yellow indicates co-localisation of XOR and TUNEL), indicated by a blue arrow, is most likely aggregation.*

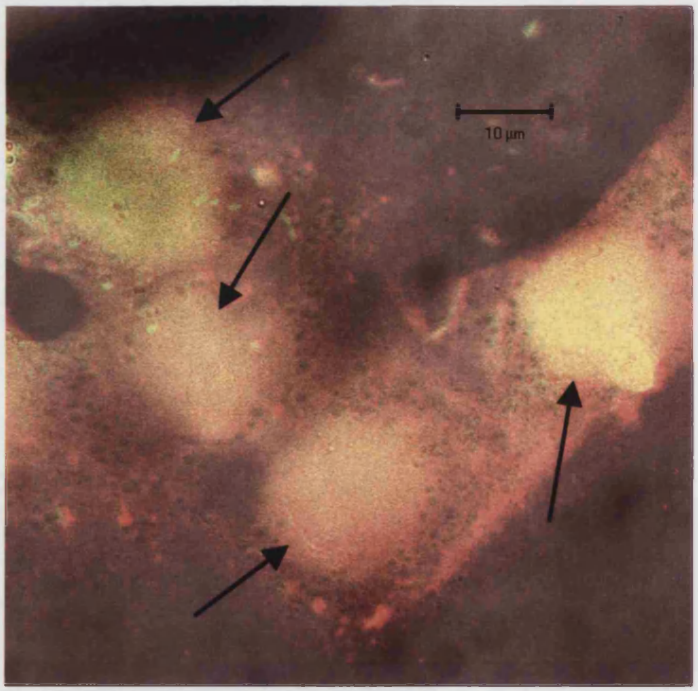

Fig 6.18: *Localisation of XOR (red) and TUNEL (green) in apoptotic HB4a cells after treatment with sodium butyrate. The nuclei, marked by black arrows, appear yellow where the XOR label is co-localising with TUNEL. Very little of the normal punctate labelling can be seen and the XOR labelling is weaker than in other samples.*

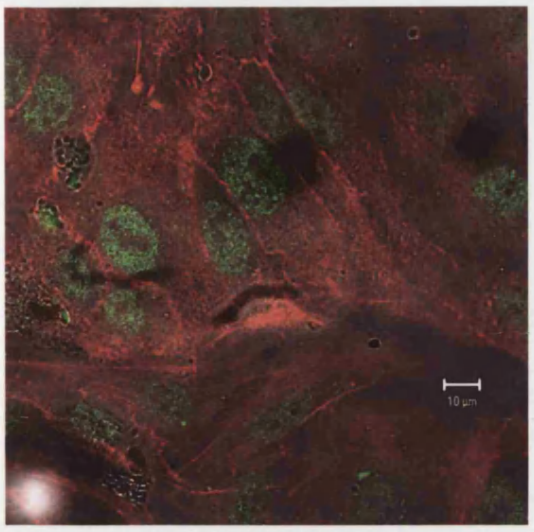

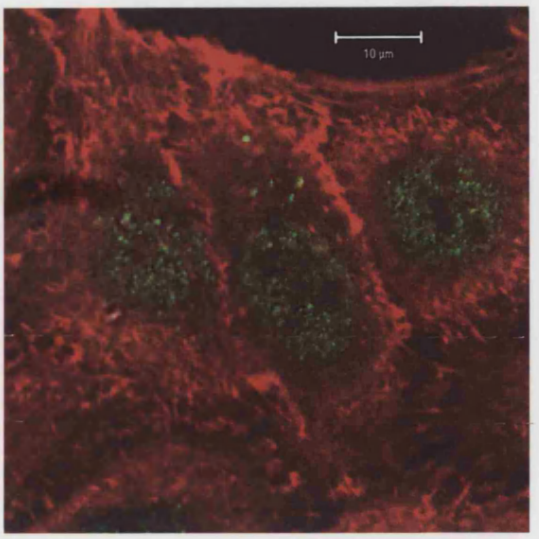

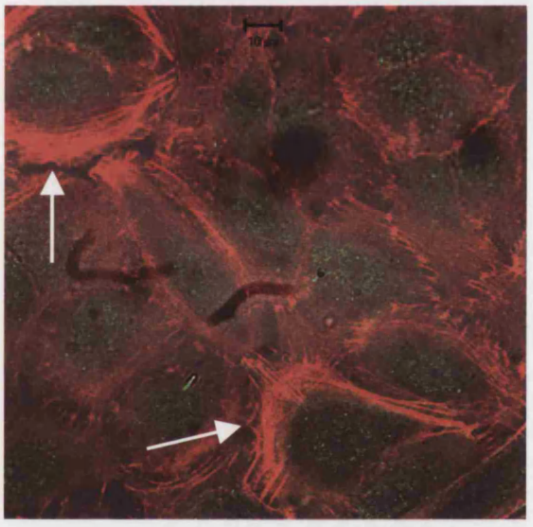

Fig 6.19, 6.20 and 6.21: *Localisation of XOR (green) and actin (red) in HB4a cells. XOR is seen as green, largely nuclear, punctate staining. Some cytoplasmic staining can be seen in Fig 6.20. The bundles of actin, indicated by a white arrow, are clearly labelled in Fig 6.21, although the lack of yellow colouration in any of the images indicates a lack of co-localisation.*

6.5 Discussion

Levels of XOR activity, detected by the pterin assay (Beckman *et al,* 1989), as described in Section 4.3, were at the limit of detection for the HB4a cell line. Attempts to compensate for this by increasing the sample concentration resulted in an increase in light scattering and difficulty in calibrating the assay. Although it can be seen that pterin dependent XOR activity increases with cell numbers (Fig 6.1), it is difficult to draw any further conclusions.

The activity of XOR in these cells seemed to be dependent on when the cell medium was changed. Pterin-dependent XOR activity could be detected 24h after the medium was changed, but after 48h the activity dropped to either low or undetectable levels. This phenomenon was more pronounced at the end of the growth curve, and reflects the limited nutrients and acidification of the media after 48h, but it is odd that it was not observed in the endothelial cells. Taken at face value, the observation suggests medium-dependent switching on and off of XOR activity. While intriguing, this idea is clearly highly speculative and would require considerable further study for its confirmation.

NO production was not detected from HB4a cells, probably because of the intrinsically low XOR activity. Immortalisation of the HB4a cell line may have resulted in a down-regulation of the enzyme, as observed in cancerous cells (Ikegami 1986). Detergents were incorporated into the assay to ensure access of the substrates to any cytosolic enzyme, all to no avail. It was impossible to predict what NO scavengers were present in the assay due to the use of whole cells. For example, the

normal purine catabolism of XOR produces urate, a known NO scavenger (Doel, 2001).

Localisation of XOR by means of electron microscopy showed discrete 'packets' of cytosolic gold labelling (see Figs 6.4, 6.5), often seen to be concentrated in the apical part of the cell. In both epoxy resin and LR White embedded samples, the pattern of staining and surrounding ultrastructure indicates that the enzyme was localised in vesicles. There also appeared to be staining within the Golgi apparatus (see Figs 6.9, 6.10), although this was not as well defined as in the other cell lines. Overall these results suggest that the enzyme is being packaged into vesicles for transport, possibly to the cell surface.

It is reasonable to speculate that this may be the same pathway that results in the binding of XOR, via glycosaminglycans, to the surface of endothelial cells (Radi *et al,* 1997). XOR is also found in serum (Benboubetra *et al,* 1996) and bile (H Martin, unpublished) and therefore must either be secreted or released from damaged cells.

The apparent localisation of XOR to the lysosome/endosome (see Fig 6.11) supports previous observations (Holt, 2000). If the body observed is indeed an endosome, this suggests that the enzyme is endocytosed from the cell surface (Radi *et al,* 1997), and that the cells are capable of recycling XOR.

Localisation of XOR via confocal microscopy demonstrated both nuclear and punctate staining (see Figs 6.14 - 6.16), as observed in the endothelial cells. In HB4a cells, there was no labelling of larger endosome–like structures visible on the

transmitted light image. This could be explained by the fact that HB4a cells are flatter than the endothelial cells, resulting in less clear light transmitted images and thus making cell ultrastructure more difficult to visualise. Alternatively, the lack of endosome-like structures may have been due to the fact that the correct conditions were not created for the formation of these structures, or it may be a reflection of the function of the enzyme within the cell type. If XOR were acting as a paracrine messenger from endothelial cells, then levels of enzyme would only need to be maintained on the surface of the cell. Once the necessary levels have been obtained then any further enzyme produced may well be stored. In mammary epithelial cells it is more likely that the enzyme is being constantly secreted and there would be no need for storage.

The nuclear staining was distinctly different to that seen in endothelial cells (see Chapter 5) an observation supported by the localisation seen via electron microscopy. Nearly all cells visualised under the confocal microscope showed intense staining for XOR within the nucleus, regardless of the cell density. While intense nuclear staining was observed in endothelial cells, it was largely restricted to post-confluent cells, with any nuclear staining in sub-confluent cells appearing weaker in comparison. The consistent nuclear labelling within HB4a mammary epithelial cells may reflect a role for the ROS produced by the enzyme in apoptosis or other signalling pathways resulting in the activation of transcription factors (reviewed by Hancock *et al,* 2001).

To investigate further the potential nuclear role of XOR further, apoptotic cells were stained for both XOR and TUNEL. TUNEL staining labels fragmented DNA and is an early marker of apoptosis. The results were disappointing. Cells driven into

apoptosis by sodium butyrate did not demonstrate elevated levels of labelling for XOR, and co-localisation with TUNEL was inconclusive (see Figs 6.17 and 6.18). If the enzyme were contributing to the apoptotoic pathway via the production of ROS, it would appear that it does so without any apparent change in XOR's cellular localisation.

In an attempt to further investigate the punctate staining seen in HB4a cells, samples were stained for XOR and actin (see Figs 6.19-6.21). Actin staining was accomplished by using a phallotoxin, which irreversibly binds to actin filaments. It was hoped that, if the punctate staining represented vesicular transport, that the secretion pathway was being directed by the cell cytoskeleton and co-localisation would be seen. However, in these samples, little punctate cytosolic staining was seen, with the majority of the labelling being in the nucleus. What cytosolic staining there was showed no co-localisation with the actin filaments. If the punctate staining in these cells does represent a vesicular secretion pathway, it does not appear to be regulated by the cytoskeleton.

7 ACTIVITY AND LOCALISATION OF XOR IN GUT EPITHELIAL CELLS

The interaction of immune cells with the gut epithelium plays an important role in host defence, acting to eliminate pathogens and antigens from the lumen of the gastrointestinal tract. One main function of the intestinal epithelium is to act as a barrier to limit uptake of antigenic material and microbes from the lumen. The presence of XOR activity in the small intestine (Kooij *et al,* 1992) suggests a role for the enzyme in the digestive tract, and it was decided to investigate the localisation and activity of XOR in cultured gut epithelial cells.

The permanent human colon carcinoma cell line, Caco-2, was used as a model for gut epithelial cells. These cells are of interest because they show differentiation patterns characteristic of mature enterocytes. Post-confluent cells are covered by functionally-differentiated brush border microvilli, and the cells are structurally and functionally polarised (Rothen-Rutishauser *et al,* 2000).

7.1 Growth curve and pterin activity

Cells were seeded at the same density in multiple flasks and, as described in Section 4.1, harvested at set intervals for fluorimetric assay. Assays were performed on samples from three flasks at the same stage in growth, and all assays were done in duplicate. The pterin assay was performed as described in Section 4.3 with appropriate controls.

Despite numerous attempts, pterin-dependent XOR activity was not detected in Caco-2 cells. Cell numbers were increased, preparations of whole cells, disrupted cells and cell fractions were all used and the assay conditions were varied, all to no avail. As noted with the endothelial cells (see Chapter 5), increasing the sample size created more turbidity and light scattering, making internal calibrations impossible.

7.2 Nitric oxide activity

NO levels were measured as described in Section 4.5. Results were, once again, unpredictable and difficult to reproduce. Varying the electron-donating substrates (xanthine, hypoxanthine and NADH) along with various combinations of inorganic and organic nitrates and nitrites did not lead to predictable results. Fig 7.1 shows data obtained with Caco-2 cells in the presence of 100μM xanthine and 100mM sodium nitrite and at constant pH (7.2), maintained by a pH stat.

As for the other cell lines discussed in previous Chapters, the irreproducibility of data precluded meaningful use of specific XOR inhibitors. Accordingly the only evidence to support the catalytic involvement of XOR in NO production is the requirement for XOR substrates within the assay.

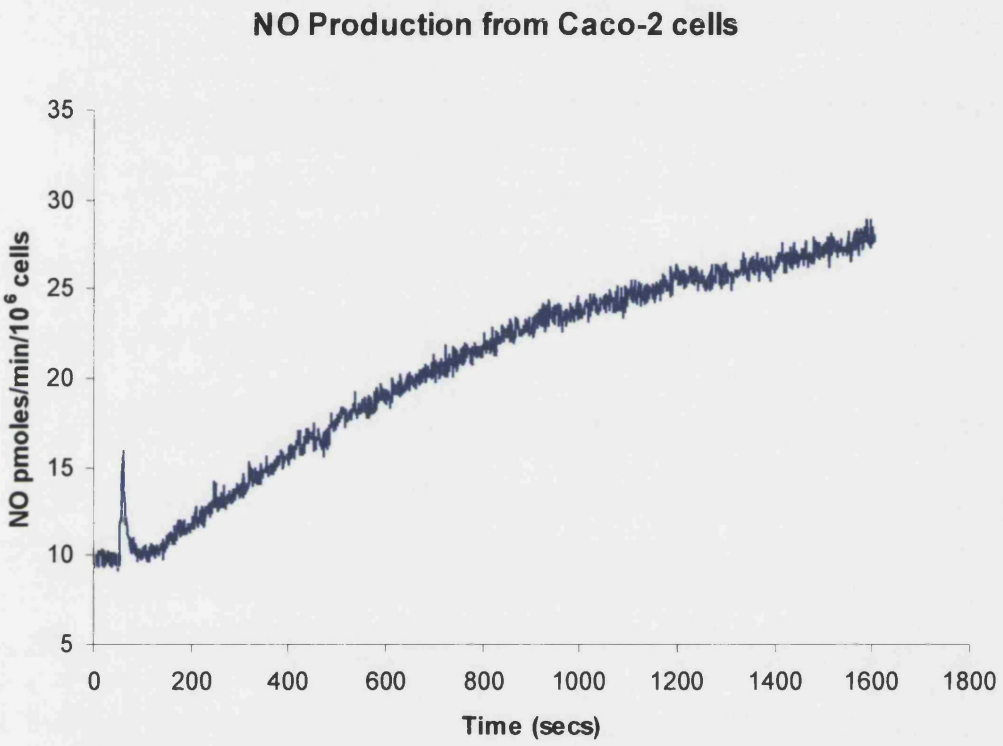

Fig 7.1: *NO production from the gut epithelial cell line Caco-2 in the presence of 100μM xanthine and 100mM sodium nitrite. The substrates were allowed to equilibrate in the reaction chamber with the buffer. The reaction was started at about 60 secs (where the peak can be seen) by the addition of of cell suspension (1ml). The reaction chamber was kept anoxic by the constant flow of oxygen-free nitrogen through the vessel and the cells were maintained in suspension by constant stirring.*

7.3 Localisation by electron microscopy

Electron microscopy was carried out as detailed in Section 4.7. Cells were embedded in either epoxy or LR White resin and samples were preserved either chemically or by slam freezing. Only monolayers of Caco-2 cells showing characteristics of dome formation were used in this Section.

7.3.1 Cell morphology

Dome formation, a characteristic of maturation in Caco-2 cells, can be seen in striking detail when viewed under an electron microscope. Fig 7.2 shows an example of the way that these cells form multiple layers. Individual cells are best identified by means of their nuclei. A cartoon below the electron micrograph indicates how cells pile up on top of the monolayer to form a dome. Many of the samples showed intense vesicular activity at the apical cell surface. This was often accompanied by an increased number of Golgi within the cell and microvilli on the cell surface. However, domes proved to be difficult to find whilst sectioning.

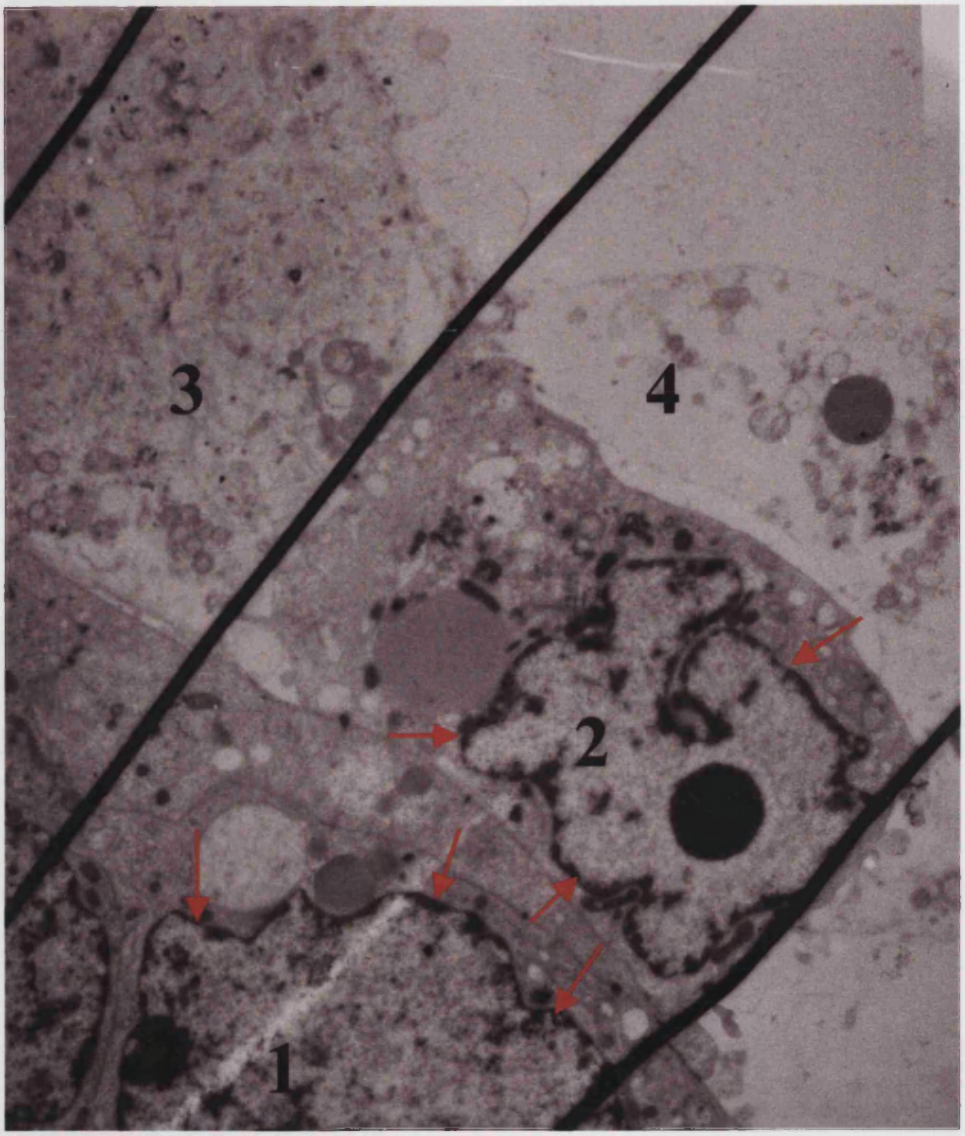

Fig 7.2: *Caco-2 cells are seen piling up to form a dome in the image above. Four cells can be seen in this image, with the nuclei of cells 1 and 2, indicated by red arrows, appearing more grainy and bordered by dark nuclear membrane. The three dark stripes are creases in the resin where the sections were cut. No gold can be seen at this magnification (x4000). Below is a cartoon of a dome with a boxed area showing how the above cells may have formed part of the dome structure.*

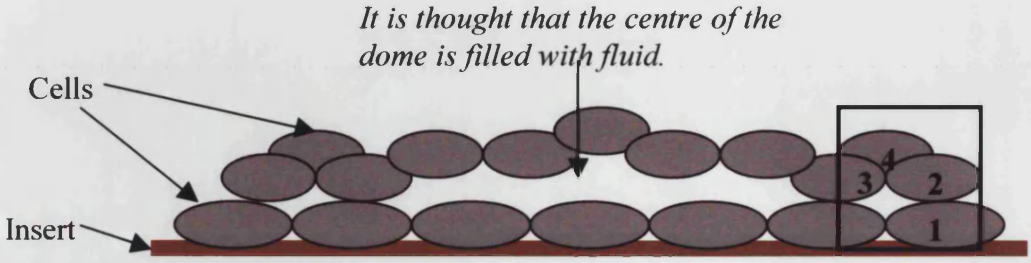

7.3.2 Localisation of XOR in cells embedded in LR White resin

As mentioned in previous Chapters, the sample preservation and resin hardening methods used with LR White resin can often result in improved labelling, but this is at the expense of ultrastructural definition in the cell. Samples preserved in this manner showed optimum levels of staining and all the images in this Section were derived from slam-frozen samples. A primary antibody concentration of 1/100 for 1D9/D1 gave the best staining with minimal background.

XOR is apparently localised to bundles or packets within the cell, as seen in Figs 7.3-7.6. This highly reproducible pattern of staining may well indicate localisation to vesicles, which in several cases are in abundance close to the cell surface.

Figs 7.7-7.9 show localisation of XOR to membrane structures within the cell. Although the ultrastructural detail in these samples is poor, the characteristics of the membrane structure suggest either Golgi apparatus or endoplasmic reticulum, organelles that are responsible for the secretion of proteins.

Figs 7.10 and 7.11 show the levels of staining seen in cells largely lacking microvilli. When compared to Figs 7.12 and 7.13 it can clearly be seen that the levels of XOR in mature cells (those with a brush border) are higher than those in immature cells. Whilst the number of clusters of gold may not differ greatly, the amount of labelling within each cluster is clearly elevated in mature Caco-2 cells.

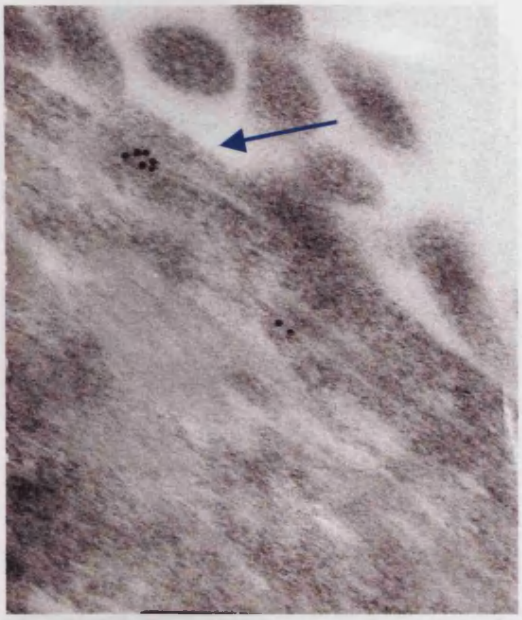

Fig7.3: *Labelling of XOR in two discrete 'packets' near the cell surface. The cluster closest to the arrow appears spherical. (Magnification x100,000)*

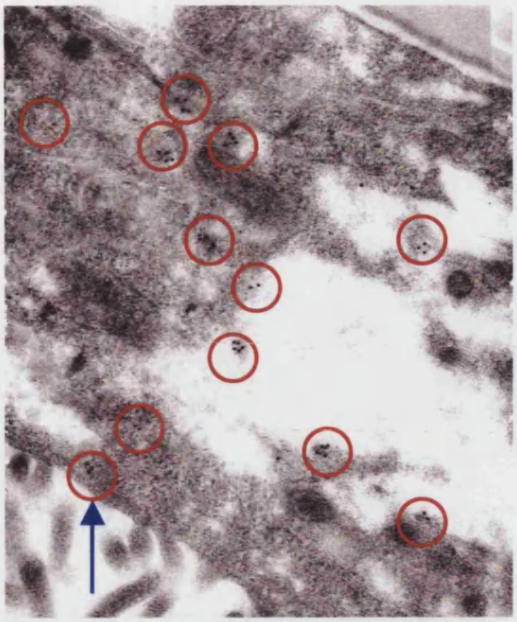

Fig 7.4: *Overview of the spread of gold clusters. Clusters are highlighted with red circles. (Magnification x50,000)*

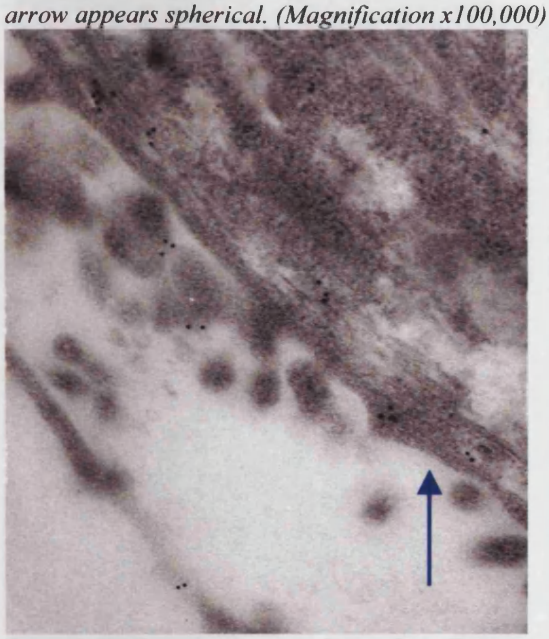

Fig 7.5: *XOR in putative vesicles at the cell surface. (Magnification x60,000)*

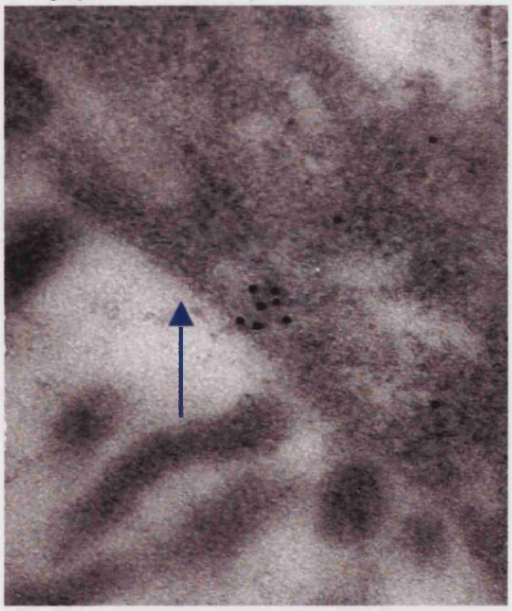

Fig 7.6: *Close up of on of the 'packets' of gold at the cell surface. Again, the gold is clustered in a circular pattern (Magnification x120,000)*

In all the images the cell surface can be identified by the blue arrow. In many of the images, microvilli, or sections of microvilli (seen as spherical dark patches where they have been sliced in cross-section) are visible beyond the cell surface.

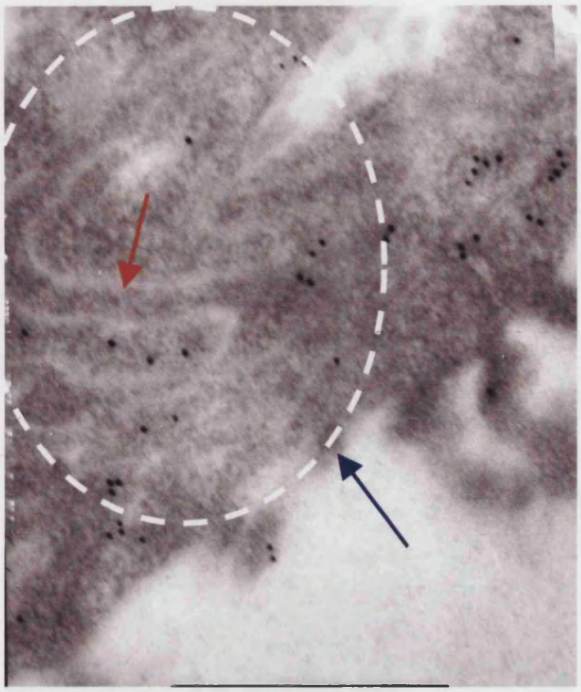

Fig 7.7: *Localisation of XOR in 'packets' adjacent to a membrane bound structure. (Magnification x75,000)*

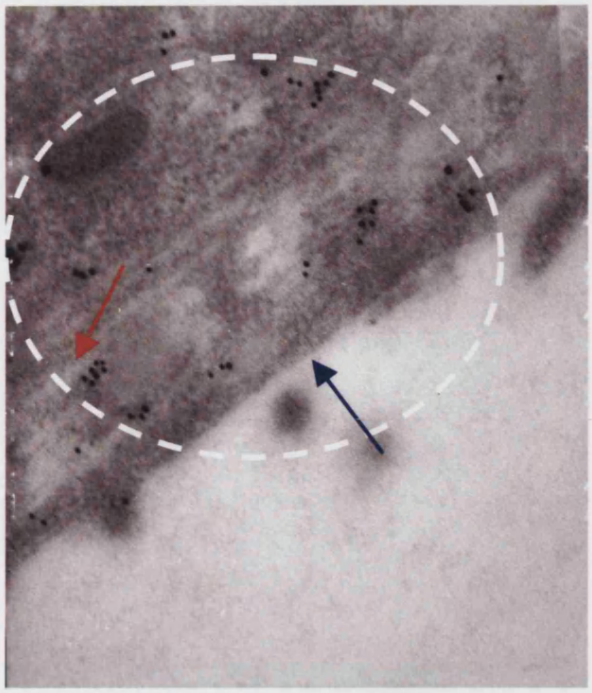

Fig 7.8: *Localisation of XOR to another membrane bound organelle. (Magnification x75,000)*

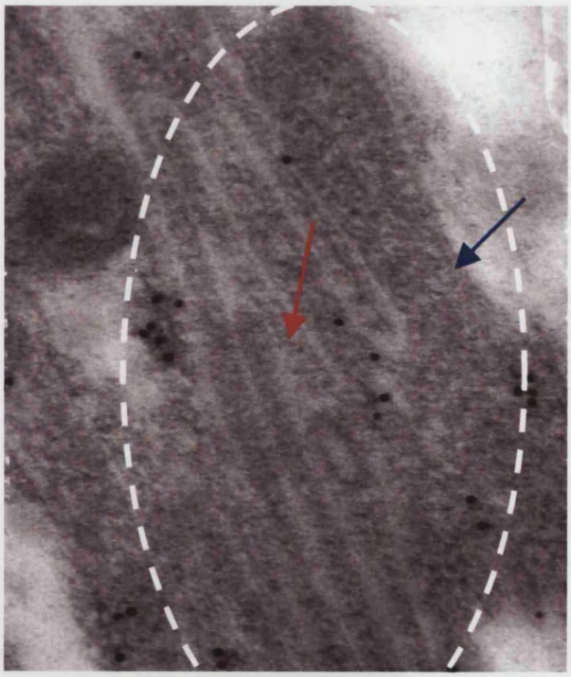

Fig 7.9: *Localisation of XOR to the Golgi or endoplasmic reticulum membrane. (Magnification x120,000)*

In all the images the membrane is indicated by the red arrow and the cell surface by a blue arrow. The membrane appears as a light stripe against the grey of the cytoplasm and a white dashed circle rings the extent of the membrane. In Figs 7.7 and 7.9, the bulbous nature of the membrane bound organelle is reminiscent of the Golgi apparatus.

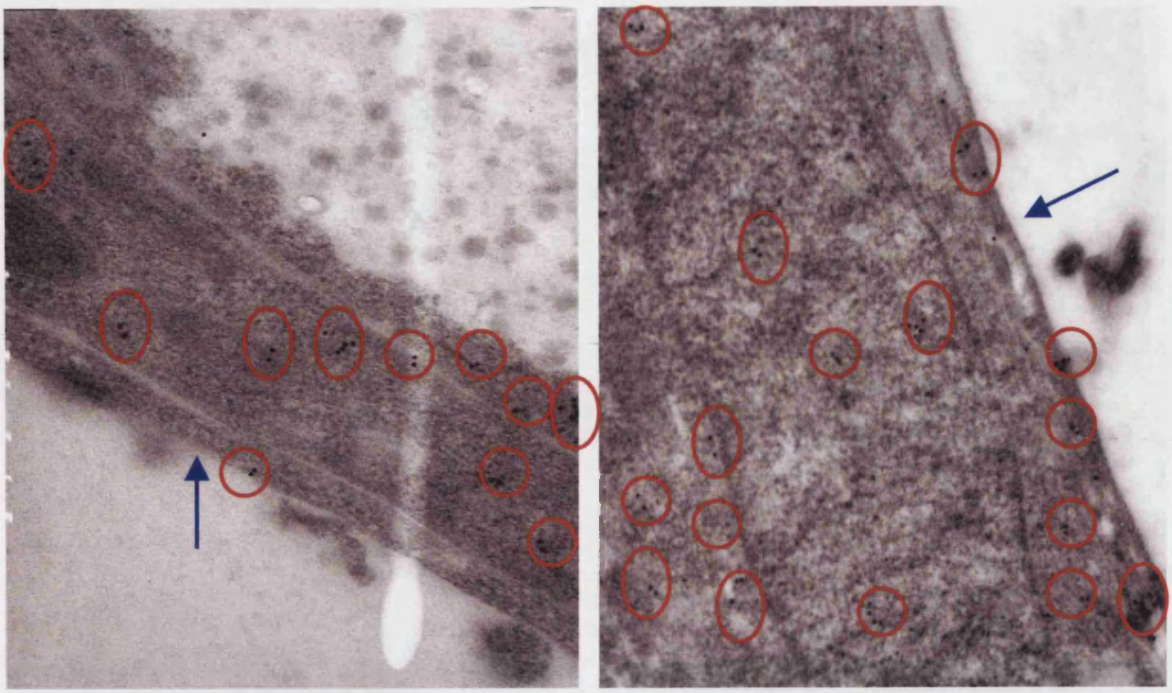

Fig 7.10 and 7.11: *Relatively low levels of staining seen in immature cells bearing few microvilli. The cell surface is shown by the blue arrow and gold labelling by red circles. (Magnification x60,000 and x50,00 respectively)*

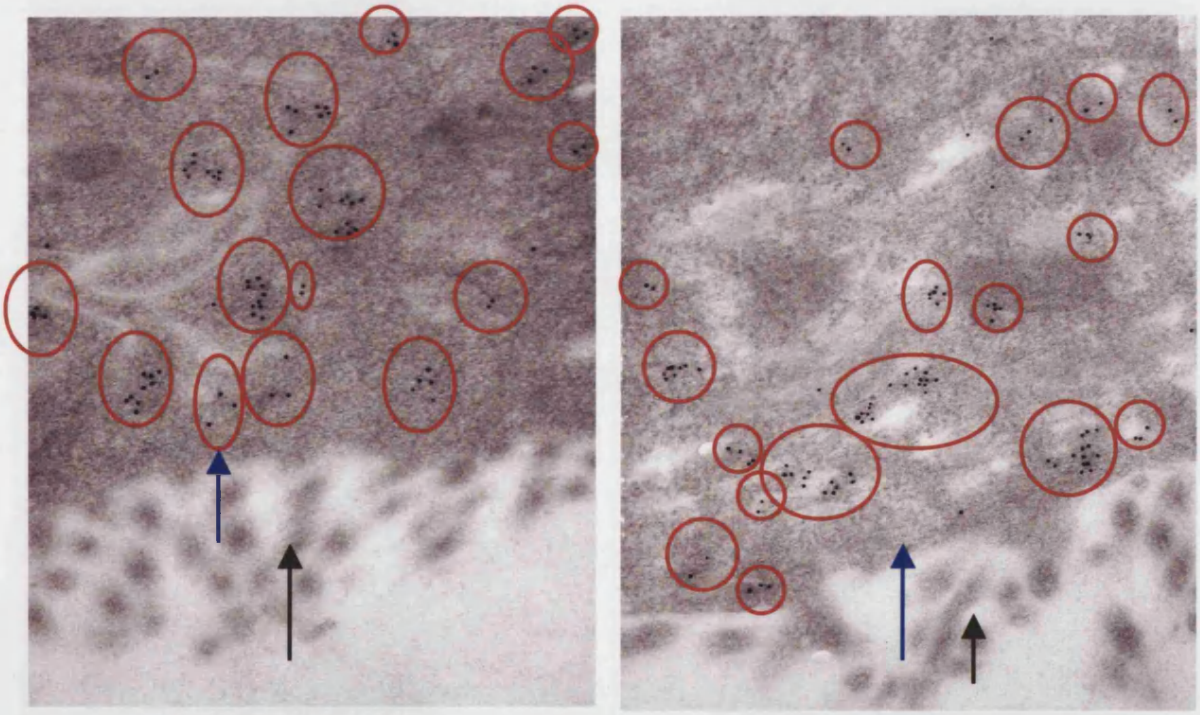

Fig 7.12 and 7.13: *High levels of staining seen in mature cells bearing microvilli. The cell surface is shown by the blue arrow, microvilli by the green arrow and gold labelling by red circles. On average, there is a greater amount of gold labelling in each of the highlighted areas than in the previous images. (Magnification x60,000 and x50,00 respectively)*

Statistical analysis of the labelling (see Appendix) showed association of the enzyme with small vesicle like packets and the Golgi apparatus. This strongly suggests involvement of XOR in cellular regulatory and secretion pathways.

7.3.3 Localisation of XOR in cells embedded in epoxy resin

Despite repeated efforts Caco-2 cells were not successfully embedded in epoxy resin. Samples viewed under both light and electron microscopy showed cells with severe plasma membrane damage and cytosolic leakage. The reason for this is unclear, but it may be that the cells were particularly sensitive to part of the fixing or embedding process.

7.3.4 Controls

Controls (see Section 5.3.4) once again showed that labelling with the primary 1D9/D1 monoclonal anti-XOR antibody was specific. Results for all controls can be found in the Appendix.

7.4 Localisation by confocal microscopy

Staining was carried out as described in Section 4.6. As with the other cell lines studied, fixation caused permeablisation of the cell membrane Therefore all the results in this section are from permeablised cells.

7.4.1 Localisation of XOR in immature and mature Caco-2 cells

The mature characteristics of Caco-2 gut epithelial cells are greatly enhanced when the cells are grown on an insert (allowing media to both sides of the cell layer) compared to when grown on coverslips (only allowing media to the apical side of the cell layer). Thus staining for XOR was carried out on cells grown on both inserts and coverslips.

Fig 7.14 shows the typical punctate staining seen in immature Caco-2 cells. In this case the cells were grown on cover slips. Once again the punctate staining seen in the other cell lines can be observed. The edge of the clump of cells appears devoid of any labelling. This is undoubtedly misleading and the reason why no fluorescence is seen is that the edge of the clump of cells is below the plane of focus and does not reflect an absence of XOR.

Fig 7.15 also shows localisation of XOR in Caco-2 cells, but this time the cells have been grown on inserts. The pattern of staining was similar to that seen before, although there appear to be larger areas of punctate staining. It is hard to tell whether

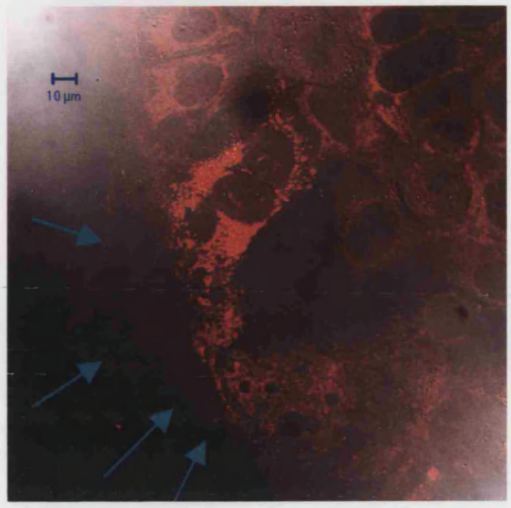

Fig 7.14: *Localisation of XOR in Caco-2 monolayer. A clump of cells can be seen in in this image. The cell boundary is shown by blue arrows.*

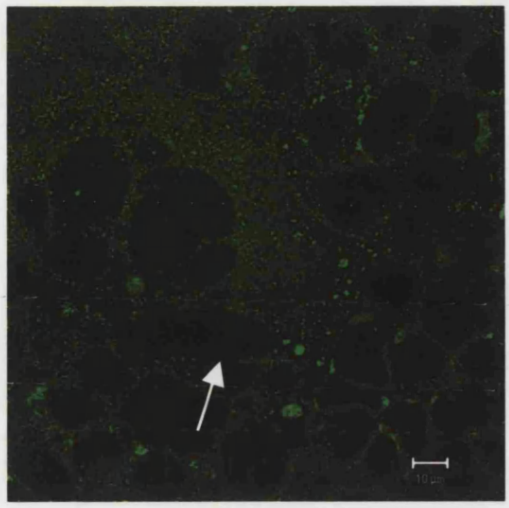

Fig 7.15: *Localisation of XOR in Caco-2 in a confluent monolayer. Cell nuclei appear free of staining (indicated by a white arrow) and the cytosol is filled with both large and small punctate staining.*

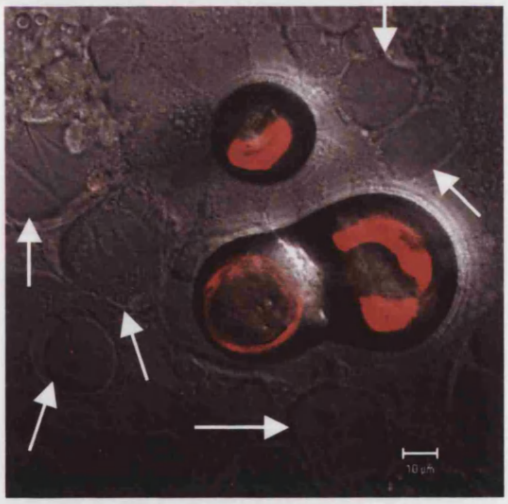

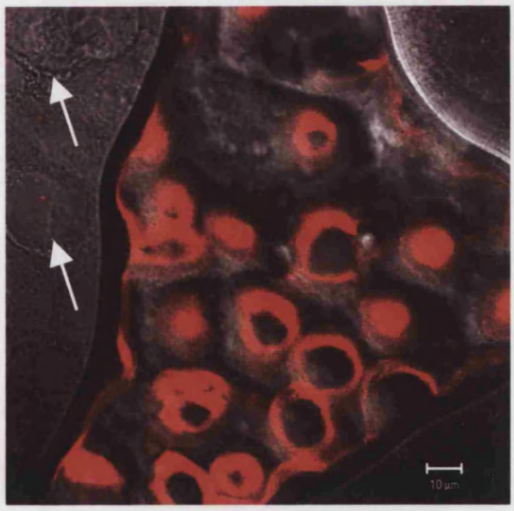

Fig 7.16 and 7.17: *Localisation of XOR in Caco-2 domes. In the first image two small, newly formed domes can be seen. The upper dome consists of one cell and the lower dome of two and in both cases the cells appear ringed with staining for XOR. In the second image the dome has spread so much that it appears as a sheet over the monolayer and comprises of in the region of 20 cells. In both images white arrows indicate the nuclei of the cells in the monolayer benath the dome. No staining at all can be seen in the monolayer.*

or not this is membrane associated, as it was difficult to resolve a light transmitted image of cells grown on inserts. One instantly striking feature is the complete absence of staining in the cell nuclei.

Figs 7.16 and 7.17 show typical patterns of localisation in mature cells grown on cover slips. The cells ringed with red labelling for XOR are growing on top of the cell monolayer and form part of a 'dome' (see Fig 7.2). Dome formation is one of the characteristics of Caco-2 maturation. The cells forming the domes always show more intense staining than those forming the monolayer beneath, and it would seem from the pattern of staining that the enzyme was located at the apical periphery of these cells. It is noteworthy that the labelling for XOR seen in Caco-2 domes grown on coverslips is diffuse and shoes none of he punctate staining seen in all other samples. The complete lack of labelling observed in the monolayer of these images is artifactual. No fluorescence can be detected because the sensitivity of the equipment needed to be reduced to prevent the intense staining within the dome turning into a blur. Whilst this results in false negative results for the monolayer in many of the images, it does give an indication of the intensity of the staining in the domes.

Fig 7.18 shows a progression of images taken through a Caco-2 dome formed from a monolayer of cells grown on coverslips. The top left hand image is of the basal layer of the cells (including the unstained cell monolayer beneath) and each subsequent image (viewing left to right, top to bottom) is slightly further up (distance is indicated on each picture) in the domes until finally the apical side of the cells is seen. Once again these cells were grown on cover slips. This 'z sectioning', demonstrates further

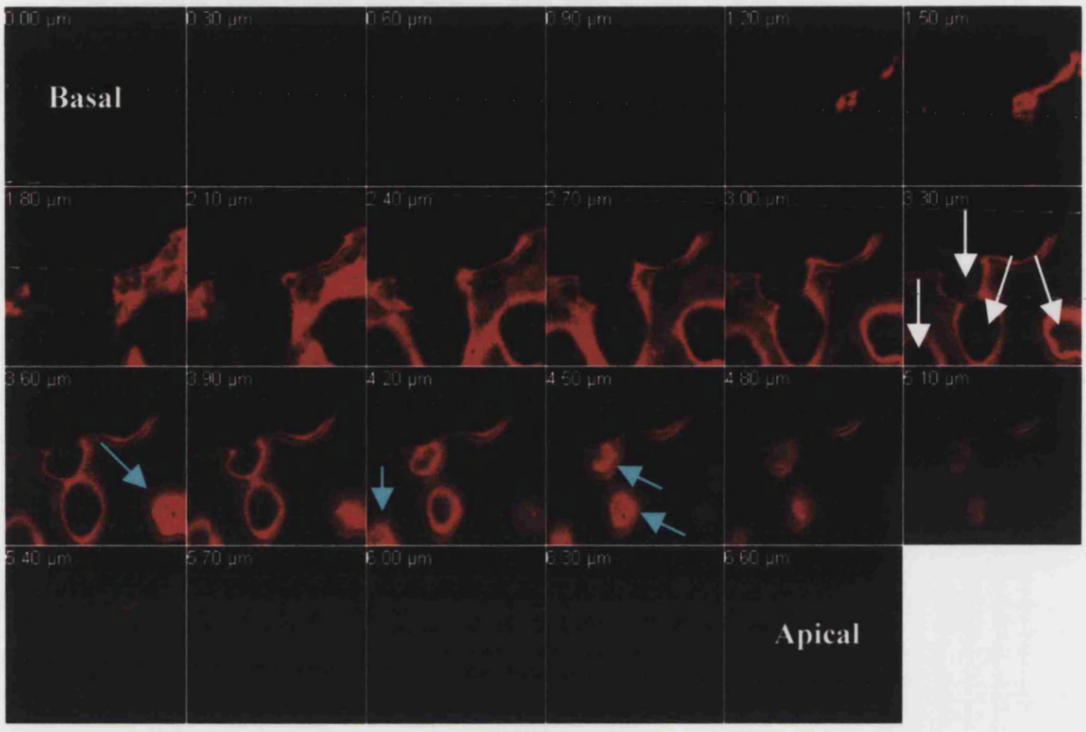

Fig 7.18: *Localisation of XOR in a Caco-2 dome, showing serial slices from basal to apical side of a single dome. As the confocal microscope scans from the case of the cells up, it can be seen that the staining seen to 'ring' the cells in the earlier images is in fact diffuse staining covering the entire periphery of the cells in the dome. Four cells can clearly be seen in this image and are indicated by white arrows in one of the middle sections. As the view moves upwards, the top of each of the cells can be seen by the red 'cap' of fluorescent labeling (indicate by a blue arrow).*

that the staining for XOR is most intense at the outer edge of the cells forming the dome.

Fig 7.19 shows the localisation of XOR in a Caco-2 dome formed from a monolayer of cells grown on an insert. A network of lines of XOR can be seen crossing the dome, along with more punctate staining for the enzyme. The 'hairnet'-like pattern of staining seems to be localised to the boundaries between cells making up the dome. Fig 7.21 shows the 3D image of the dome being turned through 360°. Viewed from the side it can be seen that the dome actually protrudes from the monolayer, and the greater intensity of staining in the dome, compared to the monolayer becomes evident. This staining is markedly different from that of cells grown on coverslips, where the staining in the domes was more diffuse. However, Fig 7.20 shows z-sectioning through the same dome as that pictured in Figs 7.19 and 7.21 (this time travelling from the apical side of the dome to the basal side). This demonstrates that, whilst the pattern of staining was quite different from that seen in Caco-2 domes grown on coverslips, the staining was still at its most intense at the outer edge of the dome.

7.4.2 Localisation of XOR in barrier- positive and barrier-negative Caco-2 cells

Caco-2 cells grown on cell culture inserts were provided, ready fixed, by Dr Roger Hurst of the University of the West of England, Bristol. These cells are grown in the same manner as the cells described in Section 5.4.2, with the intention of modelling the blood-brain barrier (Roger Hurst, verbal communication). 'Barrier-positive' is shorthand for co-cultures that have developed high transcellular resistance, tight

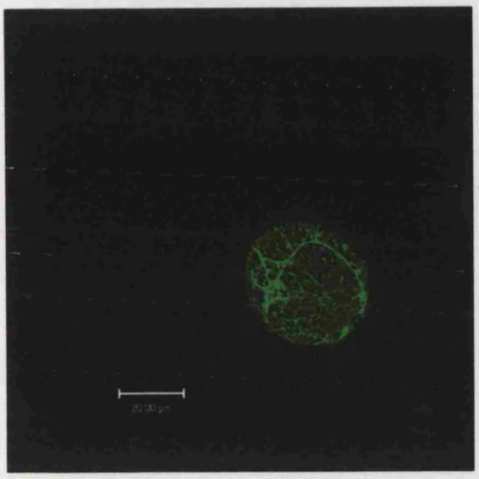

Fig 7.19: *Localisation of XOR in a Caco-2 dome. Many cells make up this single dome and some of the cell boundaries can be seen highlighted by the hairnet like fluorescent staining for XOR.*

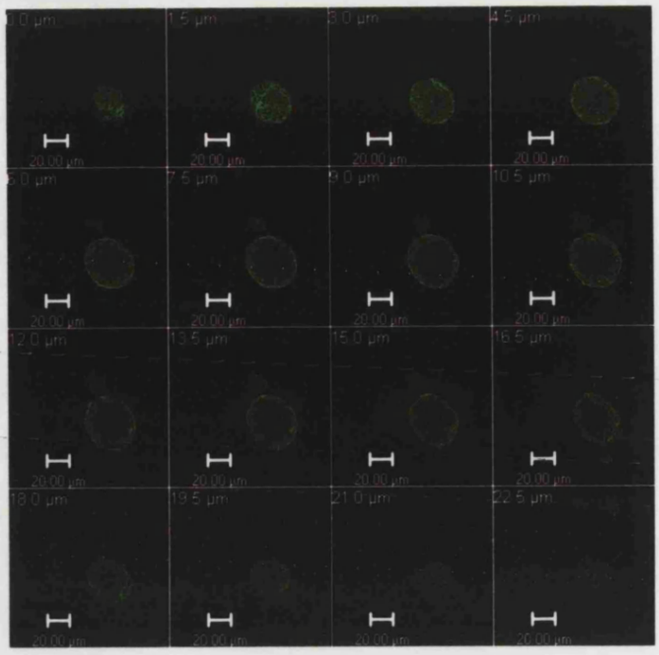

Fig 7.20: *Localisation of XOR in the same dome. The image shows serial z-sections of a single dome starting at the top of the dome and passing on down to the monolayer the some is formed upon. The brightest staining is around the periphery of the dome.*

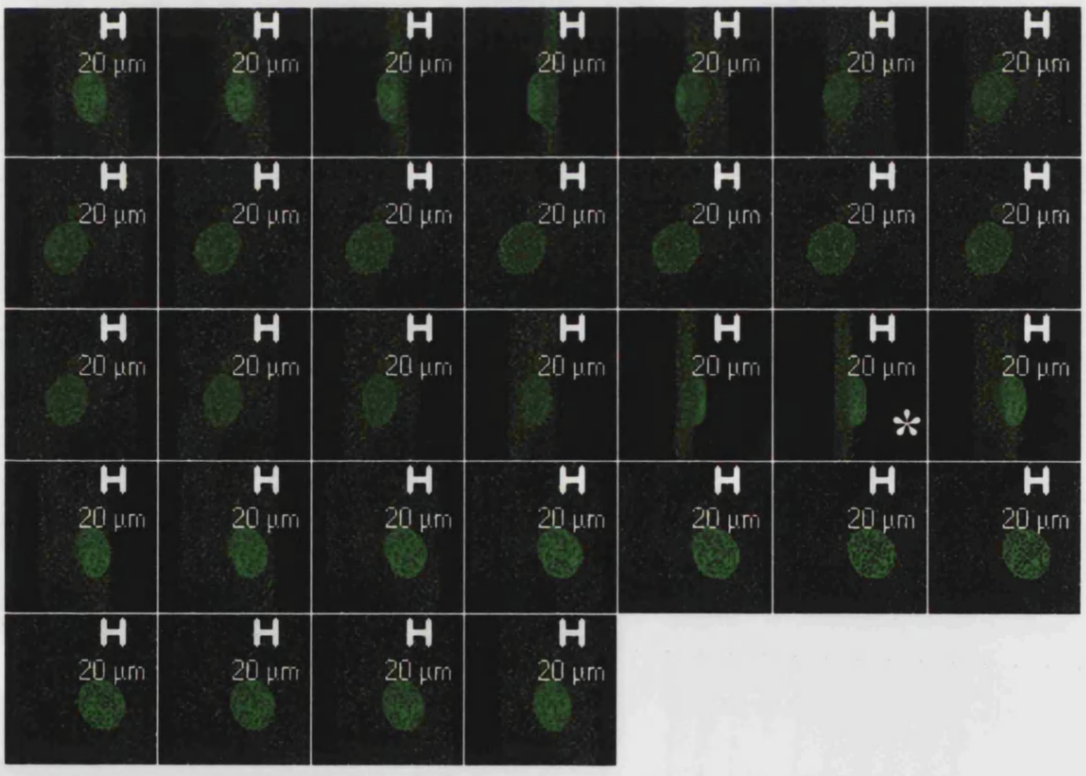

Fig 7.21: *Localisation of XOR in the same caco-2 dome: 3D image turned through 360°. This image is built up by layering the serial z-sections, seen in previous images, on top of each other to generate a 3D image. This image can then be rotated so that the localisation of XOR can be seen from above the dome, from the side and below. The side on image is indicated by a *. The intensity of the staining in the dome when compared to the monolayer is apparent, as is the height of the dome.*

junctional complexes and restricted permeability that can be modulated by osmotic shock (Garberg 1998). The aim of this Section was to determine if cells displaying 'barrier-positive' characteristics showed different patterns of localisation of XOR compared to normal cells. Localisation of XOR was carried out as described in Section 4.6.

Fig 7.22 shows localization for XOR (green) and actin (red) on barrier-positive Caco-2 cells. The network of staining seen on the domes in Fig 7.19 is repeated but seems to be more pronounced. There is no co-localisation with actin, showing that the XOR staining was not linked to the actin infrastructure of the cells.

Fig 7.23 shows serial z-sections, going from the basal through to the apical side (see legend), of a dome formed on a monolayer of barrier positive cells. Again, XOR is shown in green and actin in red. This image demonstrates that the centre of the dome lacks any comparable labelling for XOR, showing itself as a circular area devoid of fluorescence (almost the reverse of the 'yolk of the egg' anology used previously to describe nuclear labelling). It seems strange that there is a complete lack of nuclear staining within these cells.

Figs 7.24 and 7.25 show the pattern of XOR localisation seen in barrier negative cells. The 'hairnet' like network of staining was much more apparent in these samples, seeming to mark out the boundaries between individual cells within the dome. Again, XOR is shown in green and actin is shown in red. In these cases, low levels of punctate XOR staining can be seen in the monolayer. The lack of yellow (seen when

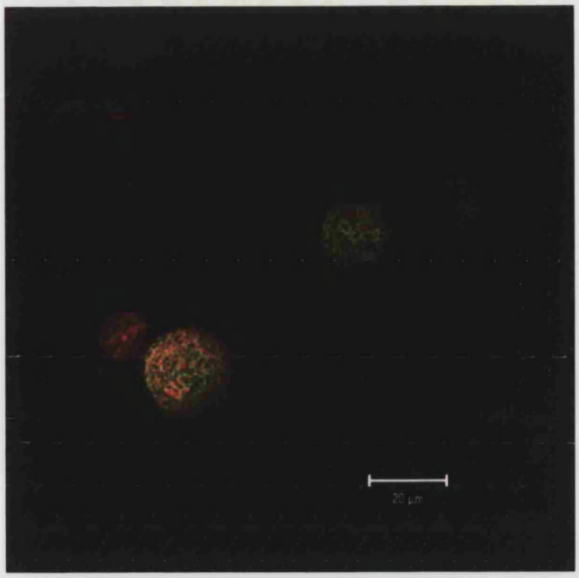

Fig 7.22: *Localisation of XOR and actin in barrier positive Caco-2 domes (XOR – green, actin – red). Three ball like domes can be seen in this image. No labelling can be seen in the monolayer beneath.*

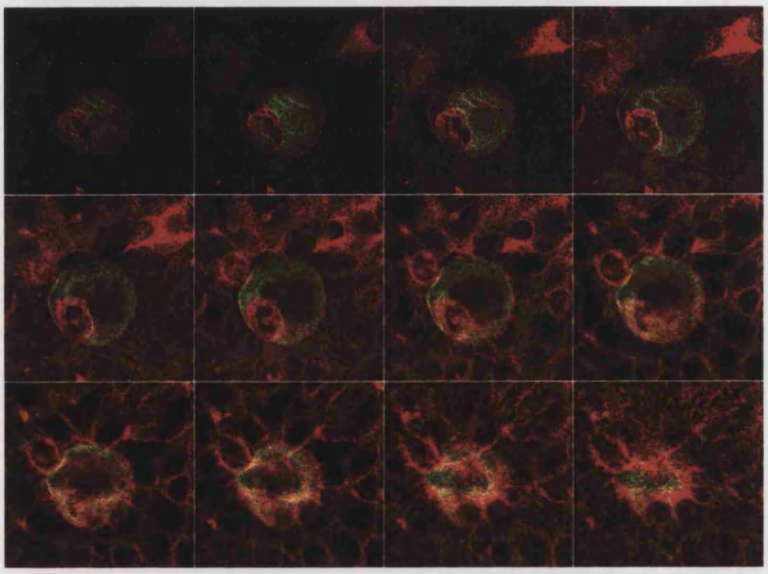

Fig 7.23: *Localisation of XOR and actin in barrier positive caco-2 domes, serial z-sections (XOR – green, actin – red). Once again the sections start at the top of the cell and move down to the monlayer beneath. There is a spherical area within the dome that is devoid of all staining, indicating the lack of XOR in the centre of the dome. The cells within the domes are smaller than those comprising the monolayer and there are many cells in this single dome.*

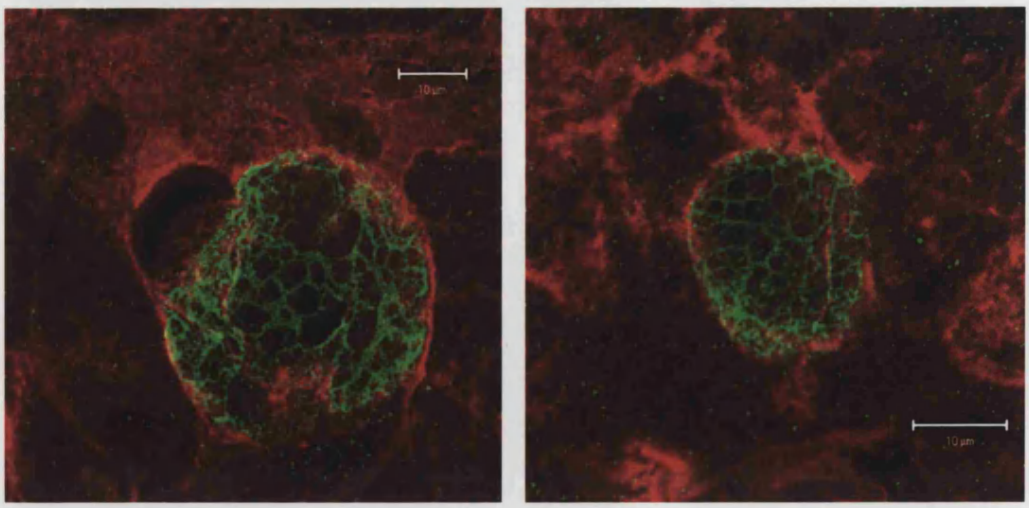

Fig 7.24 and 7.25: *Localisation of XOR in caco-2 barrier negative domes (XOR – green, actin – red). The network of staining in these images can clearly be seen to outline the cells within the dome, although there is no co-localisation with actin, apparent by the lack of yellow labeling (yellow labeling is generated when both red and green labeling co-incide). Punctate staining can clearly be seen in the monolayer.*

the two fluorescent tags co-inside) shows that there was no co-localisation between the XOR and actin.

7.4.3 Localisation of XOR in apoptotic Caco-2 cells

Enterocytes are dynamic cells that, *in vivo,* are constantly undergoing a process of maturation and cell death. It has been previously hypothesised that the free radicals produced by XOR may play a part in the signalling cascade, which eventually results in apoptosis and cell death (Page, 1999). Fig 7.26 shows Caco-2 cells that have been stained for XOR (red) and TUNEL (green), which labels fragmented DNA and is an early indicator of apoptosis. Whereas a degree of co-localisation can be seen, as demonstrated by the yellow colour produced when the two fluorescent tags coincide, this result was not consistent.

7.4.4 Localisation of XOR, zonular occludens and catenin β

In the next Section, XOR is shown to be localised alongside various proteins that form complexes in the junctions between cells. Fig 7.27 gives an overview of a cell junction and is useful when interpreting the data. Fig 7.28 shows localisation of tight junctions within a monolayer of Caco-2 cells. This was achieved using the primary monoclonal antibody ZO-1, which is directed against zonula occludens, a protein within the tight junction complex (see Fig 7.27). The staining appears as crazy paving and the boundaries between cells can be clearly seen.

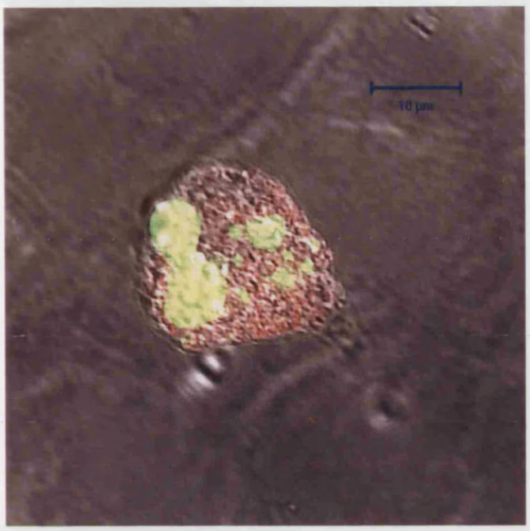

Fig 7.26: *Localisation of XOR (red) and TUNEL (green) in Caco-2 cell monolayer. Yellow indicates co-localisation of TUNEL and XOR although the shape of the cell and its Distance from the monolayer indicate that the Staining is probably due to aggregation within a dead cell.*

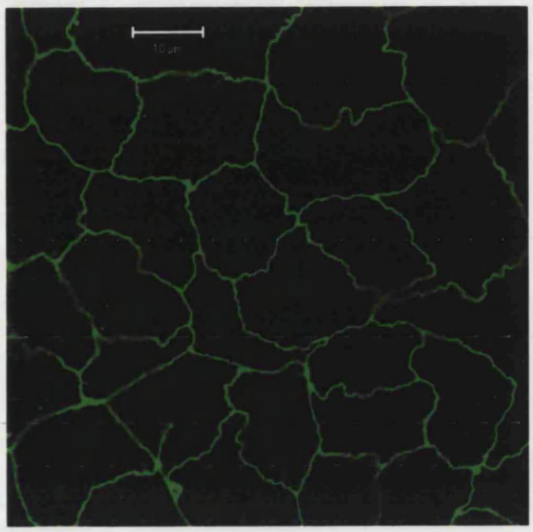

Fig 7.28: *Localisation of zonular occludens in a Caco-2 monolayer. The cell boundaries where this tight junction protein is found are clearly marked by the green staining.*

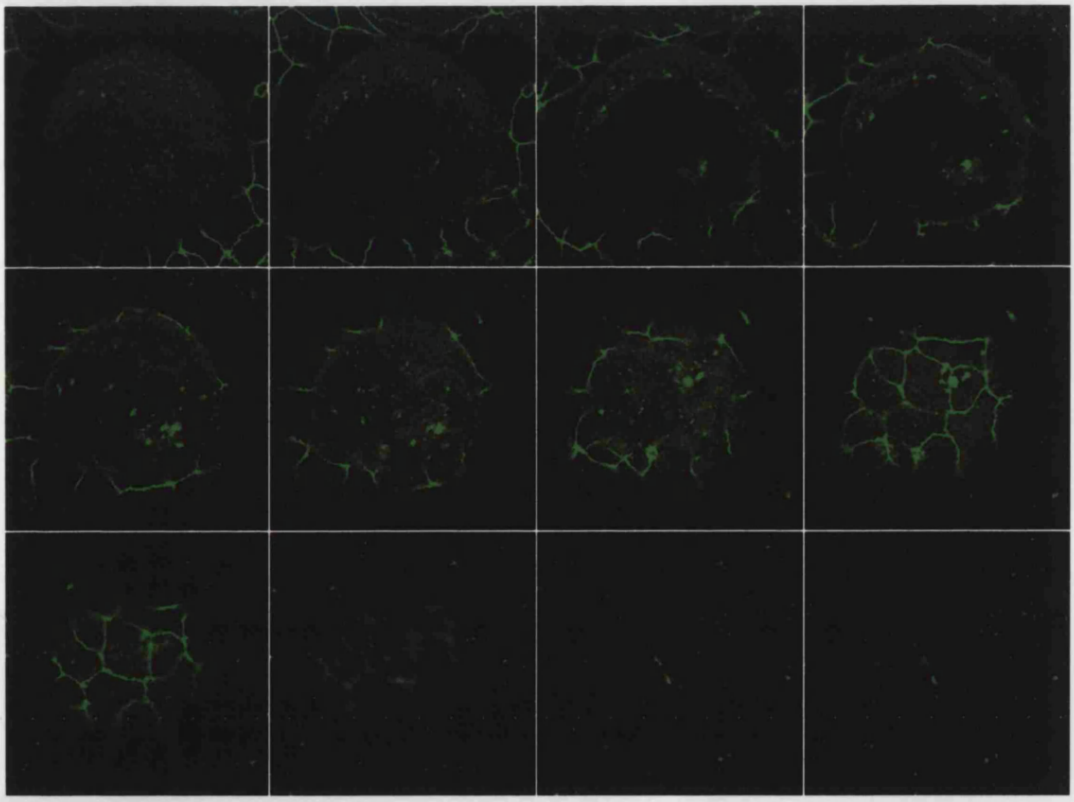

Fig 7.29: *Localisation of zonular occludens in a caco-2 dome: serial z-slices from basal to apical side of the dome. Once again, the cell boundaries between the cells in the monolayer can clearly be seen in the first few images. Then, as the perspective shifts up into the dome, the boundaries of the cells within the dome can be seen.*

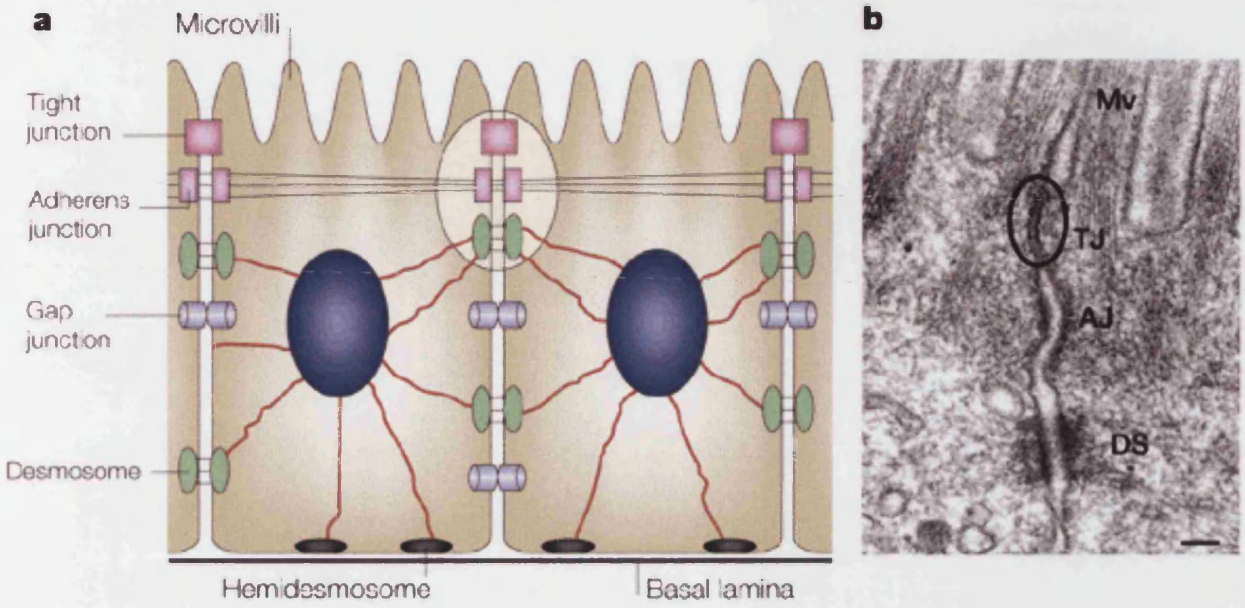

Fig 7.27: *The localisation of various junctional complexes formed between epithelial cells. The actual size of the gap between the cells can clearly be seen in b, where the gap can be seen to widen towards the basal side of the cells (taken from Tsukita et al, 2001)*

.

Fig 7.29 shows the localisation of tight junctions within a dome formed by post-confluent mature Caco-2 cells. The series of images are z-sections progressing from the basal side of the dome up to the apical layer. Again, the tight junctions appear as crazy paving, outlining each individual cell and revealing the structure of the dome more clearly.

Fig 7.30 demonstrates the staining seen with a polyclonal antibody against catenin β. This is a protein that is found lower down in the junction, in the adherens junction (see Fig 7.27). The gap between the neighbouring cells is wider in this area; hence the less well defined staining. However, the boundaries between the cells can just be seen in the serial images.

XOR staining is again seen in Fig 7.31 (red fluorescence) alongside that for catenin β (green fluorescence) in a dome of Caco-2 cells. This image is of the very top of a dome. Once more the XOR appears in a network, as does the adherens junction protein. When the two images are overlaid, in Fig 7.32, co-localisation is evident by the yellow colour. This indicates that XOR is indeed localised to the junctions between dome-forming cells.

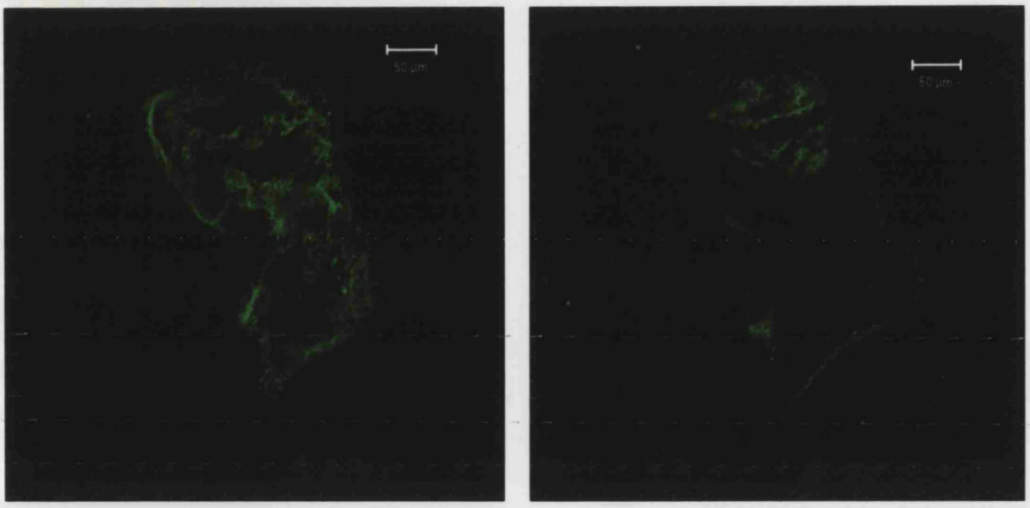

Fig 7.30: *Two sections through the same area of a Caco-2 dome stained with anti-catenin β. This protein localises further down in the cell boundary than ZO-1 and it is less easy to see the cell boundaries.*

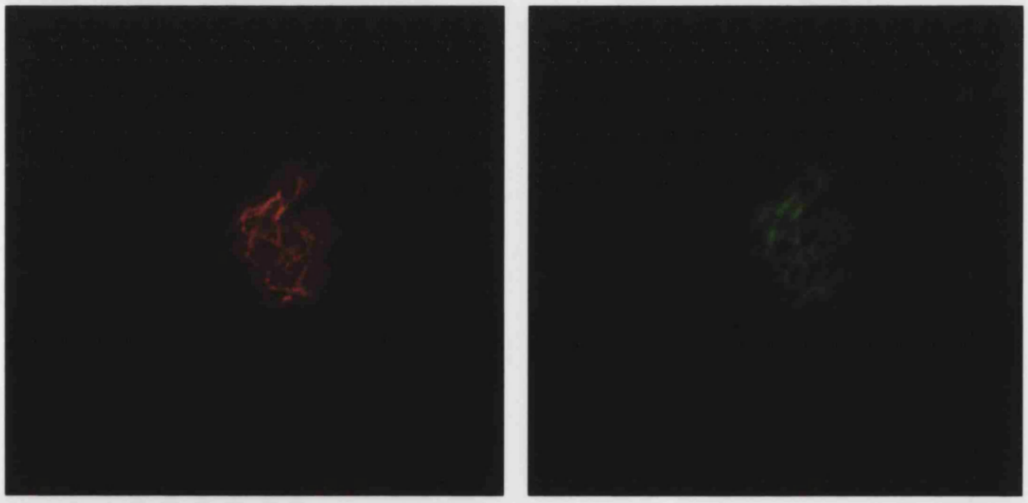

Fig 7.31: *Two pictures of the same area showing XOR (red) and catenin β (green). This image is taken from the very top of a dome, where the cell boundaries of the uppermost cells within the dome can be seen.*

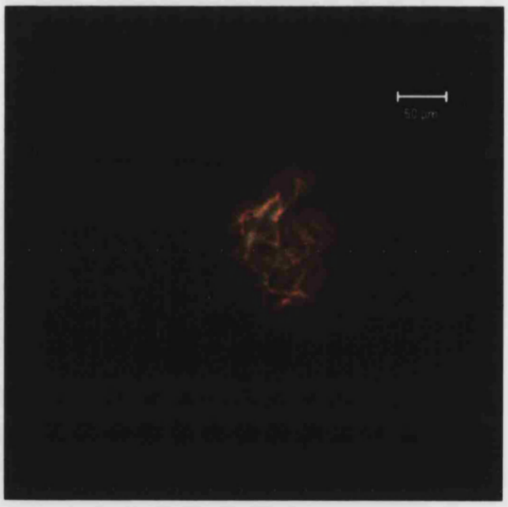

Fig 7.32: *Overlay of images in 7.30, yellow signifies co-localisation of XOR and catenin β, indicating that XOR is localized to the junctions of dome forming cells.*

7.5 Discussion

XOR activity in cells is typically measured by using the pterin assay (Beckman *et al,* 1989), as described in Section 4.3. This is a sensitive fluorimetric assay able to detect low levels of XOR activity (down to as low as 0.5pmole/min/mg isoxanthopterin production). However, no pterin-dependent XOR activity was detected in Caco-2 cells, despite several variations in protocol. Such changes included the use of whole cells and cell fractions, detachment of cells by trypsinisation and mechanical scraping. Detergents were also used in attempts to allow better access of the substrates to the enzyme. Any XOR activity within these cells was clearly below the lower limit of detection of the pterin assay.

Confocal microscopy, electron microscopy and Western blotting (results not shown due to difficulties encountered scanning the blots) all showed that XOR protein was present in this cell line, which leaves the question of why no activity could be detected. One possible explanation is that XOR activity has been shown to be down-regulated (Weber *et al,* 1978) or non-existent (Moriwaki *et al,* 1996) in cancerous cells, and the Caco-2 cell line is derived from a human colon carcinoma. Another potential explanation is that the preparation of the cells for assay resulted in the loss of the enzyme, whilst preparation of the cells for microscopy did not. Both of these possibilities are explored in Chapter 8.

It is possible that, for all the cells considered in this study, the low levels of XOR activity reflect the activity of the enzyme in most human tissues (Harrison, 1997). Moderately high levels of XOR activity have only been reported histochemically in the liver and small intestine (Kooij *et al,* 1992), and it is possible that other human tissues contain largely inactive XOR protein (Harrison, 1997). However, low xanthine oxidase activity does not necessarily not preclude other (eg NADH oxidase) functions.

Nitric oxide production from Caco-2 cells proved to be unpredictable, despite many attempts at optimizing the assay by varying conditions, substrates, buffer and even the reaction vessel used. Positive results were obtained occasionally, although the source of detected NO was uncertain. Non-enzymic production of NO by acidification of nitrites was ruled out by the use of a pH stat, as described in Chapter 5, and NO production by NOS is unlikely due to the fact the the assay was carried out under anoxic conditions. Nevertheless, the only evidence supporting XOR as the source of NO is the requirement for XOR substrates in the assay.

Immunolocalisation of XOR via electron microscopy demonstrated that the enzyme was associated with the microvilli, vesicular-like structures and either the Golgi apparatus or endoplasmic reticulum. The labelling suggests some kind of active transport from the secretory apparatus into secretory vesicles and then, potentially, to the external surface of the cell. The staining in the microvilli in these cultured cells is consistent with the localisation of XOR activity, via electron microscopy, to the microvillli of epithelial cells in intestinal brush border (Van den Munckhof *et al,* 1995). What is interesting to note is that, in the present study, the level of enzyme

seemed higher in cells with microvilli compared to those without (see Figs 7.10-7.13), suggesting that mature cells express more XOR.

The localisation pattern of XOR, as determined by electron microscopy, was similar to that seen in the endothelial and mammary epithelial cells (see Chapters 5 and 6). However, localisation of the enzyme as determined by confocal microscopy showed several distinct variations, particularly in mature cells.

Immature, sub-confluent Caco-2 cells showed punctate cytoplasmic XOR labelling (see Figs 7.14, 7.15, 7.24, 7.25). The localisation of XOR was not dependent on the substrate upon which the cells were grown and labelling frequently appeared to be more intense at the leading edge of 'clumps' of cells (see Fig 7.14). The cells at the very periphery of the clump in Fig 7.14 appear unstained, but this is simply because the cells at the very edge are below the focal plane of the microscope. Epithelial cells tend to grow in this clump formation and, unlike endothelial cells, do not put out processes. It is, accordingly, the leading edge of the clump that is involved in signalling to other cells in order to form a monolayer. Therefore this observation could indicate a cell-to-cell signalling role, as suggested for endothelial cells in Chapter 5. Whilst this pattern of localisation of XOR is similar to that seen in the other cell types studied, one distinct difference is the complete lack of nuclear labelling, even in cells that have reached confluence but not matured (Fig 7.15).

The clearly defined punctate labelling of XOR in Caco-2 cell monolayers supports the evidence, derived from the localisation of XOR by electron microscopy, of vesicular association of the enzyme. However, this is inconsistent with the findings of Jarasch

et al (1981) who found that XOR was cytosolic but did not appear to be localised to vesicles or cell organelles. The reproducibility of this observation throughout Chapter 5, 6 and 7 suggests that it is real. One explanation for the inconsistency of these findings with those of Jarasch *et al* (1981) could be that this study utilised a highly specific monoclonal anti-XOR antibody, whereas the majority of work published to date relies on polyclonal antibodies.

Localisation of XOR in dome-forming Caco-2 cells was markedly different to that observed in the other cells studied (see Chapters 5 and 6). Dome formation is a characteristic of mature Caco-2 cells (Rothen-Rutishauser *et al,* 2000) and is accompanied by enterocyte-like features such as cell polarisation and brush border microvilli. The staining for XOR within Caco-2 domes was very intense (Figs 7.16-7.25) suggesting high levels of the enzyme. Many of the images were so bright that sensitivity of the image collecting software had to be turned down to enable interpretation of the image, which resulted in the apparent loss of weaker staining in the monolayer beneath (Fig 7.16, 7.17).

The pattern of localisation of XOR associated with domes varied depending on the substrate upon which the cells were grown. Single cell and multi-cell domes grown on coverslips showed intense diffuse peripheral staining circling the cells forming domes (Figs 7.16, 7.17). When serial images were taken through the dome (Fig 7.18) it appeared that the staining was localised to the periphery of the cells within the dome. It was impossible to conclude if this staining was on the outer or inner surface of the plasma membrane, or merely localised to the cytosol in the vicinity of the plasma membrane, but the serial sections clearly show that the inside of the cells forming the

domes have little (bearing in mind the reduced sensitivity of the image collection software) to no XOR present.

Cell inserts allow access of the media to both sides of the cells, thus creating an environment closer to that found *in vivo* and promoting maturation of the cells. Caco-2 cells grown in this manner readily form mutli cellular domes in which XOR is localised in a 'hairnet' pattern at the periphery of individual dome-forming cells (Figs 7.19-7.21), along with more punctate staining, in contrast to the diffuse staining seen previously. Association of XOR with the cytoskeleton was ruled out by a lack of co-localisation with actin (Figs 7.24, 7.25). It was suggested that the 'hairnet' pattern of XOR localisation could correspond to the cell boundaries of the cells forming the domes (R Hurst, verbal communication) and this was investigated further by localisation within the domes of the tight junction complex protein, ZO-1.

Localisation of ZO-1 within Caco-2 domes did indeed show a similar pattern to that of XOR (Fig 7.29). The boundaries between the cells in both the dome and the monolayer beneath can clearly be seen. The localisation of tight junctions within the dome is strikingly similar to the localisation of XOR within domes (Fig 7.24). However, the observation that the localisation was similar does not provide enough evidence to conclude that XOR is localised to the junctions between cells.

In an attempt to determine the precise localisation of XOR within dome-forming Caco-2 cells, XOR was co-localised with catenin β (see Fig 7.32). Catenin β is a protein found lower down in the adherens junction (see Fig 7.27). The similar pattern of staining and the co-localisation is evident, indicating that the enzyme is localised to the area between cells. In this case the staining for XOR was slightly narrower than

that for catenin β, and observation that would be explained if the enzyme was located between the zonnular occludens (also known as the tight junction complex) and the top of the adherens junction, as the cleft between cells widens between these points.

The junctional localisation of XOR, along with the punctate staining observed earlier, may well indicate a transport system to the junctions between the cells forming the domes. The enzyme could be anchored in these clefts by association with glycosaminoglycans (Radi *et al,* 1997) or it may merely be secreted into the junction. However, there is some disparity between the localisation of XOR in dome-forming cells grown on inserts compared to those grown on coverslips. A potential explanation for this is that, whilst dome-forming cells grown on coverslips show more of the mature characteristics than those cells that form the monolayer beneath, they do not mature to the extent of dome-forming cells grown on inserts. It is possible that these cells are mature enough to initiate general transport of XOR to the surface of dome-forming cell, but that the barrier formed by the cell junctions is not sufficient to direct localisation of XOR to the cell junction. Hence cells grown upon coverslips show diffuse staining for XOR at the periphery of dome-forming cells and the more mature dome-forming cells grown on inserts show the 'hairnet-like' pattern of localisation of XOR that appears to correlate with the dome-forming cell junctions.

If anything, inducing barrier formation in Caco-2 cells made the network localisation less apparent. This phenomenon was only observed in one sample of cells and may be an artefact or may represent the lessened need for protection against microbial infection when a tighter barrier is present. Given that the pattern of localisation is

more apparent in mature than immature cells, it is likely that the former conclusion is the correct one.

The localisation of XOR in apoptotic cells revealed very little about the enzyme's function. Localisation did not seem to alter in apoptotic cells, nor did it become more intense. Pterin-dependent XOR assays were performed on Caco-2 cells driven into apoptosis by sodium butyrate, but once again no activity could be detected. XOR may play a role in apoptosis, but if it does, it is not revealed by the localisation of the enzyme.

Rouquette *et al* (1998) demonstrated surface staining of XOR with a polyclonal antibody raised against the enzyme, although only endothelial and mammary epithelial cells were investigated. One of the difficulties in obtaining surface staining in the present study was that the paraformaldehyde permeabilised the cells, allowing the primary antibody access beyond the cell surface. An attempt was made to circumvent this problem by performing live cell staining, hence avoiding the need to fix the cells. This proved inconclusive. Live cell staining is a relatively new technique and it was hard to tell if the enzyme was not present on the surface or if the experimental protocol was at fault. The methodology would need to be optimised and positive controls incorporated to obtain a conclusive answer.

Little nuclear staining was seen in Caco-2 cells, unlike the endothelial and mammary epithelial cell lines previously discussed. However, moderate levels of XOR were detected via electron microscopy (see Appendix) and low levels of nuclear XOR were detected by means of Western blot (data not shown). Statistical analysis of the gold

labelling for XOR generated by electron microscopy showed significantly higher levels of nuclear labelling than that seen in other cell lines. However, the inability to support this with the localisation seen under the confocal microscope casts doubts upon the authenticity of these results. It would seem that levels of XOR within the nucleus of these cells are significantly lower than that seen in mammary epithelial and endothelial cells. This could reflect the level of maturity and specialisation of these cells compared to the other cell lines studied. Nuclear staining did seem to be largely dependent on the cell type and cell density in all the cell lines studied. Endothelial cells (see Chapter 5) showed intense nuclear staining for XOR in post-confluent cells, with much weaker nuclear staining in sub-confluent cells. Mammary epithelial cells (see Chapter 6) showed much more consistent nuclear localisation of XOR that seemed independent of cell density. This variation in itself suggests that XOR has a cell or tissue specific function as opposed to a general housekeeping function.

Whilst the localisation of XOR in endothelial and mammary epithelial cells was very similar (see Chapters 5 and 6) the nuclear staining and putative localisation to the cell junction in Caco-2 cells seemed to be unique to the cell type. These results are supportive of an alternate physiological function to that of purine catabolism.

8 OVERALL DISCUSSION

Although several different cell lines were studied, a number of general points emerge. Prominent among these is the evidence of 'vesicle-like' association of XOR molecules within the cytoplasm.

In the confocal microscope studies described in this thesis, the punctate nature of cytoplasmic staining, suggestive of vesicular packaging, was, in many cases, strikingly obvious. This was less apparent in the confocal images shown by Rouquette *et al* (1998); a fact that may reflect the earlier use of polyclonal antibodies as apposed to the present employment of high affinity monoclonals.

Rouquette and coworkers (1998) demonstrated localisation of XOR on the outer surface of endothelial cells, as did Vickers *et al* (1998), using monoclonal antibodies. In the present work, I was unable to explore extracellular localisation with confidence because the fixing processes, however mild, always led to antibody penetration of the plasma membrane. Nevertheless, I found that, in many cases, XOR was concentrated towards the outer periphery of the cytoplasm, particularly in those areas apposed by neighbouring cells (Figs. 5.11,5.21). These findings complement the similar localisation of extracellular enzyme shown by Rouquette *et al* (1998) and proposed by them to reflect an intercellular signalling role for XOR.

If, for the sake of discussion, the punctate cytoplasmic staining represents vesicular location of XOR, then the enzyme could be seen as being transported to the plasma membrane for eventual export to the outer cell surface, where it assumes a signalling or other function. Support for this paradigm is provided by electron microscopy. In these studies, two different resins were used for embedding, each with its peculiar strength and weakness. The requirements of sample preparation were such that one resin showed good definition of cell ultrastructure, but low density of antigen, while the other gave higher antigenic density with poorly preserved ultrastructure. Nevertheless, use of the two resins in parallel indicated strongly that XOR was often packaged within vesicle-like bodies (Figs. 5.4, 5.6, 5.7, 6.4-6.6, 7.3-7.6). Moreover, such vesicles were seen, in particular cases, to be either emerging from Golgi-like structures or approaching and merging with the plasma membrane (Figs. 5.5, 5.8, 6.8-6.10, 7.7-7.9)

Apart from the histochemical evidence cited above, further support for the cellular export of XOR is provided by Partridge *et al* (1992), who reported that the enzyme is constitutively released from microvascular endothelial cells. The question arises as to what extent such export is compatible with established secretory mechanisms. XOR lacks an N-terminal signal sequence (Ichida *et al,* 1993) and so is not an obvious candidate for the classic biosynthetic and secretory pathway of proteins destined for export from the cell or incorporation into the plasma membrane (Stroud and Walter, 1999). This does not necessarily exclude XOR from targetting to the ER and incorporation into the above secretory pathway, as recent work has shown that signal sequences can occur at the C-terminus (Holscher *et al,* 2001) or even internally (Ouzzine *et al,* 1999) in proteins destined for the ER. There is also the possibility that

XOR enters the ER by post-translational protein translocation. Very little is known about the targetting mechanism employed during this translocation mode and, whereas in mammalian cells only short polypeptides have been shown to enter the ER in this manner, *S. cerevisiae* are able to translocate large precursors (Kalies and Hartmann 1998). The fact that XOR contains disulphide bonds (Godber 1998), a post-translational modification that takes part in the ER (Frand *et al,* 2000), supports this possibility.

Regarding intracellular progress subsequent to incorportation into the ER, proposed routes of newly-synthesised proteins and glycoproteins through the various compartments of the Golgi and beyond, are constantly increasing and several possibilities exist. Many of the structures seen in the present work are too large (approx. 0.5-1μm) to be coated vesicles. However, recent opinion suggests that coated vesicles may represent a minority of the carriers that operate within the secretory pathway (Glick, 2000). It is possible that the enzyme is contained within large polymorphic structures known as secretory vesicles that emerge from the trans Golgi network to travel to the plasma membrane (Glick, 2000). Another alternative to COP 1 coated vesicles are 'megavesicles', recently reported by Volchuk *et al* (2000), electron micrographs of which are strikingly similar to those seen containing XOR in this study.

Whatever the trafficking pathway, it is conceivable that XOR could associate, at an early stage, with glycosaminoglycans (GAGs) and/or syndecans, which occur on the cell surface and need to be transported there. XOR is known to have high affinity for GAGs (Radi *et al,* 1997) and may even make its way to the cell surface 'piggy-back'

on such structures, which are transported to the outer surface of the cell, where they remain anchored as part of the extracellular matrix. XOR is known to be associated with GAGs on the outer surface of vascular endothelial cells and evidence has been presented for internalization and reexport of the enzyme (Houston *et al,* 1999). Presumably, such processes involve localisation of XOR to endosomes and it may be that some of the larger 'vesicular' structures seen in confocal microscopy (eg. Figs. 5.13, 5.14) correspond to this process.

From the data in this thesis and from those of Rouquette *et al* (1998), export of XOR to the outer surface of endothelial cells, seems to be established. The question then arises as to its physiological role in this location. Discussion is necessarily speculative and must acknowledge that it is based on experimental data in cultured, immortalised cells, with limited relevance to the *in vivo* situation. Nevertheless, some observations may be significant. As noted above, XOR tends in many cases to be concentrated in peripheral regions of the cell that were directly apposed to those of neighbouring cells. This suggests involvement of the enzyme in intercellular signalling, particularly in the latter stages of monolayer formation. Such signalling could involve superoxide, hydrogen peroxide or indeed NO, although we have no direct evidence for any of these. In this context, it is noteworthy that XOR activity in the cell cultures overall rises dramatically as the monolayer forms (Fig 5.1). A further, and particularly interesting potential example of intercellular signalling is seen in the mixed cell cultures, CPA, in which extensions of endothelial cells, apparently reaching toward neighbouring smooth muscle cells (see Fig 5.21), show high density of XOR. It is tempting to see this as a manifestation of NO-mediated endothelial signalling to smooth muscle; an established physiological process (Moncada *et al,* 1991).

Similar evidence of export of XOR to the cell surface was obtained in epithelial cells. In the case of HB4a mammary cells, confocal microscopy again showed punctate staining (Figs 6.14, 6.15) and evidence of localisation of XOR to Golgi or ER was provided by electron microscopy (Figs 6.4, 6.5, 6.9, 6.10). Although HB4a cells do not actually generate milk fat globules, incoporation of XOR in the milk fat globule membrane requires the presence of the enzyme in the plasma membrane of the mammary cell and the present data can be seen as evidence that XOR is involved in a secretory pathway.

The distribution of XOR in Caco-2 cells is particularly interesting. Derived from intestinal epithelial cells, Caco-2 cells in culture grow first to a monolayer, parts of which subsequently develop domes. Domes are seen as an advanced stage of differentiation in these cells, representing the intestinal epithelial cell layer with its villi and tight junctions

In this context, the relationship between localisation of XOR and development of the cell culture is noteworthy. Prior to and at the monolayer stage, the enzyme is seen to be distributed throughout the cytoplasm. As in the other cell types studied here, both confocal and electron microscopic data are consistent with packaging of the enzyme in vesicles, at least some of which are presumably destined for export to the cell surface (Figs. 7.3 – 7.9, 7.14 – 7.15). At a later stage, single cell and multicellular domes develop and the distribution of XOR changes accordingly. In single 'dome' cells, XOR is uniformly distributed around the periphery forming a relatively dense layer. Finally, in the most highly differentiated multicellular domes, grown on cell culture inserts, the distribution of XOR changes again and most dramatically,

apparently becoming concentrated in the tight junctions. Evidence for this latter localisation comes from the strikingly similar 'hairnet' confocal images of XOR and ZO1, a tight junction protein (Figs. 7.24, 7.25, 7.29) and, more convincingly, from co-localisation of XOR and catenin β, another junctional protein (Figs. 7.30 – 7.32).

In so far as the multicellular domes constitute a model of the mature intestinal epithelium, localisation of XOR to tight junctions is perfectly understandable in terms of the antibacterial barrier function assigned to the latter (Uzzau and Fasano, 2000). In fact, this pattern of XOR localisation was especially prominent in the cells that had been grown in co-culture (Section 7.4.2) designed to induce the development of high transcellular resistance, tight junctional complexes and restricted permeability (Garberg 1998). Tight junctions are dynamic structures that adapt readily to a variety of developmental, physiological and pathological circumstances (Uzzau and Fasano, 2000). However, certain bacteria are able to exert an irreversible effect on the permeability and cytoskeletal structure of the tight junction via toxins, such as those produced by *Clostridium difficile, Bacteroides fragilis* and *Vibrio cholerae,* or via polymorphonuclear cells utilised by *Salmonella* and *Shigella* (Uzzau and Fasano, 2000). XOR can be seen as a defence against such processes.

The presence of XOR in tight junctions of intestinal epithelial cells clearly presupposes export of the enzyme from the cell and evidence of an antibacterial role for extracellular XOR in the gut has been provided by Van den Munckhof *et al.* (1995), who have shown striking electron micrographic evidence of disintegrating bacteria surrounded by XOR.

An antibacterial role for intestinal epithelial cell XOR, whether in tight junctions or excreted, can be seen as complementary to a similar role for XOR on the surface of the MFGM in the neonatal gut. In either location, XOR might be expected to actively seek out bacteria by virtue of its ability to bind to acidic glycosaminoglycans (Radi et al., 1997) commonly found on bacterial surfaces.

Van den Munckhof and coworkers (1995) assumed that the antibacterial activity of XOR depended on its ability to generate hydrogen peroxide and superoxide anion. It could also depend upon the generation of nitric oxide and, more especially, peroxynitrite, resulting from XOR-catalysed nitrite reduction (Godber *et al.,* 2000ab). In support of this idea, fresh milk has recently been shown to inhibit the metabolic activity of a pathogenic bacterium in a nitrite-dependent process. Using *E. coli* transfected with the lux operon, Hancock *et al.* (2002) were able to use chemiluminescence to monitor metabolic activity, which was shown to be significantly impaired in the presence of fresh bovine or human milk. These bacteriostatic effects were dependent on the presence of nitrite and were abolished by heating the milk or in the presence of the specific XOR inhibitor, oxypurinol (Fig 8.1). Moreover, the inhibition was only observed at low oxygen tensions, consistent with the known competition of nitrite and molecular oxygen for XOR-generated electrons (Godber *et al.,* 2000b). Bacteriostatic activity of XOR in other contexts is illustrated by its demonstrated contribution to host defence against *Burkholderia cepacia* in a mouse model of chronic granulomatous disease Segal *et al.* (2000).

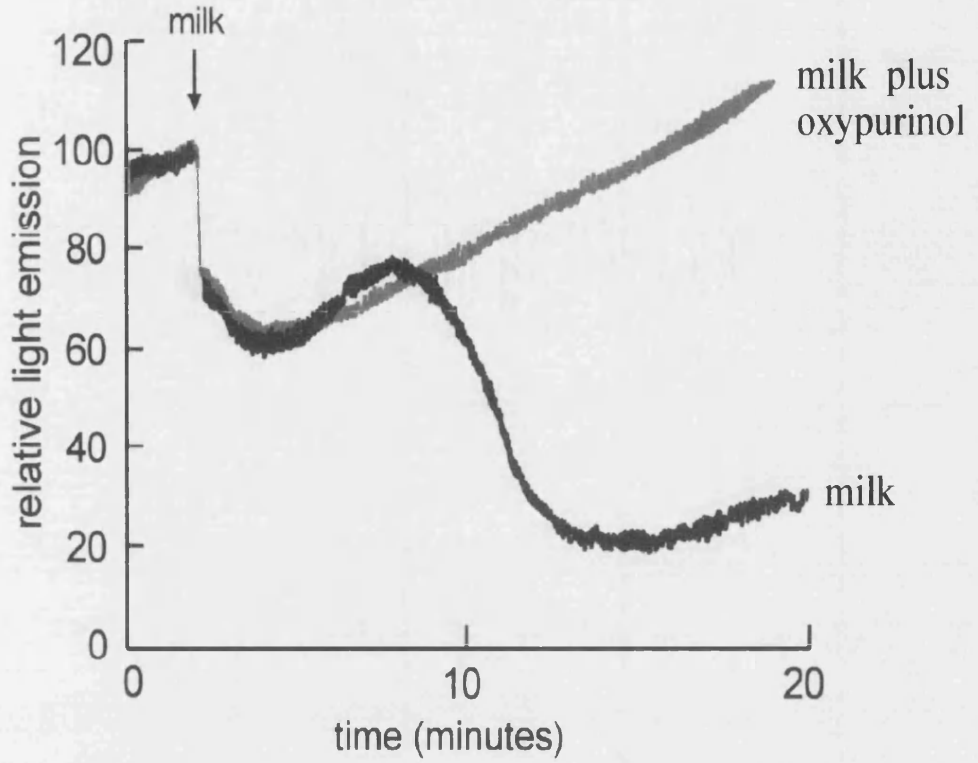

Fig 8.1: *The effect of bovine milk on the metabolism of E. coli. E. coli isolate 16906, transformed with the luxCDABE operon, was resuspended in a luminometer cuvette with 10μM pterin and 20mM sodium nitrite at 0.63% oxygen tension. Light emissions were recorded before and after the addition of milk (1ml). No reduction in light emission was seen with milk treated with 25μM oxypurinol. Similar results were obtained with human milk (not shown).*

The pattern of XOR activity seen in endothelial cells (Fig.5.1) may provide clues regarding enzyme function. The initial peak of activity, seen as the cells reach confluence, can be seen as reflecting involvement of XOR in intercellular signalling as the cells move towards confluence. A second peak is attained when the cells in the monolayer begin to die off and possible roles for XOR in the latter process should be considered. ROS and peroxynitrite are known to lead to profound biological consequences, including apoptosis and even mutation (Maeda and Akaike, 1998). In the present work, however, attempts to link apoptosis with XOR expression were inconclusive. Nevertheless, confluent and post-confluent endothelial cells showed marked staining of the nucleus. Enzyme was seen to be concentrated at the nuclear membrane and even at nuclear pores, suggesting involvement in transcriptional control. Unfortunately, such temporal association of subcellular distribution of XOR was not apparent in the other cell types studied. Mammary epithelial cells generally showed intense nuclear staining regardless of cell density, while intestinal epithelial cells showed very little staining at any stage of development. The latter observation is of interest in view of the apparent association of XOR with the proteins of tight junctions. ZO-2, which localises to tight junctions of confluent cells, is found in the nucleus of sub-confluent cells and migrates to the cell surface as confluence is attained (Islas *et al*, 2002).

9 APPENDIX

Controls

Localisation by means of electron microscopy, secondary antibody only

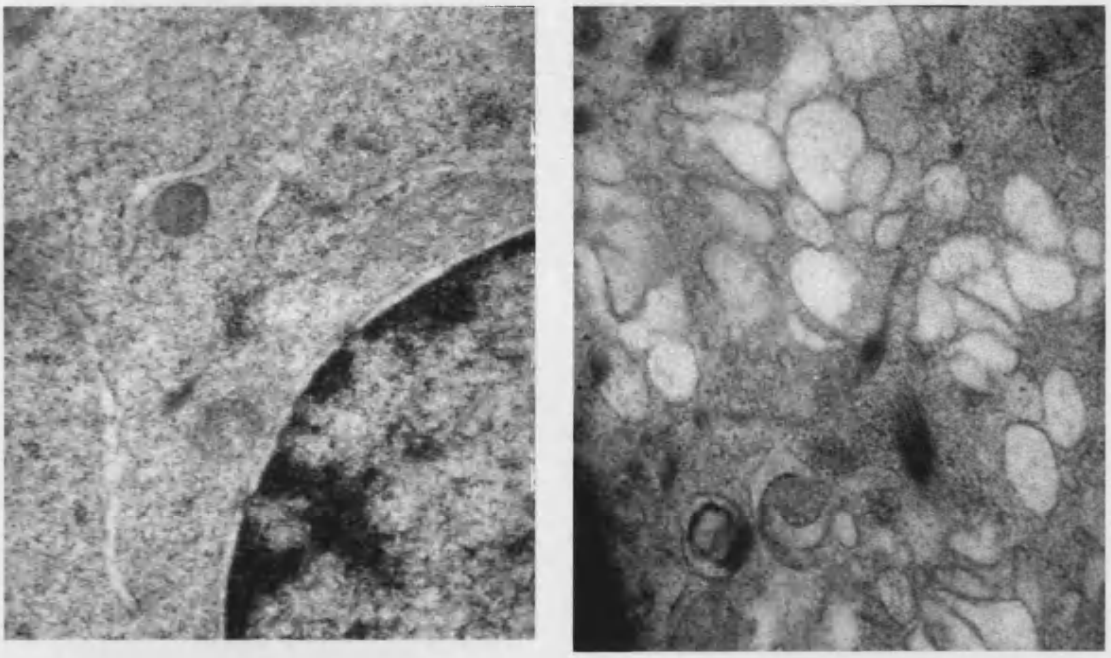

EA-hy-926 cells exposed to the secondary antibody only, very little non-specific labelling is seen (magnification x40,000)

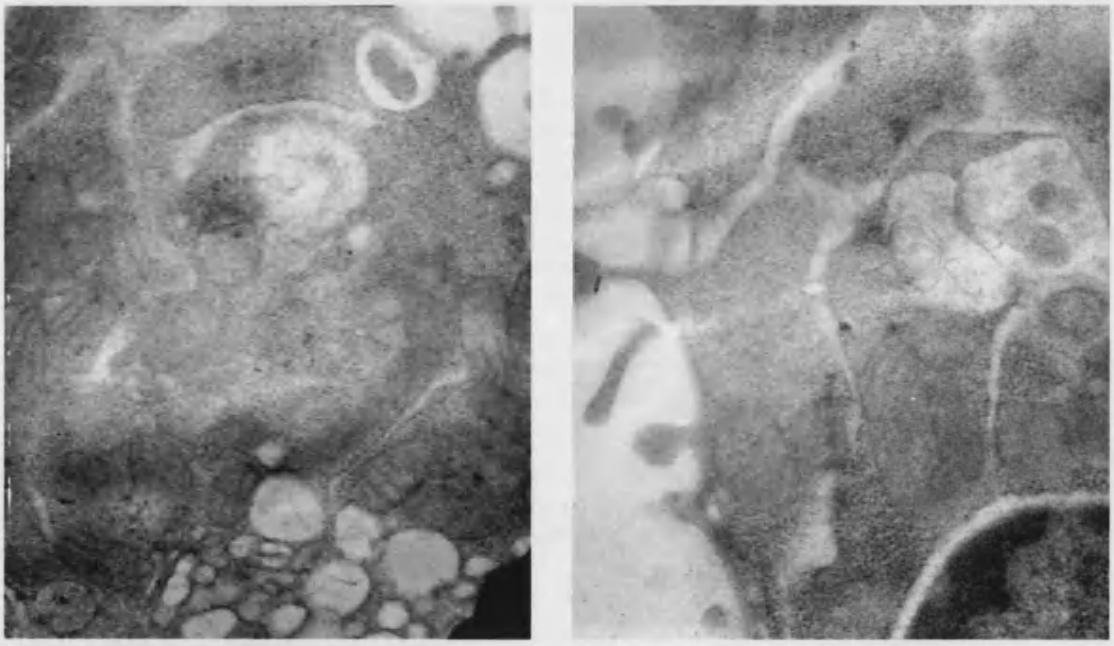

HB4a cells exposed to the secondary antibody only, very little non-specific labelling is seen (magnification x40,000)

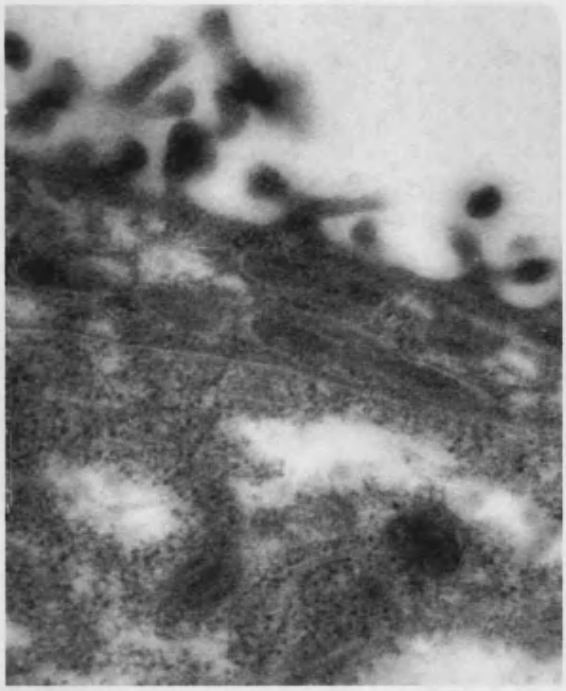

Caco-2 cells exposed to the secondary antibody only, very little non-specific labelling is seen (magnification x60,000)

Localisation by means of electron microscopy, monoclonal anti-golgi antibody

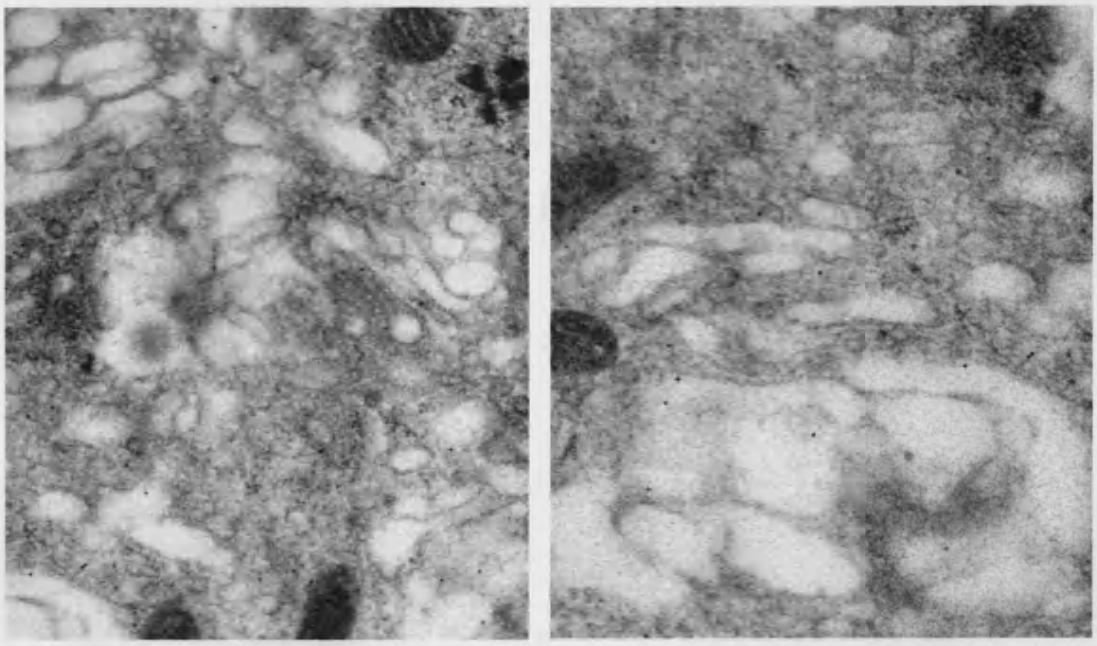

EA-hy-926 and HB4a cells respectively subjected to the same staining protocol as other samples excepting that the primary mouse anti-human XOR monoclonal antibody was replaced with a mouse anti-human golgi apparatus monoclonal antibody (magnificationx50,000)

Localisation by means of confocal microscopy, secondary antibody only

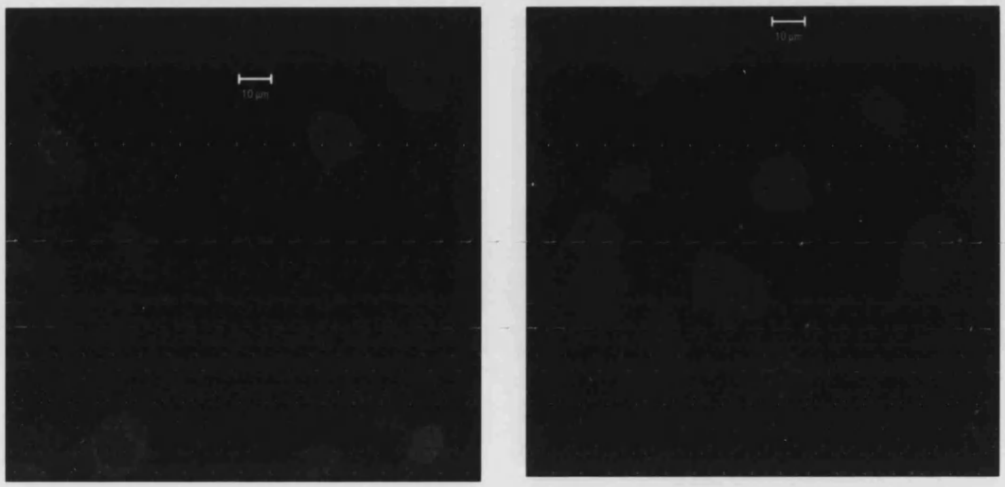

EA-hy-926 and ECV-304 cells respectivly, stained with secondary antibody FITC conjugate only. Some non-specific staining is seen but levels are low compared to samples where a primary antibody is also used

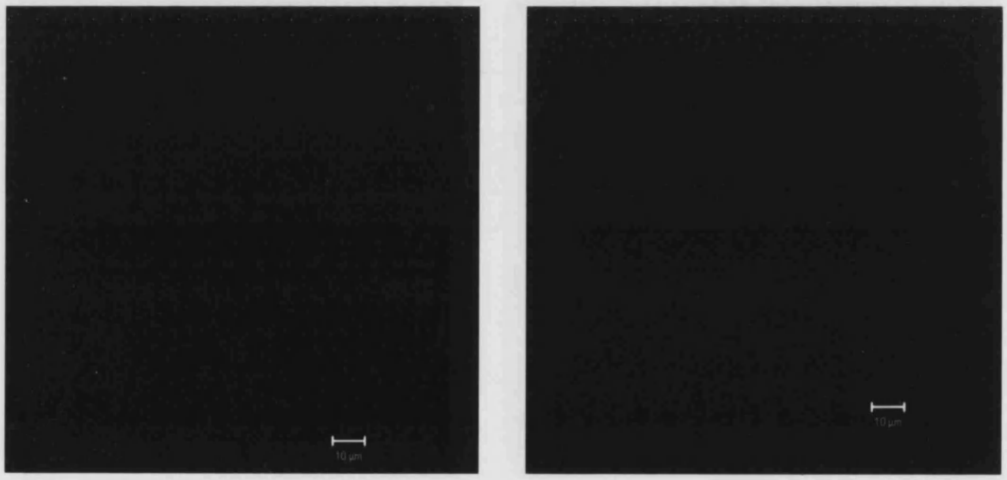

HB4a and Caco-2 (grown on coverslips)cells respectivly, stained with secondary antibody FITC conjugate only. Some non-specific staining is seen but levels are low compared to samples where a primary antibody is also used

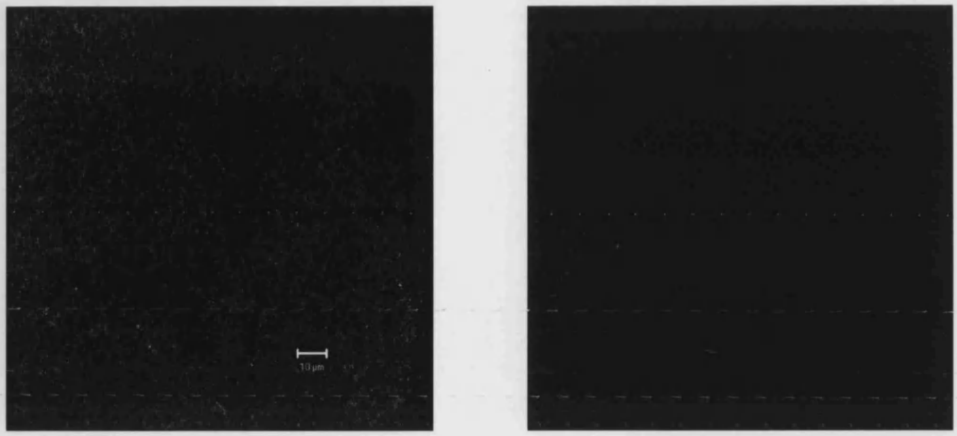

Caco-2 FITC and Caco-2 TRITC (grown on insets) cells respectivly, stained with secondary antibody only. Some non-specific staining is seen but levels are low compared to samples where a primary antibody is also used

Secondary only controls for both electron microscopy and confocal microscopy where performed for each batch of staining with whichever secondary atnibody conjugate that was used. The images shown here are an example of those routinly seen, as hundreds of control images were obtained. If background levels were above those shown in the Section, the results were rejected.

Statistical analysis of gold labelling

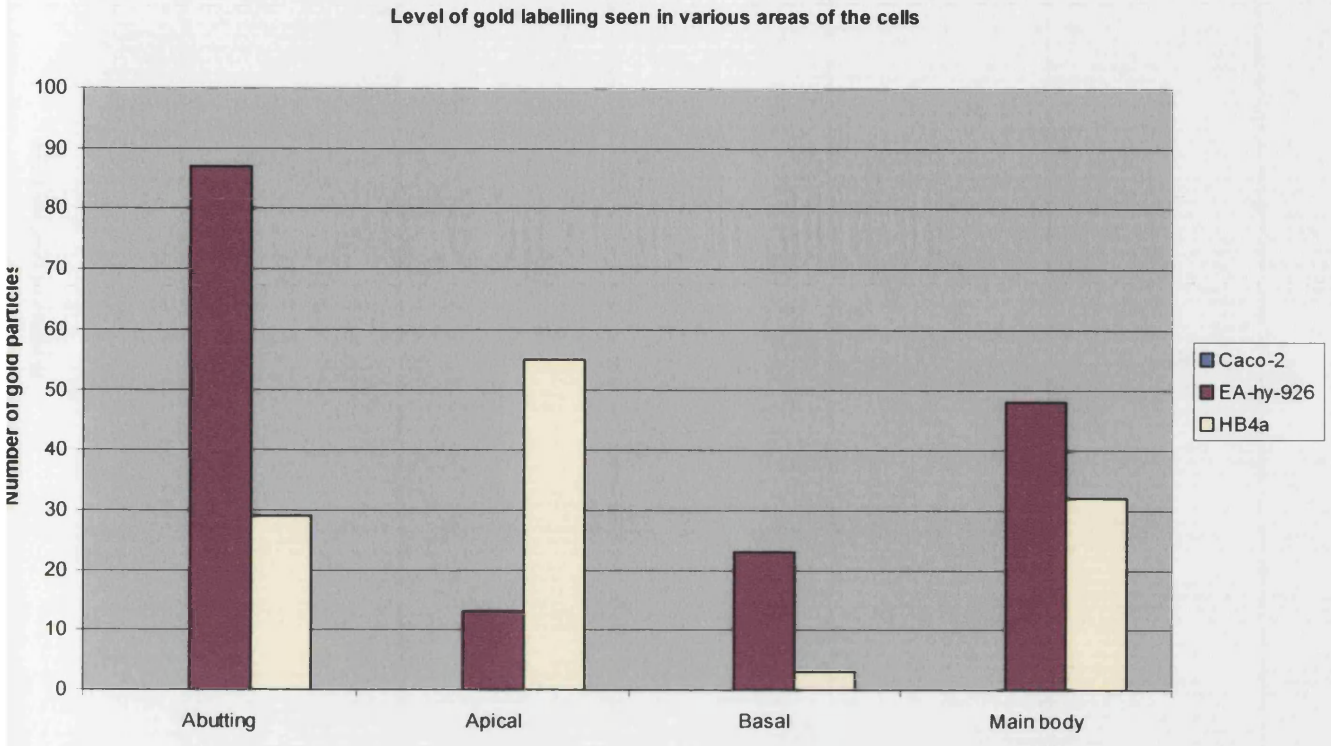

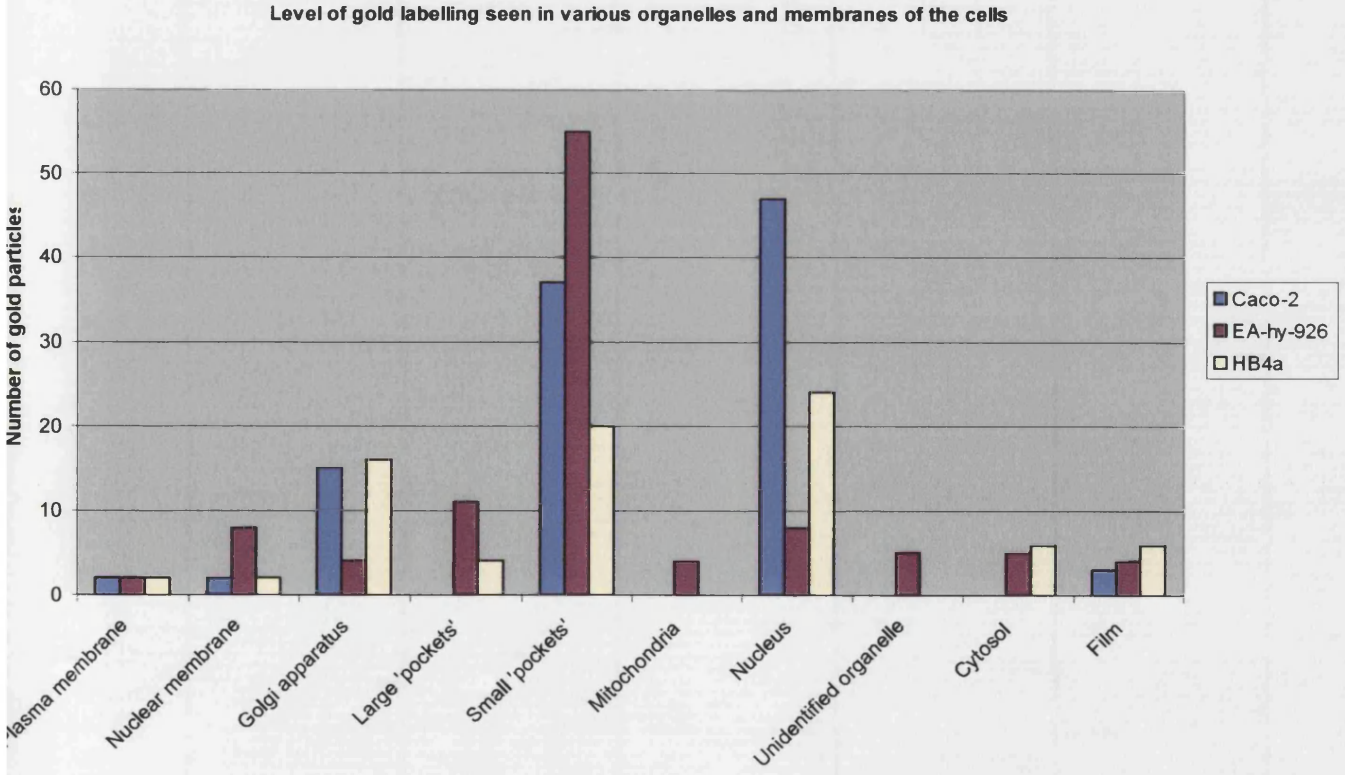

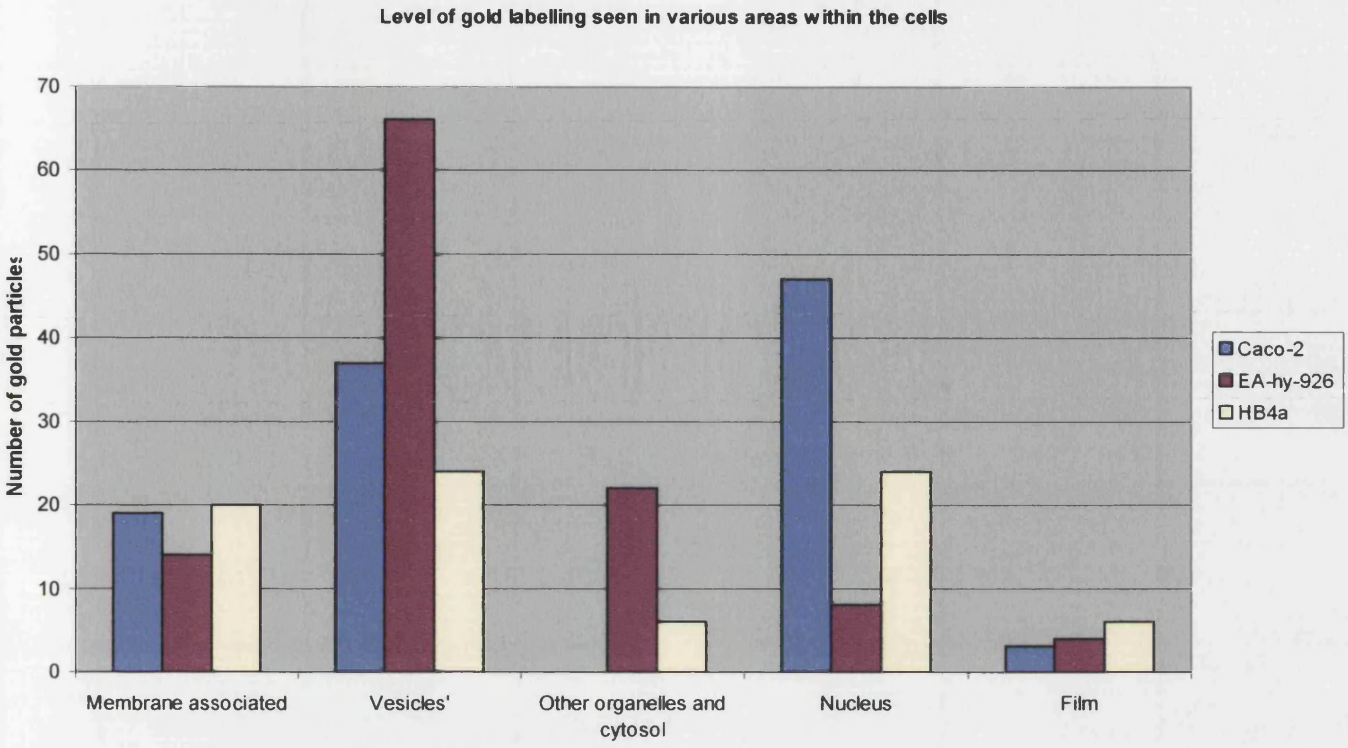

Statistical analysis showing significance of labelling by the χ^2 test

	Observed	*Expected*	*Observed*	*Expected*	*Observed*	*Expected*
	Caco-2		**EA-hy-926**		**HB4a**	
Abutting			**87**	*42.75*	**29**	*29.75*
Apical			**13**	*42.75*	**55**	*29.75*
Basal			**23**	*42.75*	**3**	*29.75*
Main body			**48**	*42.75*	**32**	*29.75*
Average			*42.75*		*29.75*	
Chi Test (P value significance level)			*1.931E-16*		*6.66E-10*	
Plasma membrane	**2**	*17.66666667*	**2**	*10.6*	**2**	*10*
Nuclear membrane	**2**	*17.66666667*	**8**	*10.6*	**2**	*10*
Golgi apparatus	**15**	*17.66666667*	**4**	*10.6*	**16**	*10*
Large 'pockets'		*17.66666667*	**11**	*10.6*	**4**	*10*
Small 'pockets'	**37**	*17.66666667*	**55**	*10.6*	**20**	*10*
Mitochondria		*17.66666667*	**4**	*10.6*		*10*
Nucleus	**47**	*17.66666667*	**8**	*10.6*	**24**	*10*
Unidentified organelle		*17.66666667*	**5**	*10.6*		*10*
Cytosol		*17.66666667*	**5**	*10.6*	**6**	*10*
Film	**3**	*17.66666667*	**4**	*10.6*	**6**	*10*
Average	*17.66667*		*10.6*		*10*	
Chi Test (P value significance level)	*1.32E-19*		*7.927E-41*		*3.19E-08*	

Primary cells

There was some concern that the inability to obtain reproducible data for NO production was an artefact of using a permanent cell line. Discrepancies between the characteristics and behaviour of primary cells and their immortalised counterparts have been revealed in other reports (Claise, Edeas, Chaouchi *et al,* 1999). To rule this out primary white blood cells were obtained from fresh blood (as per Section 4.3) and subjected to NO analysis (as per Section 4.5). No activity could be detected in these cells, despite the fact that XOR has been localised and enzyme activity has been detected in leucocytes (Hellsten, Hansson, Johnson *et al,* 1996). This suggested that the failure to detect NO from some cells and the lack of reproducible data from others was a function of the assay, due to the complexity of working with a whole cell system or a reflection of the low levels of XOR activity seen in all human cells irrespective of whether the cells originated from a cell line or a primary cell source.

10 REFERENCES

Abadeh S, Killacky KS, Benboubetra M, Harrison R. (1992). Purification and partial characterisation of xanthine oxidase from human milk. *Biochimica et Biophysica Acta.* **1117,** 25-32.

Abati A, Cajigas A, Holland SM, and Solomon D. (1996). Chronic granulomatous disease of childhood; respiratory cytology. *Diagnostic Cytopathology.* **15,** 98-102

Abrams J, Elkyam U, Thadani U and Fung H. (1998). Tolerance; an historical overview. *American Journal of Cardiology.* **81(1A),** 1-14A.

Ahlner J, Andersson RG, Torfgard K and Axelsson KL. (1991). Organic nitrate esters: clinical use and mechanisms of actions. *Pharmacological Review.* **43(3),** 351-423.

Alderton WK, Couper CE and Knowles RG. (2001). Nitric oxide synthases: structure, function and inhibition. *Biochemical Journal.* **357,** 593-615.

Beckman JS, Dale PA, Pearson JD, Marshall PA and Freeman BA. (1989). A sensitive fluorometric assay for measuring xanthine dehydrogenase and oxidase in tissue. *Free Radical Biology and Medicine.* **6,** 607-615.

Benboubetra M, Gleeson A, Harris CPD, Khan J, Arrar L, Brennard D, Reid J, Reckless JD and Harrison R. (1997). Circulating anti-(xanthine oxidoreductase) antibodies in healthy human adults. *European Journal of Clinical Investigation.* **27,** 611-619.

Bradford M. (1976). A rapid and sensitive method for the quantification of microgram quantities of protein utilising the principle of protein dye binding. *Annuals of Biochemistry.* **72,** 248-254.

Brass CA. (1995). Xanthine oxidase and reperfusion injury: major player or minor irritant? *Hepatology.* **21,** 1757-1758.

Bray RC. (1975). Molybdenum iron-sulphur hydroxylases and related enzymes, in: P.D. Boyer (Ed.), The Enzymes, Vol. XII, 3rd edn., Academic Press, New York, pp. 229-419

Brown AM, Benboubetra M, Ellison M, Powell D, Reckless JD and Harrison R. (1995). Molecular activation-deactivation of xanthine oxidase in human milk. *Biochimica et Biophysica Acta.* **1245,** 248-254.

Carey DJ. (1997). Syndecans: multifunctional cell-surface co-receptors. *Biochemical Journal.* **327,** 1-16.

Choudhury S. (2001). The purification and characterisation of xanthine oxidoreductase from liver. *pH. D. Dissertation.* University of Bath.

Claise C, Edeas M, Chauchi N, Chalas J, Capel L, Kalimouttou S, Vazquez A and Lindenbaum A. (1999). Oxidized-LDL induce apoptosis in HUVEC but not in the endothelial cell line EA-hy-926. *Atherosclerosis.* **147,** 95-104.

Cleere WF and Coughlan MP. (1975). Avian xanthine dehydrogenase I. Isolation and characterisation of the turkey liver enzyme. *Complete Biochemical Physiology.* **508,** 311-322.

Cole J. (1996). Nitrate reduction to ammonia by enteric bacteria: redundancy, or a stratergy for survival during oxygen starvation? *FEMS Microbiological Letters.* **136,** 1-11.

Cook WS, Chu R, Saksela M, Raivio K and Yeldandi AV. (1997). Differential immunohistochemical localization of xanthine oxidase in normal and neoplastic human breast epithelium. *International Journal of Oncology.* **11,** 1013-1017.

Coon HG. (1968).Clonal culture of differentiated rat liver cells. *Journal of Cell Biology.* **39,** 29a

Doel JJ. (2000). Production of nitric oxide from nitrites and nitrates catalysed by xanthine oxidoreductase. *Ph. D Dissertation.* University of Bath.

Doel JJ, Godber BLJ, Goutl TA, Eisenthal R and Harrison R. (2000). Reduction of organic nitrites to nitric oxide catalysed by xanthine oxidase: possible role in metabolism of vasodilators. *Biochemical and Biophysical Research Communications.* **270,** 880-885

Doel JJ, Godber BLJ, Eisenthal R and Harrison R. (2001). Reduction of organic nitrates catalysed by xanthine oxidoreducatse under anaerobic conditions. *Biochemica et Biophysica Acta.* **1527,** 81-87.

De Jong JW, Van der Meer p, Nieukoop AS, Huizer T, Stroeve RJ and Bos E. (1990). Xanthine oxidoreductase activity in perfused hearts of various species; including humans. *Circulation Research.* **67,** 770-773.

Della Corte E and Stripe F. (1972). The regulation of rat liver xanthine oxidase. *Biochemical Journal.* **126,** 739-745.

DeMoss JA and Hsu P-Y. (1991). NarK enhances nitrate uptake and nitrite excretion in *Escherichia coli. Journal of Bacteriology.* **173,** 3303-3310.

de Silva AM, Balch WE and Helenius A. (1990). Quality control in the endoplasmic reticulum: folding and misfolding of vesicular stomatitis virus G protein in cells and *in vitro. Journal of cell biology.* **3,** 857-866.

Dykhuizen RS, Frazer R, Duncan C, Smith C, Golden M, Benjamin N and Leifert C. (1996). Antimicrobial effect of acidified nitrite on gut pathogens: importance of dietary nitrate in host defense. *Antimicrobial agents and chemotherapy.* **40(6),** 1422-1425.

Eckermann L, Laurent F, Langford TD, Hetsko ML, Smith JR, Kagnoff M and Gillin FD. (2000). Nitric oxide production by human intestinal epithelial cells and comptition for arginine as potential determinants of host defense against lumen-dwelling pathogen *Giardia lamblia. Journal of Immunology.* **164,** 1478-1487.

Edgell C-J S, McDonald CC and Graham JB. (1983). Permanent cell line expressing human factor VIII-related antigen established by hybridisation. *Proceedings of the National Academy of Science USA.* **80,** 37-34-3737.

Enroth C, Eger BT, Okamoto K, Nishino T, Nishino T and Pai E. (2000). Crystal structure of bovine milk xanthine dehydrogenase and xanthine oxidase: structure based mechanism of conversion. *Proceedings of the National Academy of Science USA.* **97,** 21479-21485

Frederiks WM and Bosch KS. (1996). The proportion of xanthine oxidase activity of total xantine oxidoreductase activity *in situ* remains constant in rat liver under various (patho)physiological conditions. *Hepatology.* **24,** 1179-1184

Frederiks WM, Marx F and Kooij A. (1993). The effect of ischemia on xanthine oxidase activity in rat intestine and liver. *Investigative Journal of Experimental Pathology.* **74,** 21-26.

Frederiks WM, Vreeling-Sindelarova H, and Straatsburg IH. (1999). Localisation of xanthine oxidase activity at the luminal surface of sinusoidal endothelial cells in rat liver, in: *Cells of the hepatic sinusoid, Volume 7.* Kupfer Cell Foundation. 123-124

Feelisch M, Brands F and Kelm M. (1995). Human endothelial cells bioactivate organic nitrates to nitric oxide: implications for the reinforcement of endothelial defence mechanisms. *European Journal of Clinical Investigation.* **25,** 737-745.

Feelisch M and Kelm M. (1991). Biotransformation of organic nitrates to nitric oxide in vascular smooth muscle and endothelial cells. *Biochemical and Biophysical Research Communications.* **180(1),** 286-293.

Frand AR, Cuozzo JW and Kaiser CA. (2000). Pathways for protein disulphide bond formation. *Trends in Cell Biology.* **10,** 203-210.

Garberg P. (1998). *In vitro* models of the blood-brain barrier. *Alternatives to Laboratory Animals.* **26,** 821-847.

Glick BS. (2000). Organization of the Golgi apparatus. *Current Opinions in Cell Biology.* **12,** 450-456

Godber BLJ, Physiochemical and kinetic properties of human milk xanthine oxidoreductase. (1998). *Ph. D. Dissertation.* University of Bath.

Godber BLJ, Doel JJ, Durgan J, Eisenthal R and Harrison R. (2000). A new rote to peroxynitrite: arolefor xanthine oxidoreductase. *FEBS Letters.* **475,** 93-96.

Godber BLJ, Doel JJ, Goult TA, Eisenthal R and Harrison R. (2001). Suicide inactivation of xanthine oxidoreductase during reduction of inorganic nitrite to nitric oxide. *Biochemical Journal.* **358,** 325-333.

Godber BLJ, Doel JJ, GP, Blake DR, Stevens CR, Eisenthal R and Harrison R. (2000a). Reduction of nitrite to nitric oxide catalyzed by xanthine oxidoreductase. *Journal of Biological Chemistry.* **275(11),** 7757-7763.

Godber B, Stevens S, Harrison R, Eisenthal R and Bray RC. (1997). ≥95% of xanthine oxidase in human milk is present as the demolybdo form, lacking molybdopterin. *Biochemical Society Transactions.* **25,** 519S.

Granger DN, Rutili G and McCord JM. (1981). Role of superoxide in feline intestinal ischemia. *Gastroenterology.* **81,** 22-29

Gustafson DL and Pritsos CA. (1992). Bioactivation of mitomycin C by xanthine dehydrogenase from EMT6 mouse mammary carcinoma tumours. *Journal of the National Cancer Insitutue.* **84(15),** 1180-1185.

Gutteridge S, Tanner SJ and Bray RC. (1978). Comparison of the molybdenum centres of native and desulpho xanthine oxidase. *Biochemical Journal.* **175,** 887-897.

Hancock JT. (1997). Nitric Oxide, Hydrogen Peroxide and Carbon Monoxide, in: *Cell Signaling,* Addison Wesley Longman Limited, Harlow, pp. 167-184.

Hancock JT, Desikan R and Neil SJ. (2001). Role of reactive oxygen species in cell signalling pathways. *Biochemical Society Transactions.* **29,** 345-350.

Hancock JT, Salisbury V, Ovejero-Boglione MC, Cherry R, Hoare C, Eisenthal R and Harrison R. (2002). Milk contains anti-microbial activity: mediated by the enzyme xanthine oxidoreductase and peroxynitrite. *In press.*

Hanson LA, Ceafalau L, Mattsby-Baltzer I, Lagerberg M, Hjalmarsson A, Ashraf R, Zaman S and Jail F.(2000). The mammary gland-infant immunologic dyad. *Advanced Experimental Medical Biology.* **478,** 65-76

Hara I, Miyake H, Hara S, Arakawa S and Kamidono S. (2000). Sodium butyrate induces apoptosis in human renal cell carcinoma cells and synergistically enhances their sensitivity to anti-fas-mediated cytotoxicity. *International Journal of Oncology.* **17(6),** 1213-1218.

Harrison DG and Bates JN. (1993). The nitrovasodilators; new ideas about old drugs. *Circulation.* **87,** 1461-1467.

Harrison R. (1997). Human xanthine oxidoreductase: in search of a function. *Biochemical Society Transactions.* **25,** 786-791.

Harrison R, Benboubetra M, Bryson S, Thomas RD, and Elwood PC. (1990). Antibodies to xanthine oxidase: elevated levels in patients with acute myocardial infarction. *Cardioscience.* **1,** 183-189

Hassoun PM, Yu FS, Shedd AL, Zulueta JJ, Thannickal VJ and Lanzillo JJ. (1994). Regulation of endothelial cell xanthine dehydrogenase xanthine oxidase gene expression by oxygen tension. *American Journal of Physiology.* **266(2 Pt1),** L163-171.

Hayat MA. (1989). Principles and techniques of electron microscopy. *The MacMillan Press Ltd.* **3rd Ed.** 92-119.

Hellsten Y, Hansson HA, Johnson L, Frandsen U and Sjödin BS. (1996). Increased expression of xanthine oxidase and insulin-like growth factor 1 (IGF-1) immunoreactivity in skeletal muscle after strenuous activity in humans. *Acta Physiological Scandinavia.* **157,** 191-197.

Hille R. (1996). The mononuclear molybdenum enzymes. *Chemistry Reviews.* **96,** 2757-2816

Holscher C, Bach UC and Dobberstein B. (2001). Prion protein contains a second endoplasmic reticulum targeting signal sequence located at its C terminus. *Journal of Biological Chemistry.* **276(16),** 13388-13394.

Holt L. (2000). Cellular localisation of XOR. *Final year project undergraduate report.* The University of Bath.

Houstan M, Estevez A, Chumley P, Aslan M, Marklund S, Parks DA and Freeman BA. (1999). Binding of xanthine oxidase to the vascular endothelium. *Journal of Biological Chemistry.* **8(19),** 4985-4994.

Hurst RD and Fritz IB. (1996). Properties of an immortartalised vascular endothelial/glioma cell co-culture model of the blood brain barrier. *Journal of Cellular Physiology.* **167,** 81-88.

Hurst RD, Heales SJR, Dobbie MS, Barker JE and Clark JB. (1998). Decreased endothelial cell glutathione and increased sensitivity to oxidative stress in an *in vitro* blood-brain barrier model system. *Brain Research.* **802,** 232-240.

Ichida K, Amaya Y, Noda K, Minoshima S, Hosoya T, Sakai O, Shimizu N and Nishino T. (1993). Cloning of the cDNA-encoding human xanthine dehydrogenase (oxidase): structural analysis of the protein and chromosomal localisation on the gene. *Gene.* **40(8),** 279-284.

Ichikawa M, Nishino T, Nishino T and Ichikawa A.(1992). Subcellular localization of xanthine oxidase in rat hepatocytes: high-resolution immunoelectron microscopic study combined with biochemical analysis. *Journal of Histochemisrty and Cytochemistry.* **40(8),** 1097-1103.

Iizuka T, Sasaki M, Oishi K, Uemura S, Koike M and Shinozaki M. (1999). Non-enzymatic nitric oxide generation in the stomachs of breastfed neonates. *Acta Paediatrician.* **88,** 1053 1055

Ikegami T and Nishino T. (1986). The presence of desulfo-xanthine dehydrogenase in purified and crude enzyme preparations from rat liver. *Archives of Biochemical Biophysics.* **247,** 254-260.

Ikegami T, Natsumeda Y and Weber G. (1986). Decreased concentration of xanthine dehydrogenase (EC 1.1.1.204) in rat hepatomas. *Cancer Research.* **46,** 3838-3841.

Irani K. (2000). Oxidant signalling in vascular cell growth, death and survival. *Circulation Research.* **87,** 179-183.

Islas S, Vega J, Ponce L and Gonzalez-Mariscal L. (2002). Nuclear localization of the tight juction protein ZO-2 in epithelial cells. *Experimental Cell Research.* **274(1),** 138-148.

Jarasch ED, Grund C, Bruder G, Heid HW. Keenan TW and Franke WW. (1981). Localization of xanthine oxidase in mammary gland epithelium and capillary endothelium. *Cell.* **25,** 67-82

Kalies KU and Hartmann E.(1998). Protein translocation into the endoplasmic reticulum (ER). *European Journal of Biochemistry.* **254,** 1-5

Kayyali US, Donaldson C, Huang H, Abdelnour R and Hassoun PM. (2001). Phosporylation of xanthine dehydrogenase/oxidase in hypoxia. *Journal of Biological Chemistry.* **276(17),** 14359-14365.

Keenan TW and Patton S. (1995). The structure of milk: implications for sampling and storage, in: *Handbook of Milk Composition.* New York Academic Press. 5-50.

Kelm M, Dahmann R, Winks D and Feelisch M. (1997). The nitric oxide/superoxide assay. *Journal of Biological Chemistry.* **272,** 9922-9932.

Knowles RG and Moncada S. (1994). Nitric oxide synthases in mammals. *Biochemical Journal.* **298,** 249-258.

Kooij A, Bosch KS, Frederiks WM and Van Noorden CJF. (1992). High levels of xanthine oxidoreductase in rat endothelial, epithelial and connective tissue cells. *Virchows Archive of B Cell Pathology.* **62,** 143-150.

Kooij A, Frederiks WM and Van Noorden CJF. (1995). Xanthine oxidase and reperfusion injury: major player or minor irritant? Reply. *Hepatology.* **21,** 1758-1760.

Kooij A, Schiller HJ, Schijns M, Van Noorden CJF and Fredricks WM. (1994). Conversion of xanthine dehydrogenase to xanthine oxidase in rat liver and plasma at the onset of reperfusion after ischemia. *Hepatology.* **19,** 1488-1495.

Kooij A, Schijns M, Fredricks WM, Van Noorden CJF and James J. (1992). Distribution of XOR activity in human tissues – a histochemical and biochemical study. *Virchows Archives of B Cell Pathology.* **63,** 17-23.

Krenitsky TA, Neil SM, Elion GB and Hitchings GH. (1972). A comparison of the specificities of xanthine oxidase and aldehyde oxidase. *Archives of Biochemical Biophysics.* **150,** 585-599.

Krenitsky TA, Spector T and Hall WW. (1986). Xanthine oxidase from human liver; purification and characterisation. *Archives of Biochemical Biophysics.* **247,** 108-119.

Kurose I and Granger DN. (1994). Evidence implicating xanthine oxidase and neutrophils in reperfusion-induced microvascular dysfunction. *Annual of the New York Academy of Science.* **723,** 158-179

Lepore DA, Kozlov AV, Stewart AG, Hurley JV, Morrison WA and Tomasi A. (1999). Nitric oxide synthase-independent generation of nitric oxide in rat skeletal muscle ischemia-reperfusion injury. *Nitric Oxide: Biology and Chemistry.* **3(1),** 75-84.

Lin CT, Chen LH and Chan TS. (1983). A comparative study of polyclonal and monoclonal antibodies for immunohistochemical localization of cytosolic aspartate and aminotransferase in rat liver. *Journal of Histochemical Cytochemistry.* **31(7),** 920-926.

Linder N, Rapola J and Raivio KO. (1999). Cellular expression of xanthine oxidoreductase protein in normal human tissue. *Laboratory Investigation.* **79,** 967-974.

Lorenz B, Schluter T, Bohnensack R, Pergande G and Muller WE. (1998). Effect of flupirtine on cell death of human umbilical vein endothelial cells induced by reactive oxygen species. *Biochemical Pharmacology.* **56(12),** 1615-1624.

Maeda H and Akaike T. (1998). Nitric oxide and oxygen radicals in infection, inflammation and cancer. *Biochemistry (Moscow).* **6(7),** 854-865

Massey V and Harris CM. (1997). Milk xanthine dehydrogenase: the first one hundred years. *Biochemical and Biophysical Acta.* **25,** 750-755.

McCord JM. (1985). Oxygen-derived free radicals in postischemic tissue injury. *New England Journal of Medicine.* **312,** 159-163.

McManaman JL, Hanson L, Neville MC and Wright RM. (2000). Lactogenic hormones regulate xanthine oxidoreductase and β-casein levels in mammary epithelial cells by distinct mechanisms. *Archives of Biochemistry and Biophysics.* **373(2),** 318-327.

McManaman JL, Neville MC and Wright RM. (1999). Mouse mammary gland xanthine oxidoreductase: purification, characterisation and regulation. *Archives of Biochemical Biophysics.* **371,** 308-316.

Menconi MJ, Unno, N, Smith M, Aguirre DE and Fink MP. (1998). Nitric oxide donor-induced hyperpermeabiity of cultured intestinal epithelial monolayes: role of superoxide radical, hydroxyl radical and peroxynitrite. *Biochimica et Biophysica Acta.* **1425,** 189-203.

Miesel R and Zuber M. (1993). Elevated levels of xanthine oxidase in serum of patients with inflammatory and autoimmune rheumatic diseases. *Inflammation.* **17,** 551-561.

Millar TM, Stevens CR, Benjamin N, Eisenthal R, Harrison R and Blake DR. (1998). Xanthine oxidoreductase catalyses the reduction of nitrates and nitrite to nitric oxide under hypoxic conditions. *FEBS Letters.* **427,** 225-228.

Moncada S, Palmer RMJ and Higgs EA. (1991). Nitric oxide: physiology, pathophysiology and pharmacology. *Pharmacological Reviews.* **43(2),** 109-142.

Moorhouse PC, Grootveld M, Halliwekk B, Quinlan JG and Gutteridge JMC. (1987). Allopurinol and oxypurinol are hydroxyl radical scavengers. *FEBS Letters.* **213,** 23-28.

Moriwaki Y, Yamamoto T, Yamaguchi K, Suda M, Yamakita JI, Takahashi S and Hagashino K. (1996). Immunohistochemical localization of xanthine oxidase in human tissues. *Acta Histochemical Cytochemistry.* **29,** 153-162

Nishino T and Nishino T. (1989). The nicotinamide adenine dinucleotide-binding site of chicken liver xanthine dehydrogenase. *Journal of Biological Chemistry.* **264,** 5468-5473.

O'Bryne S, Shirodaria C, Millar T, Stevens C, Blake D and Benjamin N. (1999). Inhibition of platelet aggregation with glyceryl trinitrate and xanthine oxidoreductase. *Journal of Pharmacology and Experimental Therapeutics.* **292(1),** 326-330.

Olson J, Ballou D, Palmer G and Massey V. (1974). The mechanisms of action of xanthine oxidase. *Journal of Biochemistry.* **249,** 4363-4382.

Ouzzine M, Magdalou J, Burchell B and Fournel-Gigleux S. (1999). An internal signal sequence mediates the targeting and retention of the human UDP-glucuronosyltransferase 1A6 to the endoplasmic reticulum. *The Journal of Biological Chemistry.* **274(44),** 31401-31409.

Page S. (1999). Regulation and immunolocalisation of human xanthine oxidoreductase. *Ph. D Dissertation.* University of Bath.

Page S, Powell D, Benboubetra M, Stevens CR, Blake DR, Selase F, Wolstenhome AJ and Harrison R. (1998). Xanthine oxidoreductase in human mammary epithelial cells: activation in response to inflammatory cytokines. *Biochimica et Biophysica Acta.* **1381,** 191-202.

Parks DA and Granger DN. (1986). Xanthine oxidase: biochemistry, distribution and physiology. *Acta Physiology Scandinavia.* **548 (sp),** 87-99

Patton S and Keenan TW. (1975). The milk fat globule membrane. *Biochimica et Biophysica Acta.* **415,** 273-309.

Pfeffer KD, Huecksteadt TP and Hoidal J. (1994). Xanthine dehydrogenase and xanthine oxidase activity and gene expression in renal epithelial cells. (1994). *Journal of Immunology.* **153(4),** 1789-1797.

Poss WB, Huecksteadt TP, Panus PC, Freeman BA and Hoidal JR. (1996). Regulation of xanthine dehydrogenase and xanthine oxidase activity by hypoxia. *American Journal of Physiology.* **270(6 Pt1),** L941-946.

Prajda N, Donohue JP and Weber G. (1981). Increased amidophosphoribosyltransferase and decreased xanthine oxidase activity in human and rat renal cell carcinoma. *Life Science.* **29,** 853-860.

Prajda N, Morris HP, and Weber G. (1976). Imbalance of purine metabolism in hepatomas of different growth rates as expressed in behaviour of xanthine oxidase (EC 1.2.3.2). *Cancer Research.* **36,** 4639-4646.

Pritsos CA. (2000). Cellular distribution, metabolism and regulation of the xanthine oxidoreductase enzyme system. *Chemico-Biological Interactions.* **129,** 195-208.

Radi R, Rubbo H, Bush K and Freeman BA. (1997). Xanthine oxidase binding to glycosaminoglycans: kinetics and superoxide dismutase interactions of immoblized xanthine oxidase-heparin complexes. *Archives of Biochemistry and Biophysics.* **339(1),** 125-135.

Ramboer C, Piessins F and DeGroote J. (1972). Serum xanthine oxidase and liver disease. *Digestion.* **7,** 183-195.

Rapoport TA. (1992). Transport of proteins across the endoplasmic reticulum membrane. *Science.* **258(5084),** 931-936.

Rothen-Rutishauser B, Braun A, Günthert M and Wunderil-Allenspach H. (2000). Formation of mutlilayers in the Caco-2 cell culture model: a confocal laser scanning microscopy study. *Pharmaceutical Research.* **17(4),** 460-465.

Rouquette M, Page S, Bryant R, Benboubetra M, Stevens CR, Blake DR, Whish WD, Harrison R and Tosh D. (1998). Xanthine oxidoreductase is asymmetrically localised on the outer surface of human endothelial and epithelial cells in culture. *FEBS Letters.* **426,** 397-401.

Rytkonen EM, Halila R, Laan M, Saksela M, Kallioniemi OP, Palotie A and Raivio KO. (1995). The human gene for xanthine dehydrogenase (XDH) is localised on chromosome band 2q22. *Cytogenetic Cell Genetics.* **68,** 61-63.

Saksela M, Lapatto R and Raivio KO. (1998). Xanthine oxidoreductase gene expression and enzyme activity in developing human tissues. *Biology of the Neonate.* **74,** 274-280.

Sampath V, Zhao X and Caughey W. (1994). Characterisation of interactions of nitric oxide with human haemoglobin A by infrared spectroscopy. *Biochemical and Biophysical Research Communications.* **198,** 281-287.

Sanders SA, Eisenthal R and Harrison R. (1997). NADH oxidase activity of human xanthine oxidoreductase: generation of superoxide anion. *European Journal of Biochemistry.* **245,** 541-48.

Sawa T, Wu J, Akaike T and Maeda H. (2000). Tumour-targeting chemotherapy by xanthine oxidase-polymer conjugate that generates oxygen-free radicals in tumour tissue. *Cancer Research.* **60,** 666-671.

Sears CL. (2000). Molecular physiology and pathophysiology of tight junctions: assault of the tight junction by enteric pathogens. *American Journal of Physiological Gastrointestinal Liver Physiology.* **279,** G1129-G1134.

Segal BH, Sakamoto N, Patel M, Maemura K, Klein AS, Holland SM and Bulkley GB. (2000). Xanthine oxidase contributes to host defense against *Burkholderia cepacia* in the p47phox-/- mouse model of chronic granulomatous disease. *Infection and Immunity.* **68 (4),** 2374-2378.

Smail N, Catania RA, Wang P, Cioffi WG, Bland KI and Chaudry IH. (1998). Gut and liver: the organs responsible for increased nitric oxide production after trauma-hemorrhage and resuscitation. *Archives of Surgery.* **133,** 399-405.

Stamps AC, Davies SC, Burman J and O'Hare MJ. (1994). Analysis of proviral integration in human mammary epithelial cell lines immortalized by retroviral infection with a temperature-sensitive SV40 T-antigen construct. *International Journal of Cancer.* **57,** 865-874.

Stevens CR, Millar TM, Clinch JG, Kanczler JM, Bodamyali T and Blake DR. (2000). Antibacterial properties of xanthine oxidase in human milk. *Lancet.* **356,** 829-830.

Stevenson BR and Keon BH. (1998). The tight junction: morphology to molecules. *Annual Review of Cell Developmental Biology.* **14,** 89-109.

Stroud MS and Walter P. (1999). Signal sequence recognition and protein targeting. *Current Opinion in Structural Biology.* **9,** 754-759

Sumi S and Wada Y. (1996). Xanthine oxidase deficiency (hereditary xanthinuria), molybdenum cofactor deficiency. *Nippon Rinsho.* **54,** 3333-3336.

Sussman MS and Bulkley GB. (1990). Oxygen derived free radicals in reperfusion injury. *Methods Enzymology.* **186,** 711-723.

Tan KH, Dobbi MS, Felix RA, Barrand MA and Hurst RD. (2001). A comparison of the induction of immortalized endothelial cell impermeability by astrocytes. *Neurochemistry.* **12(7),** 1-6.

Terada LS, Piermattei D, Shibao GN, McManaman JL and Wright RW. (1997). Hypoxia regulates xanthine dehydrogenase activity at pre- and posttranslational levels. *Archives of Biochemistry and Biophysics.* **348(1),** 16-168.

Terao M, Kurosaki M, Zanotta S and Garattini E. (1997).The xanthine oxidoreductase gene: structure and regulation. *Biochemical Society Transactions.* **25,** 791-794.

Trewick AL, Elhassan K, Round JM and Adiseshiah M. (1996). Xanthine oxidase in critically ischemic and claudicant limbs: profile of activity during early reperfusion. *British Journal of Surgery.* **83,** 798-802.

Tsukita S, Furuse M and Itoh M. (2001). Multifunctional strands in tight junctions. *Nature Reviews Molecular Cell Biology.* **2(4),** 285-293.

Tumova S, Hatch BA, Douglas JLAW and Bame KJ. (1999). Basic fibrobalst growth factor dos not prevent heparan sulphate proteogycan catabolism in intact cells, but it alters the distribution of the glycosamioglycan degradation products. *Biochemical Journal.* **337,** 471-481.

Uzzau S and Fassano A. (2000). Cross-talk between enteric pathogens and the intestine. *Cellular Microbiolgy.* **2(2),** 83-89

Van den Munckhof RJM, Vreeling-Sindelarova H, Schellens JPM, Van Noorden CJF and Frederiks WM. (1995). Ultrastructural localization of xanthine oxidase activity in the digestive tract of the rat. *Histochemical Journal.* **27,** 897-905.

Vickers S, Schiller HJ, Hildreth JE and Bulkley GB. (1998). Immunoaffinity localization of the enzyme xanthine oxidase on the outside surface of endothelial cell plasma membrane. *Surgery.* **124,** 551-560.

Volchuk A, Amherdt M, Ravazzola M, Brügger B, Rivera VM, Clackson T, Perrelet A, Söllner TH, Rothman JE and Orci L. (2000). Megavesicles implicated in the rapid transport of intracisternal aggregates across the Golgi stack. *Cell.* **102,** 335-348.

Wajner M and Harkness RA. (1989).Distribution of xanthine dehydrogenase and oxidase activities in human and rabbit tissues. *Biochemica et Biophysica Acta.* **991,** 79-84.

Weber G, Kizaki H, Tzeng D, Shiotani T and Olah E. (1978). Colon tumour: enzymology of the neoplastic program. *Life Science.* **23,** 729-736.

Weitzburg E and Lundberg JON. (1998). Nonenzymatic nitric oxide production in humans. *Nitric Oxide Biology and Biochemistry.* **2(1),** 1-7.

Wiezorek JS, Brown DH, Kupperman DE and Brass CA. (1994). Rapid conversion to high xanthine oxidase activity in viable Kupfer cells during hypoxia. *Journal of Clinical Investigation.* **94,** 2224-2230.

Yoshikawa T, Kokura S, Tainaka K, Naito Y and Kondo M. (1995). A novel cancer therapy based on oxygen radicals. *Cancer Research.* **55,** 1617-1620.

Zhang Z, Naughton D, Winyard PG, Benjamin N, Blake DR and Symons MC. (1998). Generation of nitric oxide by a nitrite reductase activity of xanthine oxidase: a potential pathway for nitric oxide formation in the absence of nitric oxide synthase activity. *Biochemical and Biophysical Research Communications.* **249(3),** 767-72 .